NASA Technical Memorandum 110440

Phenolic Impregnated Carbon Ablators (PICA) as Thermal Protection Systems for Discovery Missions

Huy K. Tran, Christine E. Johnson, Daniel J. Rasky,
Frank C. L. Hui, Ming-Ta Hsu, Timothy Chen,
Y. K. Chen, Daniel Paragas, and Loreen Kobayashi

April 1997

National Aeronautics and
Space Administration

NASA Technical Memorandum 110440

Phenolic Impregnated Carbon Ablators (PICA) as Thermal Protection Systems for Discovery Missions

Huy K. Tran, Christine E. Johnson, Daniel J. Rasky, and Frank C. L. Hui,
Ames Research Center, Moffett Field, California
Ming-Ta Hsu and Timothy Chen, H.C. Chem, San Jose, California
Y. K. Chen, Thermosciences Institute, Moffett Field, California
Daniel Paragas and Loreen Kobayashi, Foothill-De Anza College, Cupertino, California

April 1997

National Aeronautics and
Space Administration

Ames Research Center
Moffett Field, California 94035-1000

Phenolic Impregnated Carbon Ablators (PICA) as Thermal Protection Systems for Discovery Missions

HUY K. TRAN, CHRISTINE E. JOHNSON, DANIEL J. RASKY, FRANK C. L. HUI, MING-TA HSU,*
TIMOTHY CHEN,* Y. K. CHEN,† DANIEL PARAGAS,‡ AND LOREEN KOBAYASHI‡

Ames Research Center

Summary

This report presents the development, characterization, and arc-jet testing of Phenolic Impregnated Carbon Ablators (PICA), a member of the Lightweight Ceramic Ablators (LCA) family developed at Ames Research Center. LCAs consist of a low density fibrous substrate impregnated with an organic resin. PICA uses a pre-formed fibrous carbon tile manufactured by Fiber Materials, Inc. as the substrate, and phenolic as the organic infiltrant. Innovative infiltration techniques were developed to produce PICA with densities ranging from 14 to 65 lbm/ft^3; however, only the low density PICA samples were used to evaluate the material's thermal performance. Arc-jet testing of low density PICA showed that these materials can withstand very high heating rates and surface pressures and are more mass efficient than most traditional ablative materials (ref. 1). The manufacturing process of PICA has since been refined to give repeatable performance among batches, and its thermal performance is being further evaluated. Surface densification was also recently developed to improve the ablation characteristics in high heating and surface pressure environments.

The thermal performance and ablation characteristics of PICA were evaluated in an oxidizing environment in the Ames Research Center 60 megawatt (MW) Interaction Heating Facility (IHF). Samples of PICA with and without surface densification, the carbon preform, and Avcoat-5026 (the Apollo heat shield), were tested at cold wall heat fluxes of 375 to 2960 Btu/ft^2-s and surface pressures from 0.1 to 0.43 atm. Resulting heat loads during these tests ranged from 5500 to 29,600 Btu/ft^2. Surface and in-depth temperatures were measured using optical pyrometers and thermocouples, respectively. Mass loss was measured for each sample and surface recession was measured using a height gage. Various material characterization tests were also performed on virgin (pre-test) and charred (post-test) PICA samples.

Introduction

During the past two decades, there has been very little effort toward developing new lightweight ablative heat shields for planetary entry vehicles. Traditional ablators, such as SLA-561V and Avcoat-5026H/C, were developed several decades ago to support the Viking and Apollo missions. In recent years, the national priority has been re-focused on the exploration of other planets, and the need for advanced ablative materials became apparent. These planetary missions would require a heat shield that can withstand very high heating rates and shear loads, while providing the necessary thermal protection for the interior of the vehicle. In addition, a low density material is desirable to minimize the weight of the heat shield, allowing the weight of the scientific payload to be maximized.

A family of materials called Lightweight Ceramic Ablators (LCAs) were developed at Ames Research Center to fulfill the needs of these future planetary missions. LCAs are low density materials that utilize precursor technologies to simplify the manufacturing process and minimize manufacturing costs. Arc-jet tests show that these materials can withstand very high heating rates and shear loads with a savings in weight up to 50% when compared to traditional ablators (ref. 1).

The manufacturing processes of LCAs have been significantly improved since their initial conception, and several optimization approaches were investigated. The objective of this arc-jet test series was to investigate the thermal performance and ablation characteristics of various compositions of PICA at a wide range of heat fluxes, surface pressures, and heat loads.

Materials

LCAs, in general, consist of a fibrous ceramic substrate impregnated with an organic resin. PICA utilizes a fibrous carbon Fiberform® insulation manufactured by

*H.C. Chem, 15221 Skyview Dr., San Jose, CA 95133.
†Thermosciences Institute, Moffett Field, CA 94035.
‡Foothill-De Anza College, 21250 Stevens Creek Blvd., Cupertino, CA 95014.

Fiber Materials, Inc.[1] and phenolic resin as the infiltrant. Fiberform is a commercial insulation material which has been optimized for vacuum or inert furnaces. Fiberform is produced by chopping carbon fibers of 14–16 μm diameter and 1600 μm length in a water slurry. A water soluble phenolic resin is added to the slurry, mixed and vacuum cast. The green billet is then dried, resin cured, and carbonized to 1440°F, and then heat treated at 3240°F. Due to its high porosity, the Fiberform, in general, has fairly low thermal conductivity compared to the high density solid graphite and its counter part, the carbon foam. It is also the basis in the selection of high temperature substrates for LCA materials.

The SC1008 phenolic infiltrant used in the production of PICA is a phenol-formaldehyde resin formed through polycondensation reactions between phenol and formaldehyde in the presence of suitable catalysts by a one- or two-stage process (ref. 2). Figure 1 shows the polymerization process of the phenolic resins using a one-stage process (a); the reaction is interrupted at A- or B-stage resins to prevent crosslinking. For the two-stage process (b), the reaction can be carried out nearly to completion without three-dimensional crosslinking. Final crosslinking is accomplished after application of A- or B-stage resins or molding powder to produce a thermoset material. Figure 2 shows the molecular structure of the cured phenolic resins.

Initial densities of the carbon Fiberform used in this test series ranged from 8.5 to 11 lbm/ft^3. Innovative impregnation techniques[2] were used to produce standard PICA test samples with final densities ranging from 14 to 17 lbm/ft^3.

Surface densification was performed on several test samples to investigate the difference in ablation characteristics and thermal performance when compared with standard PICA samples. Surface densification increased the final densities of the PICA materials, ranging from 18 to 23 lbm/ft^3. Table 1 summarizes the composition of each densified test sample, denoted with a “D” following the sample identification number. Several samples of the carbon substrate (10 to 11 lbm/ft^3) and one sample of the traditional ablator Avcoat-5026 (32 lbm/ft^3) were tested to compare with the PICA samples.

[1]Fiber Materials, Inc., “Some Comments on the Thermal Conductivity of Carbon Fiberform Insulation,” FMI internal report.
[2]Patent pending.

Material Testing and Analysis

It is necessary to obtain the thermophysical and thermochemical properties of the material to evaluate the ablation characteristics and thermal performance. Various tests were performed to characterize and fully understand the performance of the various compositions of PICA.

1. Thermal Properties Measurements

Initial thermal property measurements were taken to characterize PICA material. Thermal conductivity measurements were made on the Fiberform and PICA materials, and thermogravimetric analysis was performed on the phenolic resins and PICA material in an inert and oxidizing environment.

a. Thermal conductivity

Fiberform is commercially used as insulation for vacuum and inert furnaces, thus, its thermal conductivity is fairly low. The material exhibits an anisotropy in its thermal and mechanical performance. The thermal conductivity in the strong direction, i.e., direction of fibers, is about 2.4 times higher than that of the weak direction, through the thickness. In most cases, the ablating surface on a typical heat shield would be perpendicular to the weak direction. The thermal conductivity of this material increases with increasing temperature and can be expressed as an Arrhenius function (ref. 3),

$$K = Ae^{BT}$$

where

K the thermal conductivity, Btu-in/ft^2-hr-°F

A a material dependent constant, which is in essence, the thermal conductivity at 32°F

B a material dependent constant which is a measure of how rapidly the thermal conductivity increases with temperature

T the mean temperature, °F

Figure 3 shows the typical behavior of the thermal conductivity of the Fiberform as a function of mean temperature. The influence of density on the conductivity coefficients A and B are shown in figures 4 and 5, respectively. As expected, the coefficient A increases with density, but coefficient B is inversely proportional to density. The primary reason for this inverse trend is the influence of internal radiative heat transfer on the thermal conductivity in a fibrous material. As the density increases, the porosity decreases, and the internal structure has more integrity, which results in a reduction of the radiation contribution to the overall heat transfer.

The importance of internal radiative heat transfer on the overall thermal conductivity at high temperatures is demonstrated in figure 6, which shows the combined influence of density on conductivity for Fiberform as a function of temperature (see footnote 1). The low density materials (9 and 10.6 lbm/ft^3) have lower thermal conductivity at temperatures up to 2000°F, but cross over to a much higher conductivity above 2000°F. Fiberform with a density of 14.4 lbm/ft^3 has a slightly higher thermal conductivity at temperatures below 2000°F and significantly lower conductivities at temperatures in excess of 2700°F.

Thermal conductivities of PICA materials were measured at various pressures using the ASTM D 27766-86 and ASTM E1461-92. PICA with 30% phenolic resin in the 10 lbm/ft^3 density Fiberform was selected for this measurement. Thermal conductivity was calculated at each temperature from the measured thermal diffusivity, α, density, ρ, and heat capacity, C_p, by using the following expression, $K = \alpha \rho C_p$.

Figures 7, 8, and 9 show the heat capacity, thermal diffusivity, and thermal conductivity, respectively, of PICA-15 (10 lbm/ft^3 Fiberform and 4.5–5 lbm/ft^3 phenolic) at pressures of 0.05, 0.01, 0.001 atm. The results show that pressure has a small effect on the conductivity of PICA, and at temperatures below 2000°F, PICA has a thermal conductivity of about 2.56 Btu-in/hr-ft^2-°F. As the temperature increases to 5000°F, the thermal conductivity reaches as high as 11.91 Btu-in/hr-ft^2-°F. It is interesting to note that the thermal conductivity of PICA is a factor of two lower than that of the original Fiberform (10.6 lbm/ft^3 on fig. 6) at higher temperatures, and is almost equal to that of the Fiberform of the same density (14.4 lbm/ft^3 on fig. 6). The presence of phenolic reduces the pore size within the matrix and thus reduces the radiation term in the heat transfer balance equation. This result is consistent with internal radiative heat transfer theory.

b. Thermogravimetric Analysis (TGA)

Thermogravimetric analysis measures the mass change of a decomposing material as a function of temperature at a constant heating rate. The decomposition temperature and the char yield of the polymer can be determined from this analysis. TGA analysis on post-test samples provides insight into the amount of pyrolysis that occurred through the thickness of the material.

Figure 10 shows the char yields obtained from TGA for the phenolic resin tested in argon. Typically, phenolic has about 50–60% char yield depending on the relative degree of cross-linking of the molecules. As shown in figure 10, the phenolic begins to pyrolyze at about 300°F, and the pyrolysis is complete at 1400°F, yielding a char residue of 62.563%. Figures 11(a) and (b) show the decomposition process for PICA in argon and in air at a heating rate of 20°/min. In both air and argon, the weight loss begins at approximately 700°F and is completed at about 1300°F for the argon case, and 1500°F for the air case. In argon, the weight loss in PICA exhibits a smooth transition and yields a char residue of 78.472%. In air, the weight loss of PICA consists of two stages. The first stage, from 500°F to 1100°F, is weight loss due to gas pyrolysis of phenolic and is consistent with that observed in argon. The second stage is due to the oxidation of the carbonaceous char which is complete at 1500°F.

2. Mechanical Properties Measurements

The tensile strength of PICA-15 was measured in the transverse and in-plane directions, and the compressive strength is currently being studied.

Tensile strength of PICA-15 in both transverse and in-plane directions was measured by using the Instron 1211. The transverse direction is defined as the casting direction, which is perpendicular to the ablating surface, and the in-plane direction is parallel to the ablating surface. Fifteen one-inch cube samples were measured for each direction to give the average values, standard deviations, and the coefficient of variation listed in table 2. Coefficient of variation is defined as the ratio of standard deviation to the mean value. Figures 12 and 13 show the typical stress–strain curves of PICA-14 in both transverse and in-plane directions, respectively. As expected, PICA is quite brittle, and the failure strain is less than 1.0%, and the failure strain in the transverse direction is a factor of two higher than that of the in-plane direction. The tensile strength of the transverse direction is about one order of magnitude lower than that of the in-plane direction. This behavior is very typical in fibrous materials.

3. High Enthalpy, Hypersonic Flow Environment

a. Facility

An arc-jet test series was conducted in the Ames 60 megawatt (MW) Interaction Heating Facility (IHF). In general, an arc-jet facility uses an electrical discharge to heat a gas stream to a very high temperature. The test gas, which is air for the case of the IHF facility, is heated by an electrical discharge within a 3.15 inch diameter constrictor column (ref. 4). The heated gas is then supersonically expanded through a converging-diverging, 13 inch diameter conical nozzle exit , and discharged into an evacuated test chamber where the test model is

mounted onto a swing arm. The resulting highly energetic, or high enthalpy, flow can simulate the aerothermodynamic heating environments experienced by space vehicles during planetary entry or earth re-entry. The IHF can produce enthalpies approaching 20,000 Btu/lbm and velocities up to Mach 8.

Calibration tests were first performed to determine the heat fluxes and stagnation pressures at given facility conditions. Heat fluxes and stagnation pressures were varied by adjusting the facility current, air pressure, and test model distance from the nozzle exit. A four-inch flat faced copper calibration probe, shown in figure 14, was instrumented with two slug calorimeters to measure the heat fluxes, and a pressure port to measure the stagnation pressures. For test conditions that required high stagnation pressures at lower heat fluxes, cold air was injected downstream of the arc heater. This "add air" condition increases the total chamber pressure, and in turn, increases the stagnation pressure on the test model. Several calibration runs were conducted at each test condition to verify repeatability and to obtain statistical data. Since heat flux is dependent on the model nose radius, the data obtained from the calibration probe was related to each model size through a simplified Fay-Riddell equation (ref. 5):

$$\dot{q}_{hemi} = C\sqrt{P_{t2} / R_n} \qquad (1)$$

where $\dot{q}_{hemi}$ is the heat flux in Btu/ft^2-s on a hemispherical surface, P_{t2} is the stagnation pressure, R_n is the nose radius of the test model, and C is the total heat transfer coefficient. Stewart's correlation (ref. 6) is then used to relate the hemispherical surface to the flat faced cylinder of the same base radius:

$$\dot{q}_{FF} = 1.87\,\dot{q}_{hemi} \qquad R_n = R_b \qquad (2)$$

Table 3 shows the calibration data from the calibration probe and the resulting heat fluxes for each test model size. The facility current, arc chamber air pressure (P_{ch}), total pressure (P_t, includes P_{ch} and "add air" pressure), and calorimeter position (x) are listed in the facility conditions section of table 3. The stagnation pressure and cold wall heat flux, $\dot{q}_{cal}$, are the measurements taken from the calibration probe. The remaining columns are the resulting heat fluxes on the various model sizes. The correlation of equation 2 is only valid if the R_c/R_b ratio is less than 0.31, where R_c is the corner edge radius and R_b is the base radius of the model (ref. 7).

The stagnation point, cold wall heat flux on models with diameters less than 4.0 inches was corrected for the effect of corner radius, as shown in the last three columns of table 3. Zoby and Sullivan (ref. 7) developed a scheme to determine the effect of corner radius on stagnation-point velocity gradients on blunt bodies at 0° angle of attack. The blunt bodies used in their studies consisted of a range of ratios of body radius to nose radius, R_b/R_n, from 0.0 (flat-faced cylinder) to 1.0 (hemisphere), and ratios of corner radius to body radius from 0.0 (sharp) to 0.3. The results from Zoby's studies were used to calculate the effective radius for each model size since the heat flux is proportional to the square root of the velocity gradient.

b. Test Models

Test models of various shapes and sizes, as shown in figure 15, were produced to allow testing in a wide range of cold wall heat fluxes. Still photographs, video during tests, weight, and thickness measurements were taken at pre- and post-test for each model. The thickness measurement used a height gage and a template, shown in figure 16, to ensure that the measurements were taken at the same points on the model surface before and after testing. The thickness of the cylindrical-shaped test models was measured with a caliper due to its geometry. Most models were instrumented with one to three K-type thermocouples to measure the in-depth temperature response of the material during test and during the cool-down period. Surface temperatures were measured by two 2-color optical pyrometers; one was mounted inside the test chamber, and the other was outside the test chamber. The pyrometer outside of the test chamber viewed the test model's surface by way of a gold mirror, through a quartz viewing window; therefore, the temperature obtained from the outside pyrometer requires a correction for window transmission losses.

4. Material Thermal Response Modeling

The material thermal response model was generated using the Charring Materials Analysis code (CMA) from Aerotherm Corp. The thermal model was validated with thermocouple data from the arc jet testing. The results of the analysis consist of the B-prime table, effective thermal conductivity, effective specific heat, and decomposition kinetics of PICA. The CMA analysis uses the reaction rate information obtained from the TGA curves and XPS of the char to generate the input deck and B-prime curves. The measured thermal conductivity and thermocouple data from the arc jet testing are used in the fine adjustment and validation of the thermal model. A set of effective thermal properties and B-prime curves are generated once the model is validated.

5. X-ray Photoelectron Spectroscopy (XPS)

Elemental composition analysis of virgin PICA and a charred sample was performed using X-ray Photoelectron Spectroscopy (XPS). XPS measures the kinetic energy of

photoelectrons produced from a single x-ray source. The kinetic energy, E_{KE}, is then used to calculate the binding energy, E_{BE}, using the following equation:

$$E_{BE} = h\upsilon - E_{KE} - \Phi \quad (3)$$

XPS survey yields elemental compositions and bonding information to enable determination of composition and compound characteristics of materials.

6. Infrared (IR) and Ultraviolet (UV) Spectrophotometry[3]

The spectral hemispherical reflectance of virgin and charred PICA specimens was measured at room temperature over a wavelength range of 0.25 μm to 18 μm. A Perkin-Elmer Lambda-9 spectrophotometer was used for measurements from 0.25 μm to 2.5 μm and a BIORAD FTS-40 spectrophotometer was used for measurements from 2.5 μm to 18.0 μm.

Results and Discussion

1. Arc-Jet Test Results

Test conditions are tabulated in table 4 and test results, shown in table 5, are arranged in order of increasing heat flux and stagnation pressure. The density of each test sample is listed, as well as pre- and post-test measurements of weight and sample thickness. The resulting mass loss and stagnation point recession were then calculated and are also listed in table 5. Average recession values are the average of all recession points obtained from the template. The recession on the outer edge of the model surface is higher than that of the stagnation region due to higher heating and shear stress on the corner edge of the flat faced cylinder. Surface temperatures, measured by the optical pyrometers, are also reported in table 5. The effective heat of ablation, H_{eff}, is included in the table to evaluate the performance of each material and is normalized to the virgin density. The effective heat of ablation is defined as follows (ref. 1):

$$H_{eff} = \frac{\dot{q}_{cw}}{\dot{s}\rho_v} \quad (4)$$

where $\dot{q}_{cw}$ is the stagnation point cold wall heat flux, $\dot{s}$ is the recession rate (average recession divided by test time), and ρ_v is the density of the virgin PICA sample.

[3]Estimation of temperature dependent emittances for PICA. Analysis and measurements were done by Jochen Marschall of Thermosciences Institute at Ames Research Center.

a. Standard PICA samples

Test results of standard PICA samples can be divided into three different regimes. In the first regime, at a cold wall heat flux range of 300 to 400 Btu/ft^2-s, as shown in table 5, the ablation performance is oxidation rate controlled. The recession, caused primarily by oxidation, is evident by the decreasing trend of the effective heat of ablation as the stagnation pressure increases. In this heating range, the higher the stagnation pressure, the higher the concentration of oxygen atoms diffusing into the boundary layer, therefore the higher oxidation rate and thus a higher surface recession.

At heating rates above 400 Btu/ft^2-s, up to 1400 Btu/ft^2-s, the ablation characteristic of PICA is diffusion controlled, and the main mechanism of heat rejection is re-radiation. The material becomes more efficient with increasing stagnation pressure, and is evident by the increasing trend in H_{eff}. Figure 17 shows the effective heat of ablation as a function of cold wall heat flux for standard PICA at stagnation pressures from 0.11 to 0.43 atm. The H_{eff} curve shows that PICA is most efficient at a heating rate range of 1200 to 1800 Btu/ft^2-s at 0.43 atm. Due to arc jet facility limitations, it was not possible to test PICA material at stagnation pressures above 0.43 atm. Major modification to the facility is required to accomplish such testing.

The third regime, sublimation rate controlled, occurs at heating rates above 1800 Btu/ft^2-s where the surface recession is primarily due to sublimation of the carbon. The surface temperature at this heating range is extremely high, such that the carbon fibers at the surface begin to sublime, thus contributing to the high recession. It is interesting to note that H_{eff} at these heating rates is still significantly higher than that of the oxidation regime.

Visual inspection of models at post test shows no sign of spallation, i.e., the recessed surface is very smooth, including the corner edge where the heating rate and shear stress is almost double that of the stagnation region (ref. 8). Appendix E shows two examples of the pre- and post-test condition the PICA models.

Figure 18 shows the in-depth temperature response for a standard PICA sample at 500 Btu/ft^2-s, 0.42 atm stagnation pressure, and a total heat load of 12,500 Btu/ft^2. Surface temperature, measured by the optical pyrometer and corrected for actual material emissivity and transmission losses due to the viewing window and mirror, is plotted on the primary y-axis. In-depth temperatures, measured by thermocouples, are plotted on the secondary y-axis. Thermocouple locations were measured more precisely after testing, and actual locations are labeled on the plots. While the surface temperature is approaching

5000°F, approximately 0.5 inch from the surface the temperature peaks at about 1800°F. Even more dramatic is that at 1.2 inches from the surface, the temperature peaks at only 700°F, and at 1.6 inches from the surface, the temperature reaches only 300°F after 270 seconds. These results demonstrate the fairly good insulative properties of PICA, and indicate that most of the heat is rejected by reradiation. Figure 18 also shows that PICA has a very low heat capacity and since the material has 85% porosity, the heat is being rejected at the surface rather than stored in heat conduction. This thermal response result shows that PICA could be directly bonded to the structure of a vehicle without additional insulation, and complex heat shield ejection is not required for planetary entry missions. In most cases, the ablative heat shield is directly bonded to the spacecraft structure; however, additional thickness of the heat shield is used to maintain the desirable structure temperature. PICA thickness could be minimized due to its good in-depth thermal response. As shown in table 4, the same instrumentation scheme was used for other models at other test conditions, and the in-depth temperature responses for these models are included in Appendix A.

b. Surface densified PICA samples

Surface densification was performed on several PICA samples in an attempt to improve the ablation characteristics of PICA at high stagnation pressure test conditions without significantly increasing the overall density of PICA. The first four surface densified PICA samples were produced with different densification methods (shown in table 1) to determine the best composition. These four samples were tested at 575 Btu/ft^2-s for 25 seconds, and the result, shown in table 5, shows a variation in both surface recession and H_{eff}. A similar trend of ablation characteristics is observed for the surface densified PICA where the material is most efficient at heating rates above 1200 Btu/ft^2-s. Figure 19 shows that H_{eff} peaks at about 1200-2100 Btu/ft^2-s, and has not yet shown any signs of failure due to spallation.

A comparison of in-depth temperature responses is shown in figure 20 for standard and surface densified PICA samples at 750 Btu/ft^2-s, 0.43 atm stagnation pressure, and a total heat load of 18,750 Btu/ft^2. The surface temperature of the densified sample is approximately 4800°F, slightly less than standard PICA, and at 1 inch from the surface, the densified sample in-depth temperature peaks around 540°F, 125 degrees less than the standard PICA. At 1.5 inches from the surface, the densified sample temperature reached 335°F, approximately 15 degrees less than the standard PICA sample. These temperature profiles of standard PICA and surface densified PICA show a small difference in the in-depth temperature response between the two materials. It is perhaps due to a relatively thin layer of densification (0.25 inch depth) which absorbs more energy to pyrolyze the additional phenolic and thus allows less energy to penetrate into the model. In addition, the charred surface is being densified by the pyrolysis of the phenolic and thus reduces hot gas ingestion, or in-flow, which would influence the in-depth thermal response. More thermal response and ablation data for surface densified PICA will be obtained in future arc jet tests.

Additional in-depth thermal responses of other surface densified PICA samples, tested at a wide range of heat fluxes, are included in Appendix B. Visual inspection of the surface of the post-test models indicates that the surface densified PICA has a smoother surface than that of standard PICA. This observation is expected since the densified PICA has a higher loading of phenolic, which deposits a high char residue at the surface.

c. Carbon Fiberform samples

Several samples of the carbon substrate were tested to compare against the PICA samples at similar conditions. Figure 21 shows the performance of the carbon samples as a function of cold wall heat flux at various stagnation pressures. The H_{eff} drastically decreases at heating rates above 1200 Btu/ft^2-s where the carbon Fiberform exhibits mechanical failure. The carbon samples burned through at 750 Btu/ft^2-s and 0.34 atm stagnation pressure, and at 1200 Btu/ft^2-s and 0.34 atm stagnation pressure. The Fiberform does not have sufficient strength to withstand the high stagnation pressures, and thus recessed considerably at low heating and stagnation pressure conditions.

The carbon Fiberform test samples were instrumented with one thermocouple, and figure 22 shows an example of the carbon Fiberform tested at 1225 Btu/ft^2-s, 0.23 atm stagnation pressure, and a total heat load of 24,500 Btu/ft^2. At 1.5 inches from the surface, the temperature peaks at about 600°F. The low surface temperature measurement was due to the misalignment of the pyrometer. This in-depth thermal response demonstrates the effect of internal radiative heat transfer, mentioned above, on the thermal conductivity of carbon Fiberform. As expected, the ablating surface of the undamaged Fiberform samples was significantly rougher than that of the PICA.

d. Avcoat-5026 sample

Because of the limited supply of Avcoat and the fact that it is no longer commercially manufactured, only one sample of the material was tested to compare with PICA. Avcoat is the ablative material used as the forebody heat shield on the Apollo. The Avcoat sample was tested at a

very high heating condition; a cold wall heat flux of 2960 Btu/ft^2-s, a stagnation pressure of 0.43 atm, and a total heat load of 29,600 Btu/ft^2. Avcoat material was previously tested at lower heating rates (ref. 1), and a PICA sample was also tested at one of these conditions for comparison purposes. The Avcoat sample had a higher recession rate than the PICA material and thus its effective heat of ablation was approximately 32% of the PICA material.

To achieve the very high heating condition, the geometry of the model was limited to a 0.500 inch radius cylinder with a hemispherical nose. This geometry limits the instrumentation schemes, and thus, the thermocouple locations of the Avcoat model were not identical to that of the PICA models. The surface temperature of the Avcoat sample, as shown in figure 23, is approximately 800°F less than the surface temperature of the PICA sample tested at the same condition, due to the high blowing rate and high thermal conductivity of the Avcoat material.

2. Computational Material Response Using CMA

A material thermal response model for PICA was generated from CMA93. CMA is typically used to model one-dimensional transient transport of thermal energy in a three-dimensional isotropic material which can ablate at the surface, and can decompose in-depth. The material's preliminary physical, thermal, and optical property measurements are used to generate an input deck (included in Appendix C), and arc jet testing data is used to validate the thermal model. The thermal response model includes the B-prime table, effective thermal conductivity, effective specific heat, and decomposition kinetics. The validated thermal response model is then used in calculating the required thickness of the heat shield. Figures 24(a) and (b) are the resulting effective thermal conductivity and effective specific heat of virgin PICA and the char. As shown in figure 24(a), the thermal conductivity of virgin PICA is initially lower than that of the charred PICA, and the trend crosses over at 3100°F. This thermal response is expected since the char consists of highly conductive graphite material (see XPS analysis section below) whereas the loading of the phenolic resin in the virgin PICA reduces the pore size and thus reduces the internal radiation effect. Above 3100°F, the phenolic within the PICA layer pyrolyzes and becomes charred. However, in most analyses, the thermal conductivity of PICA is only valid at temperatures below 2000°F. Figure 24(a) also shows that the measured thermal conductivity is lower than that obtained from CMA. Figure 25 shows the B prime curves for char and gas pyrolysis at several pressures. As expected, the B prime curves shift to the right as the pressure decreases.

3. Thermogravimetric Analysis (TGA)

As an aid to understanding the thermal response and ablation characteristics of PICA, a few post-test PICA models were sectioned for further analysis. Figure 26 illustrates different regions in a cross-sectioned post-test PICA sample (PICA-M2-7) tested at 1065 Btu/ft^2-s, 0.34 atm stagnation pressure, and a total heat load of 26,625 Btu/ft^2. Material was removed at five stations and analyzed with TGA. Resin content, Re(%), for each station was calculated based on the total mass loss from the TGA results and is defined as follows:

$$\mathrm{Re}(\%) = \frac{m_r}{m_p} \times 100 \qquad (5)$$

where m_r is the mass loss of the sample, or mass removal, and m_p is the mass loss of pyrolyzed phenolic resin. The resin content at each of the five locations is shown in figure 27. The char interface is very thin compared to that of the pyrolysis interface. A sample from the pyrolysis region, approximately 0.4 inch from the surface, has a 6.1% resin content, and the pyrolysis/virgin sample, at approximately 0.75 inch from the surface, has a 23.7% resin content. The resin content reported for the station #5 was measured at 38.8%, which is consistent with the TGA results shown in figure 11(a). Thickness of the char and pyrolysis zones are estimated to be 0.12 inch and 0.6 inch, respectively. The thick pyrolysis zone is perhaps due to PICA's high porosity which allows pyrolysis gas to percolate to the front surface. Gas percolation is one of the primary advantages in heat rejection for ablative heat shield materials.

4. X-ray Photoelectron Spectroscopy (XPS)

X-ray Photoelectron Spectroscopy (XPS) analysis was conducted by Charles Evans & Associates to obtain the elemental composition of small samples from PICA-M2-7, which was tested at 1065 Btu/ft^2-s, 0.34 atm stagnation pressure, and a total heat load of 26,625 Btu/ft^2. The XPS analysis was performed on the char and the virgin portions of the sample. As shown in table 6, the char was almost entirely carbon, and the virgin sample was predominantly carbon, with some oxygen, nitrogen, and silicone. The presence of silicone was due to contamination from the machining of the samples for analysis.

5. Infrared (IR) and Ultraviolet (UV) Spectroscopy

Infrared (IR) and Ultraviolet (UV) reflectant spectra were obtained for some of the post-test samples and IR results are included in the Appendix D. A Perkin-Elmer Lambda-9 spectrophotometer was used for measurements

from 0.25 μm to 18 μm and a BIORAD FTS-40 spectrophotometer was used for measurements from 2.5 μm to 18.0 μm. Measured reflectances were converted to emittances using the expression

$$\varepsilon(\lambda, T_R) = 1 - \rho(\lambda, T_R) \tag{6}$$

which is valid for a diffusely irradiated opaque surface in thermal equilibrium with its surroundings at a temperature T_R. The temperature dependence of the wavelength integrated hemispherical emittance is estimated by averaging the room temperature spectral emittance values over the Planck distribution function at temperature T, i.e.,

$$\varepsilon(T) = \frac{\int_{\lambda_l}^{\lambda_u} \varepsilon(\lambda, T_R) e_{\lambda b}(\lambda, T) d\lambda}{\int_{\lambda_l}^{\lambda_u} e_{\lambda b}(\lambda, T) d\lambda} \tag{7}$$

Here λ_l and λ_u are, respectively, the lower and upper limits of the wavelength range over which $\rho(\lambda, T_R)$ was measured and $e_{\lambda b}(\lambda, T)$ is the Planck distribution. This estimation procedure assumes that the spectral hemispherical reflectance is a weak function of temperature and that the dominant contribution to the temperature dependence of hemispherical emittance arises from the wavelength weighting of the Planck function. Planck's distribution was used to calculate the emissivity as a function of temperature and is shown in figure 28. The emittance of the virgin PICA is 0.805 at room temperature and increases to 0.9 at 3000°F, at which PICA is charred. The emittance of the char is 0.91 and decreases with temperatures to 0.89.

Conclusion

An extensive arc-jet test series was conducted to further investigate the newly developed PICA material. The thermal performance and ablation characteristics were observed from testing in a wide range of cold wall heat fluxes, stagnation pressures, and total heat loads. Several material characterization tests were also performed to investigate various properties of the virgin and charred PICA material.

Figure 29 summarizes the thermal performance of PICA, surface densified PICA, Fiberform, and Avcoat materials as a function of cold wall heat fluxes. The effective heat of ablation of surface densified PICA is about factor of two higher than that of PICA and is an order of magnitude higher than that of Avcoat material. The Fiberform performed poorly; especially where the stagnation pressure exceeded 0.3 atm regardless of the heating rates. The ablation characteristic of PICA is very uniform, and no spallation occurred at pressures as high as 0.43 atm. In-depth temperature profiles reveal fairly good insulative properties and show that PICA heatshield thickness could be minimized due to its good in-depth thermal response.

Surface densification of PICA showed promising improvement over standard PICA, in terms of surface recession. Testing of surface densified PICA shows lower surface temperatures, less recession, and thus higher effective heats of ablation. In-depth thermal response of densified PICA showed a small difference when compared to standard PICA, which is consistent with the fact that the surface densification only affects the surface properties and performance. This improvement could be significant for future far-planet discovery missions where surface pressures could reach as high as 10 atm and heating rates above 1500 Btu/ft^2-s. Surface densified PICA and standard PICA offer great weight savings over conventional ablators, i.e., Avcoat and carbon-phenolic, due to their low density, low thermal conductivity, and high effective heat of ablation. These new materials offer a weight savings of more than 50% over the traditional ablators, and that savings could be directly translated to an increase in scientific payload.

References

1. Tran, H. K.: Development of Lightweight Ceramic Ablators and Arc Jet Test Results. NASA TM-108798, Jan. 1994.

2. Marceldekker, Inc.: Ablative Plastics. G. F. D'Alelio and J. A. Parker, eds., 1971, pp. 392–396.

3. Fiber Materials, Inc.: LCA Final Report. FMI Contract NAS2-13982 deliverable, July 1994.

4. Balter-Peterson et al.: Arc Jet Testing in NASA Ames Research Center Thermophysics Facilities. AIAA Paper 92-5041, AIAA Fourth International Aerospace Planes Conference, Dec. 1–4, 1992.

5. Fay, J. A.; and Riddell, R. R.: Theory of Stagnation Point Heat Transfer in Dissociated Air. J. Aeronaut. Sci., vol. 25, no. 2, 1958.

6. Stewart, D. A.; and Kolodziej, P.: Heating Distribution Comparison Between Asymmetric Blunt Cones. AIAA Paper 86-1307, June 1986.

7. Zoby, E.; and Sullivan, E.: Effects of Corner Radius on Stagnation-Point Velocity Gradients on Blunt Axisymmetric Bodies. NASA TM X-1067, Mar. 1965.

8. Smith, A. M. O.; and Clutter, D. W.: Machine Calculation of Compressible Boundary Layers. AIAA J., vol. 3, no. 4, Apr. 1965, pp. 639–647.

Table 1. Surface densified PICA composition

Model ID	Fiberform density, lb_m/ft^3	Final density, lb_m/ft^3	Surface densification (tip density/thickness), $lb_m/ft^3/in.$
PICA-M3-28D	9.560	18.280	63.23 / 0.125
PICA-M3-29D	9.380	18.020	63.38 / 0.125
PICA-M3-30D	9.540	16.700	60.53 / 0.125
PICA-M3-31D	9.620	16.760	58.22 / 0.125
PICA-M3-13D	11.666	23.160	46.80 / 0.25
PICA-M3-21D	11.514	22.497	47.04 / 0.25
PICA-M2-D1	10.764	22.104	46.70 / 0.25
PICA-M5-28D	8.550	20.893	55.32 / 0.25
PICA-M5-29D	8.680	21.290	46.74 / 0.25
PICA-M4-B-D	10.777	21.880	52.40 / 0.50

Table 2. Average tensile strength of PICA-14

PICA direction	Transverse	In-plane
Average tensile strength, lbf	32.9	221.8
Standard deviation, lbf	3.223	27.50
Coefficient of variation	0.098	0.124
Average modulus, Psi $\times 10^3$	3.100	62.350
Standard deviation, Psi $\times 10^3$	0.198	5.690
Coefficient of variation	0.064	0.0956
Average strain of failure, %	0.921	0.442
Standard deviation, %	0.101	0.0649
Coefficient of variation	0.11	0.147

Table 3. Calibration data

Current (amps)	P_{ch} (psia)	P_{tot} (psia)	Position (in.)	P_{t2} (atm)	$\dot{q}$ (4 in. cal) (Btu/ft^2-sec)	$\dot{q}$ (4 in. D) model	$\dot{q}$ (3 in. D) model	$\dot{q}$ (3 in. D) R_c corr*	$\dot{q}$ (2 in. D) R_c corr	$\dot{q}$ (1 in. D) R_c corr
2300	73	115	9	0.30	300	300	350	425	669	1044
2300	73	115	4	0.43	375	375	400	533	837	1305
2500	47	47	6	0.42	500	500	575	710	1116	1740
3200	101	101	14	0.21	450	450	500	639	1000	1566
4000	105	105	8	0.29	550	550	600	781	1225	1914
4500	115	115	4	0.43	750	750	900	1065	1674	2610
5500	52	52	14	0.11	400	400	450	568	893	1392
6000	115	115	14	0.23	550	550	600	781	1225	1914
6000	115	115	8	0.34	750	750	850	1065	1675	2610
6000	115	115	4	0.43	850	850	1000	1200	1900	2960

*R_c corr: corrected for model corner radius.

Table 4. Test conditions

60 MW IHF Lightweight Ceramic Ablator test											
Model ID	Diam in.	Density lb_m/ft^3	Run no./ date	Current amp	P_{ch} psia	P_{tot} psia	$\dot{q}$ Btu/ ft^2-s	P_{t2} atm	x* in.	Time sec	T/C loc (from surface) in. (nominal)
PICA-M3-10	3.978	15.933	63/4-18-95	2300	73	115	375	0.43	4	25	1.0**
PICA-M3-8	3.997	17.039	34/3-14-95	5500	50-53	50-53	400	0.11	14	25	N/A
PICA-M2-6	3.004	16.045	61/4-18-95	2300	73	115	425	0.30	9	25	0.25, 0.5, 0.75
PICA-M3-11	3.993	15.875	37/3-14-95	3200	100-102	100-102	450	0.21	14	25	N/A
PICA-21G-PS	4.001	15.260	61/10-3-95	2500	47-48	47-48	500	0.42	6	25	0.5, 1.0, 1.5
PICA-M3-12	3.982	15.591	34/7-27-95	2500	47-48	47-48	500	0.42	6	11	0.5, 0.75
PICA-M3-9	3.992	15.719	42/3-16-95	4500	115-117	115-117	750	0.43	4	25	1.0, 1.5
PICA-M3-14	3.997	15.830	73/4-24-95	6000	115-117	115-117	850	0.43	4	22	1.0
PICA-M1-1	2.007	16.185	38/3-15-95	3200	102	102	1000	0.21	14	25	1.0**
PICA-M2-7	3.003	15.978	40/3-15-95	6000	115	115	1065	0.34	8	25	1.5
PICA-M2-5	3.010	16.555	71/4-20-95	6000	115	115	1200	0.43	4	17	0.25, 0.5, 0.75**
PICA-M5-26	2.004	16.040	47/3-20-95	6000	115-117	115-117	1675	0.34	8	17	1.5
PICA-M1-2	2.001	15.840	64/4-18-95	4500	115	115	1675	0.43	4	17	1.0
PICA-M6-27	2.007	16.175	46/3-20-95	6000	116-117	115-117	1900	0.43	4	14	1.5
PICA-M4-A	1.006	16.001	50/3-21-95	6000	115-117	115-117	2960	0.43	4	10	2.5
PICA-M3-28D	3.000	18.280	56/9-27-95	2500	47-48	47-48	710	0.42	6	25	N/A
PICA-M3-29D	3.000	18.020	59/10-2-95	2500	47-48	47-48	710	0.42	6	25	0.5, 1.0, 1.5
PICA-M3-30D	3.000	16.700	60/10-3-95	2500	47-48	47-48	710	0.42	6	25	0.5, 1.0, 1.5
PICA-M3-31D	3.000	16.760	58/10-2-95	2500	47-48	47-48	710	0.42	6	25	0.5, 1.0, 1.5
PICA-M3-13D	3.990	23.160	43/3-16-95	4500	115-117	115-117	750	0.43	4	25	1.0, 1.5
PICA-M3-21D	3.991	22.497	74/4-24-95	6000	115-117	115-117	850	0.43	4	22	1.0
PICA-M2-D1	3.006	16.005	44/3-17-95	6000	115	115	1200	0.43	4	17	1.0, 1.5
PICA-M5-28D	1.989	20.893	45/3-17-95	6000	115	115	1900	0.43	4	14	1.5
PICA-M5-29D	2.005	21.290	55/3-23-95	6000	115	115	1900	0.43	4	14	1.5
PICA-M4-B-D	1.003	21.880	68/4-19-95	4500	105-107	115-117	2610	0.43	4	10	1.0
CARBON-M3-15	3.967	10.491	35/3-14-95	5500	50-53	50-53	400	0.11	14	25	N/A
CARBON-M3-20	3.992	11.424	41/3-16-95	6000	115	115	750	0.34	8	25	1.0, 1.5
CARBON-M1-16	2.008	11.035	39/3-15-95	4000	105	105	1225	0.29	8	25	1.0
CARBON-M5-30	1.989	10.890	49/3-21-95	6000	115-117	115-117	1225	0.23	14	20	1.5
CARBON-M5-31	2.005	11.079	48/3-20-95	6000	115-117	115-117	1675	0.34	3	17	1.5
AVCOAT-1	0.994	32.000	54/3-23-95	6000	115-117	115-117	2960	0.43	4	10	2.5

*Longitudinal location of model from nozzle exit.
**T/C inoperable during test.

Table 5. Test results

60 MW IHF Lightweight Ceramic Ablator test									
Model ID	Density lb_m/ft^3	$\dot{q}$ Btu/ft^2-s	P_{t2} atm	Test time sec	Mass loss lb_m	Stagnation point recession in.	Average recession in.	Surface temp deg F	H_{eff}** Btu/lb_m
PICA-M3-10	15.933	375	0.43	25	0.054	0.349	0.374	4100	18,879
PICA-M3-8	17.039	400	0.11	25	0.033	0.100	0.119	4500	59,182
PICA-M2-6	16.045	425	0.30	25	0.028	0.307	0.303	4400	26,226
PICA-M3-11	15.875	450	0.21	25	0.031	0.163	0.185	4700	45,967
PICA-21G-PS	15.260	500	0.42	25	0.043	0.147	0.210	4900	46,808
PICA-M3-12	15.591	500	0.42	11	0.024	0.102	0.115	5200	36,811
PICA-M3-9	15.719	750	0.43	25	0.041	0.211	0.255	5100	56,133
PICA-M3-14	15.830	850	0.43	22	0.043	0.203	0.219	5100	64,729
PICA-M1-1	16.185	1000	0.21	25	0.014	0.185	–	4600	100,193
PICA-M2-7	15.978	1065	0.34	25	0.025	0.242	0.262	5500	76,322
PICA-M2-5	16.555	1200	0.43	17	0.022	0.191	0.208	4700	71,092
PICA-M5-26	16.040	1675	0.34	17	0.010	0179	0.191	4400	111,534
PICA-M1-2	15.840	1675	0.43	17	0.013	0.213	–	2800*	101,277
PICA-M5-27	16.175	1900	0.43	14	0.010	0.166	0.193	5000	102,250
PICA-M4-A	16.001	2960	0.43	10	0.004	0.244	–	4500	90,978
PICA-M3-28D	18.280	710	0.42	25	0.038	0.094	0.138	4700	84,435
PICA-M3-29D	18.020	710	0.42	25	0.040	0.115	0.154	4700	76,755
PICA-M3-30D	16.700	710	0.42	25	0.037	0.159	0.212	5000	60,163
PICA-M3-31D	16.760	710	0.42	25	0.038	0.143	0.221	5100	57,506
PICA-M3-13D	23.160	750	0.43	25	0.063	0.110	0.118	4800	82,331
PICA-M3-21D	22.497	850	0.43	22	0.056	0.107	0.115	4800	86,736
PICA-M2-D1	22.104	1200	0.43	17	0.036	0.142	0.100	4900	110,749
PICA-M5-28D	20.893	1900	0.43	14	0.025	0.086	0.098	4600	155,896
PICA-M5-29D	21.290	1900	0.43	14	0.026	0.079	0.095	4700	157,821
PICA-M4-B-D	21.880	2610	0.43	10	0.007	0.087	–	4000*	164,534
CARBON-M3-15	10.491	400	0.11	25	0.013	0.137	0.153	4800	74,761
CARBON-M3-20	11.424	750	0.34	25	0.028	burn-through	–	5600	DNC***
CARBON-M1-16	11.035	1225	0.29	25	0.009	0.371	–	5500	89,766
CARBON-M5-30	10.890	1225	0.23	20	0.007	0.310	0.346	2300*	78,027
CARBON-M5-31	11.079	1675	0.34	17	0.007	burn-through	–	4300	DNC***
AVCOAT-1	32.000	2960	0.43	10	0.009	0.312	–	4000	35,577

*Pyrometer misaligned.

**H_{eff} based on average recession except where no average was taken; then based on stagnation point recession.

***DNC – did not calculate.

Table 6. Elemental compositions and bonding information of char and virgin PICA

Sample	Atomic concentration (%)			
	C	O	N	Silicone
Char	98	1.7	0	0.3
Virgin	79.1	18.2	2.1	0.6

Sample	Carbon % seen as:				
	Graphite	C-C/C-H	C-O	C=O	O=C-O
Char	100	0	0	0	0
Virgin	4.3	48.5	31.6	9.6	2.1

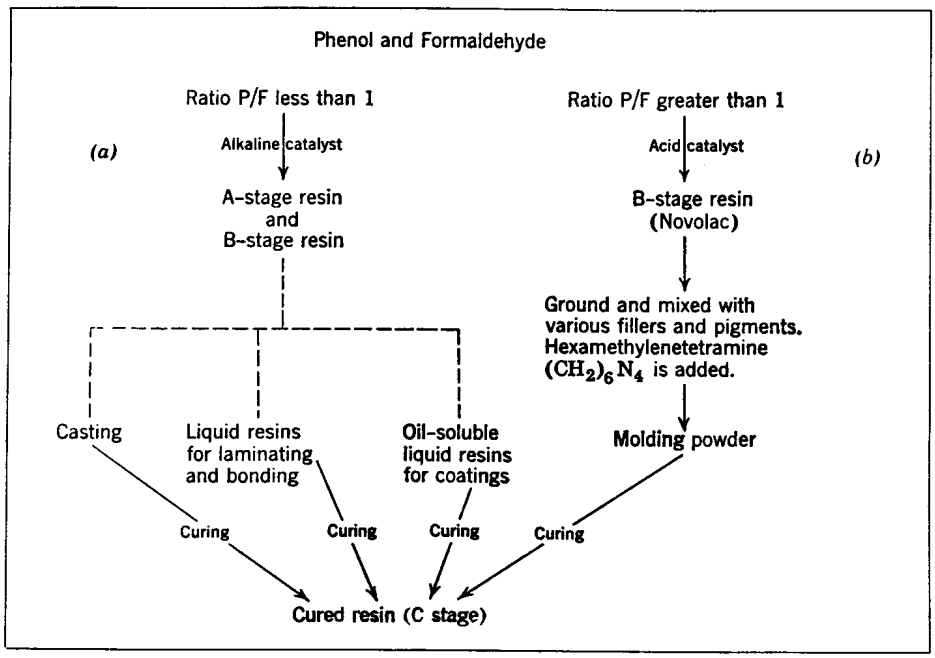

Figure 1. Production of phenol-formaldehyde resins. (a) One-stage process; the reaction is interrupted at A- or B-stage resins to prevent crosslinking. (b) Two-stage process; because of deficiency of formaldehyde (P/F >1), the reaction can be carried out nearly to completion without three-dimensional crosslinking. Final crosslinking is accomplished after application of A- or B-stage resins or molding powder to produce a thermoset material .

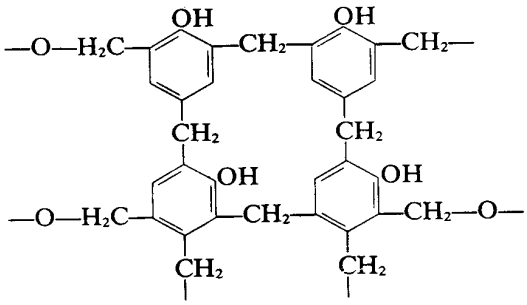

Figure 2. Molecular structure of cured phenolic resins.

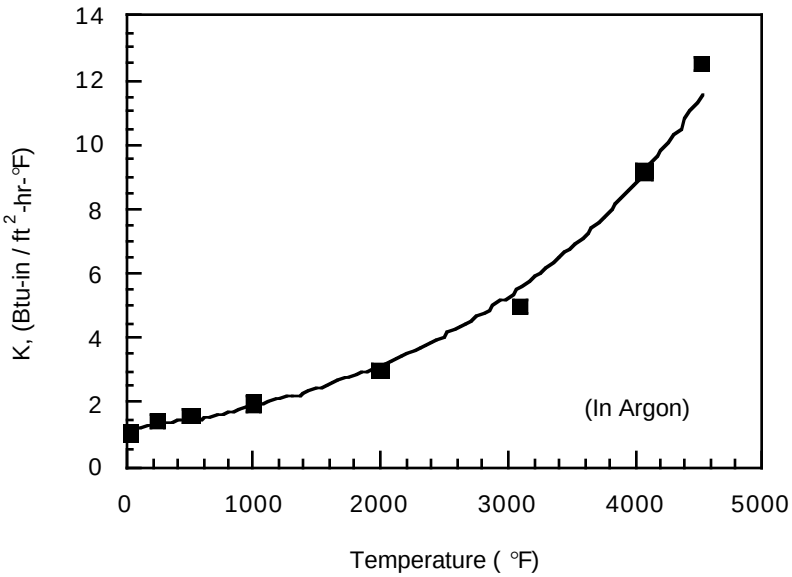

Figure 3. Thermal conductivity of carbon Fiberform.

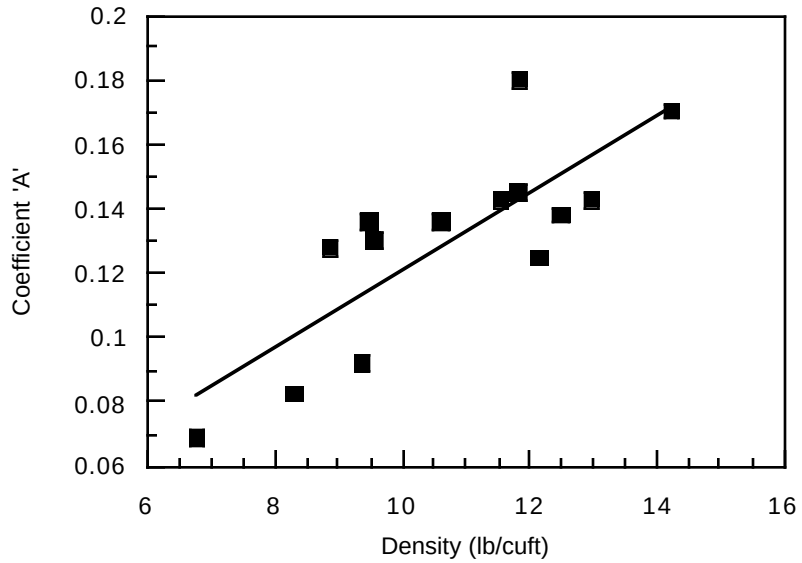

Figure 4. Influence of Fiberform density on the conductivity parameter 'A.'

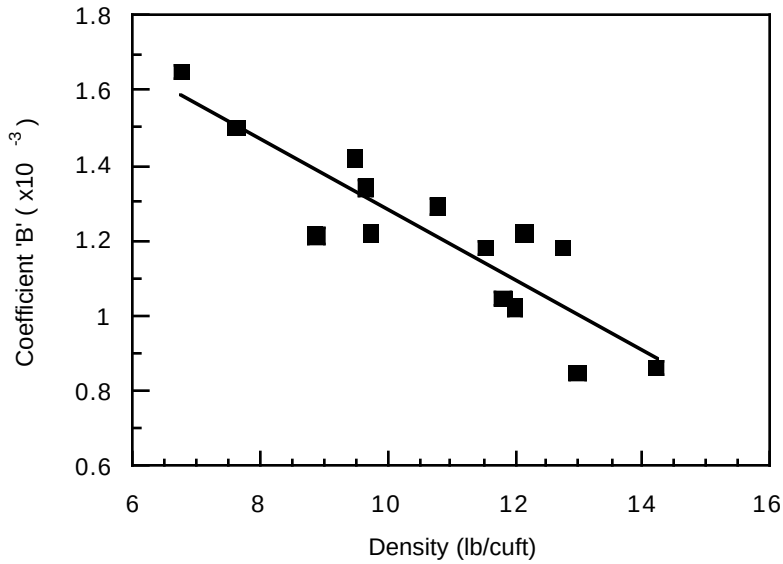

Figure 5. Influence of Fiberform density on conductivity parameter 'B.'

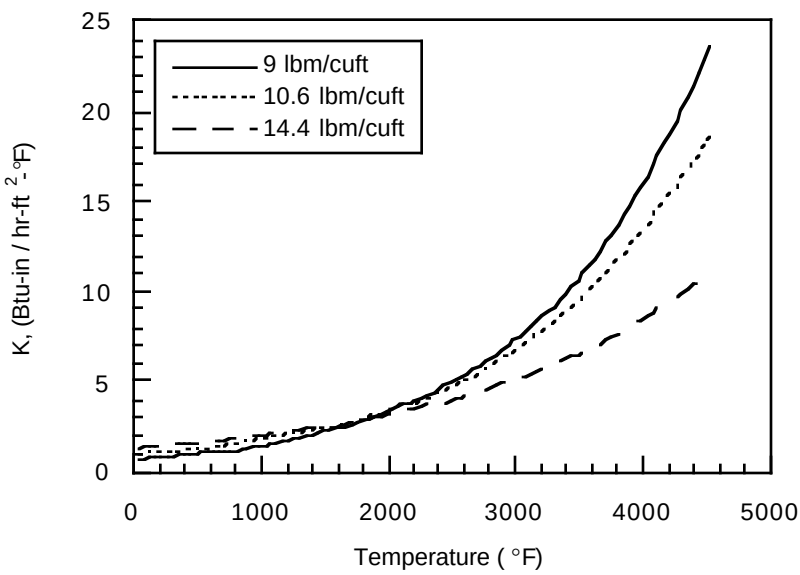

Figure 6. Influence of Fiberform density on thermal conductivity.

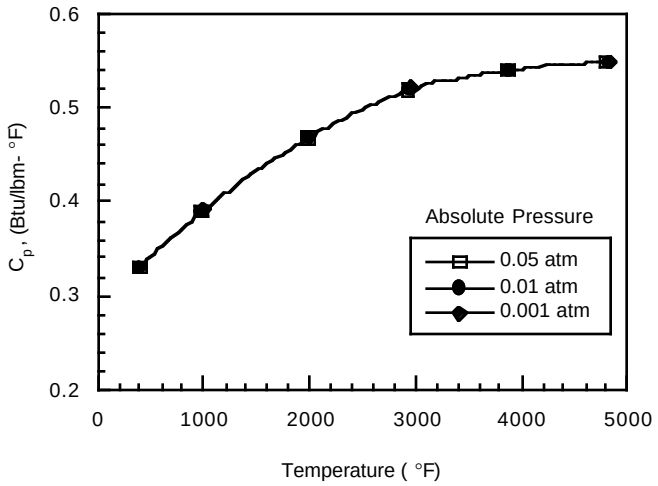

Figure 7. Heat capacity of PICA-15.

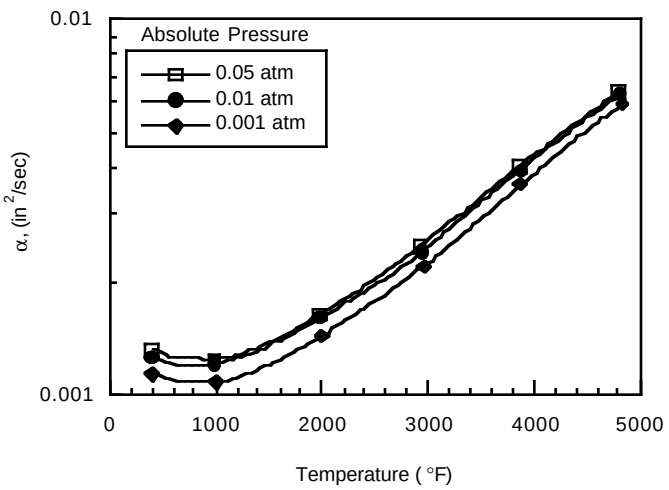

Figure 8. Thermal Diffusivity of PICA-15.

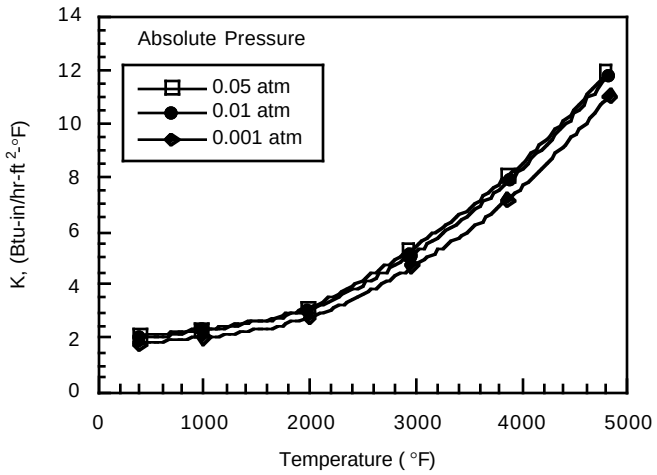

Figure 9. Thermal conductivity of PICA-15.

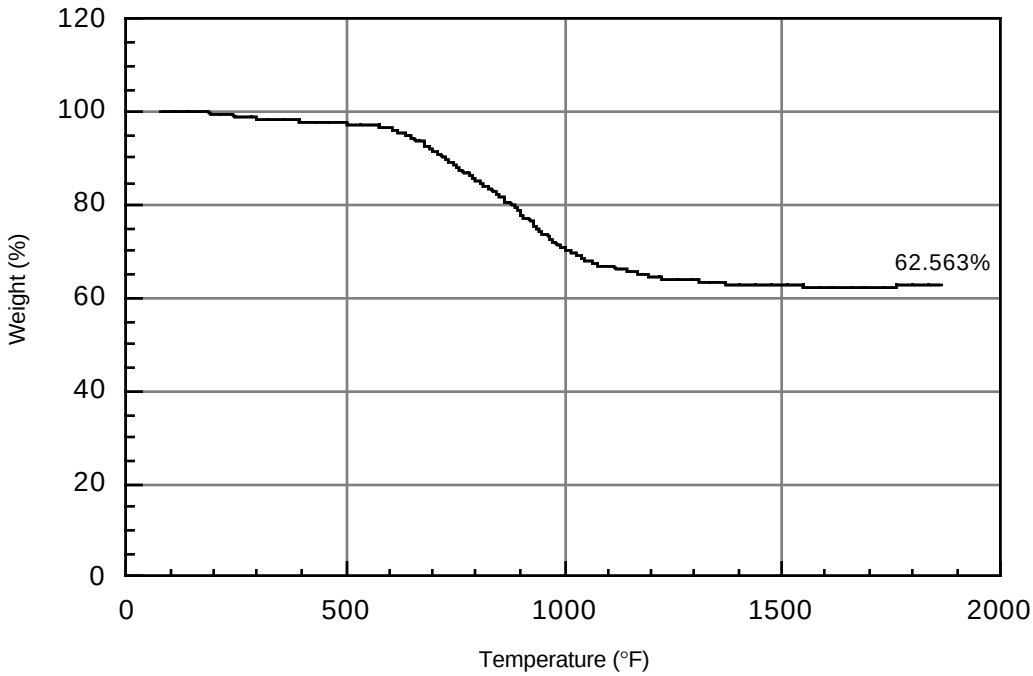

Figure 10. TGA of phenolic in argon.

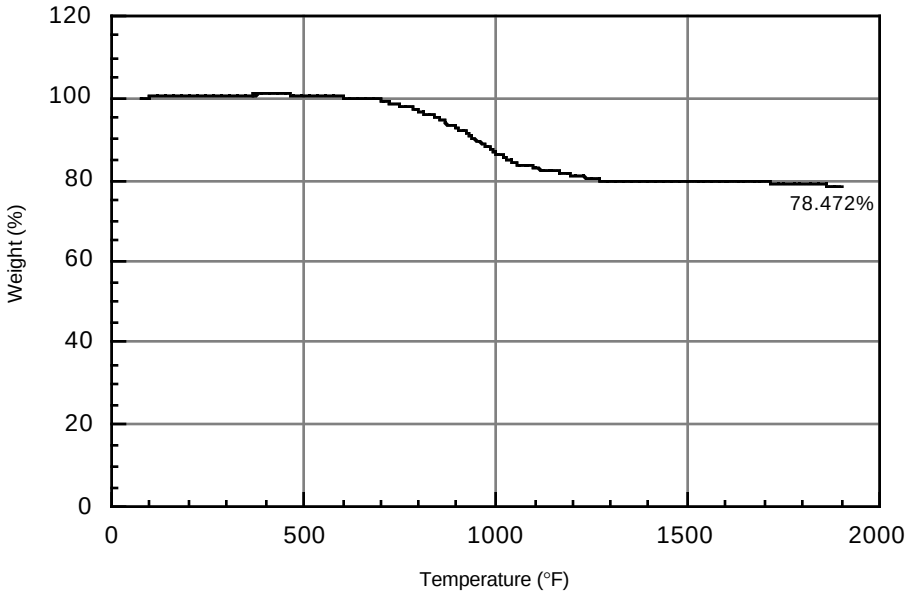

Figure 11(a). TGA of PICA in Argon.

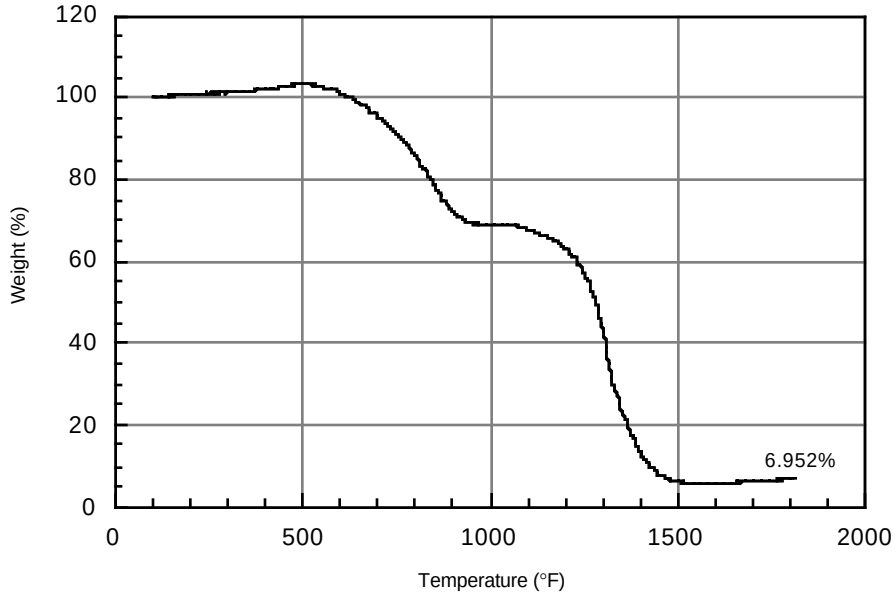

Figure 11(b). TGA of PICA in air.

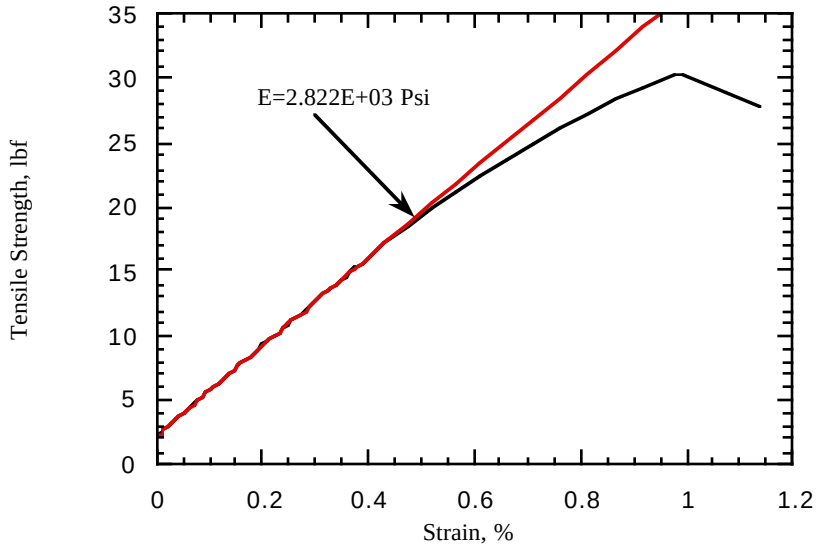

Figure 12. Tensile stress-strain curve of PICA-14 (transverse).

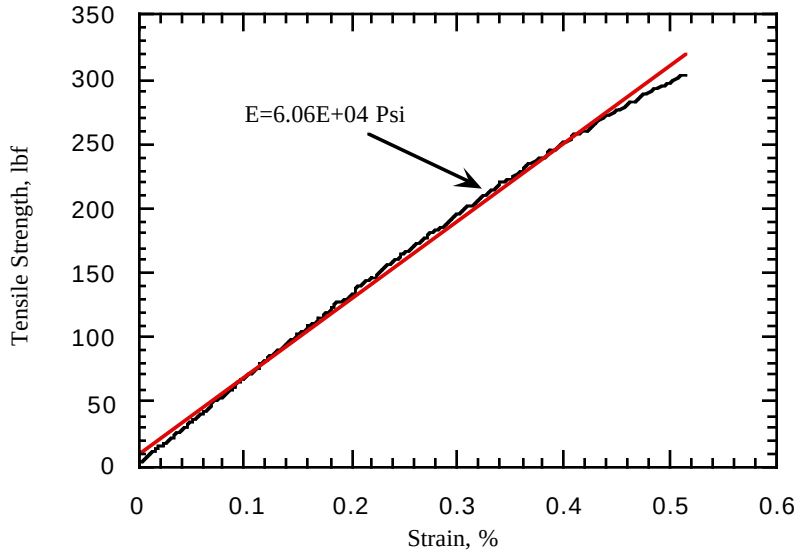

Figure 13. Tensile stress-strain curve of PICA-14 (in-plane).

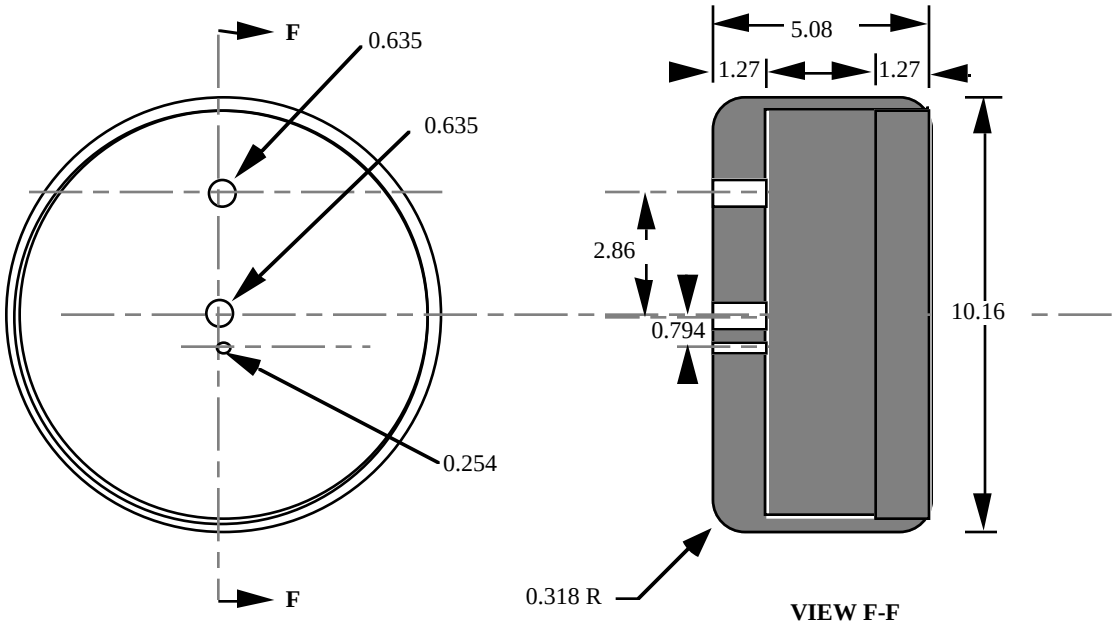

Figure 14. Calibration probe (all units in cm).

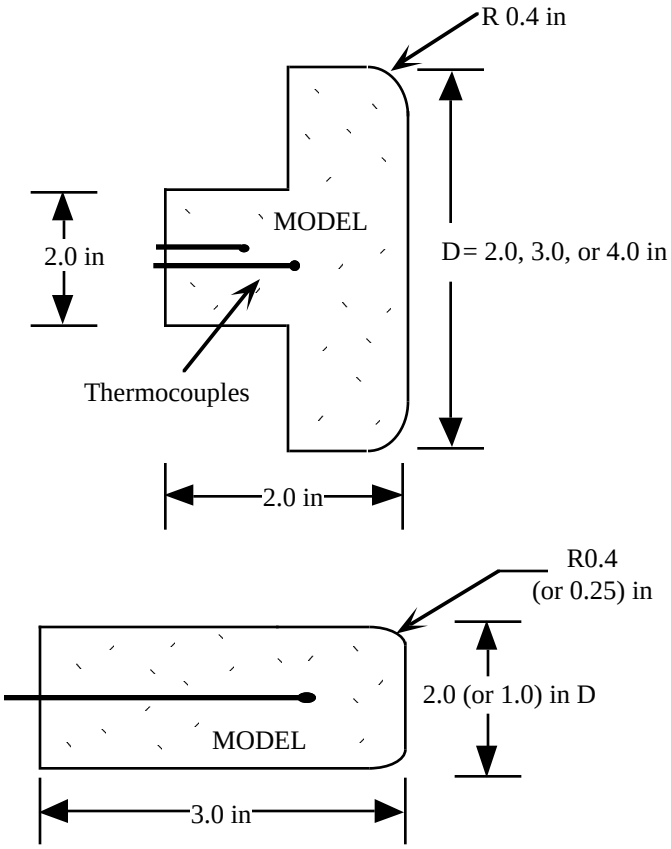

Figure 15. Arc jet test models (side view).

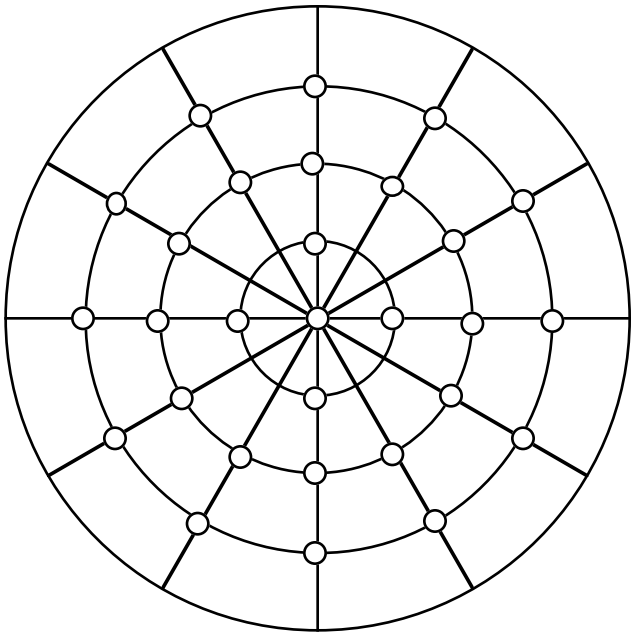

Figure 16. Template for height gage thickness measurements.

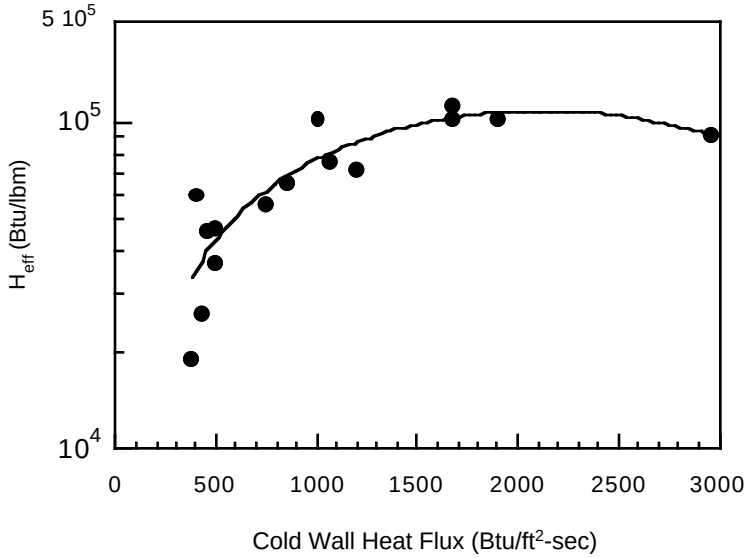

Figure 17. Effective heat of ablation for standard PICA at stagnation pressures from 0.1 to 0.43 atm.

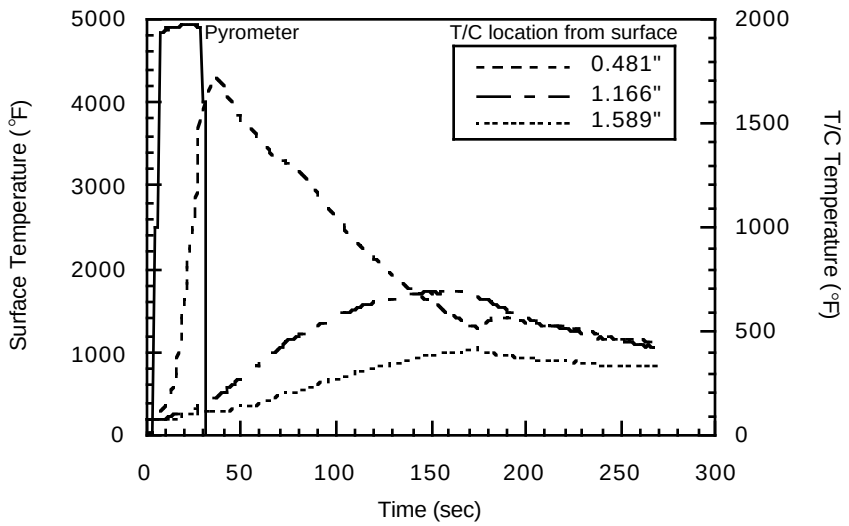

Figure 18. In-depth temperature response of standard PICA.

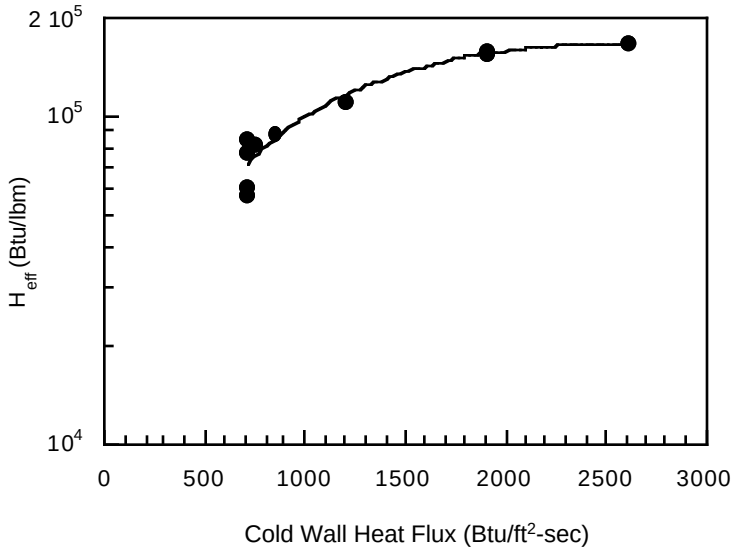

Figure 19. Effective heat of ablation for surface densified PICA at a stagnation pressure of 0.43 atm.

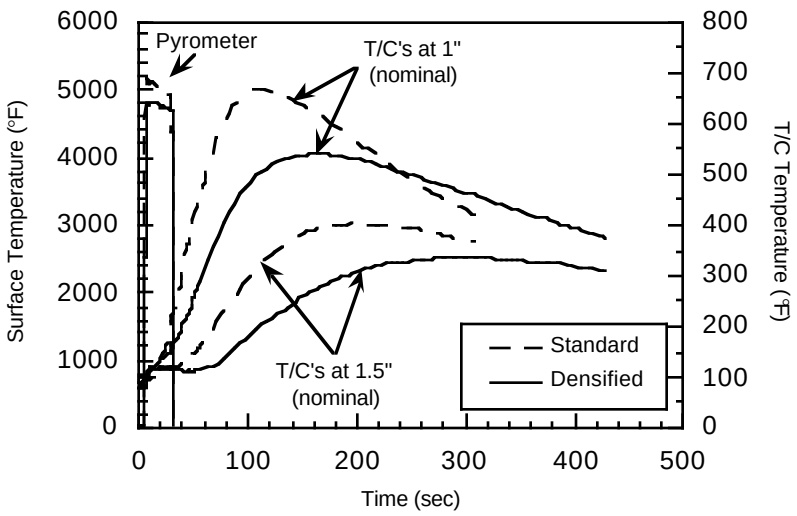

Figure 20. In-depth temperature response of surface densified PICA compared with standard PICA.

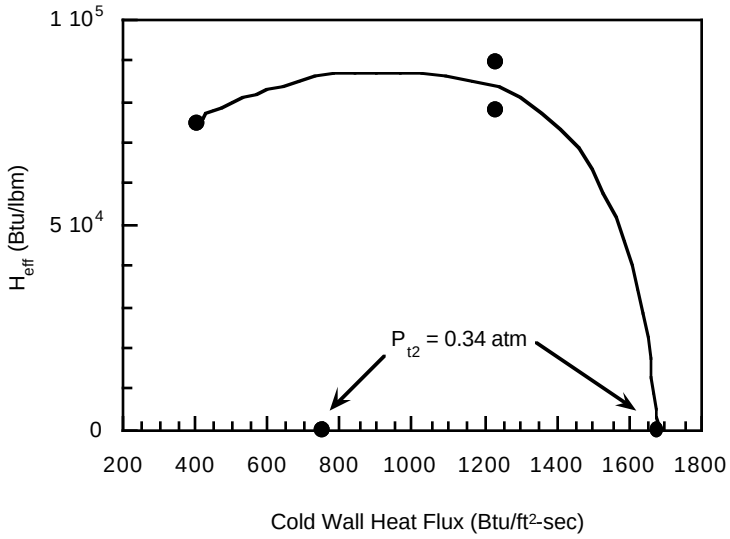

Figure 21. Effective heat of ablation for carbon Fiberform at stagnation pressures from 0.1 to 0.34 atm.

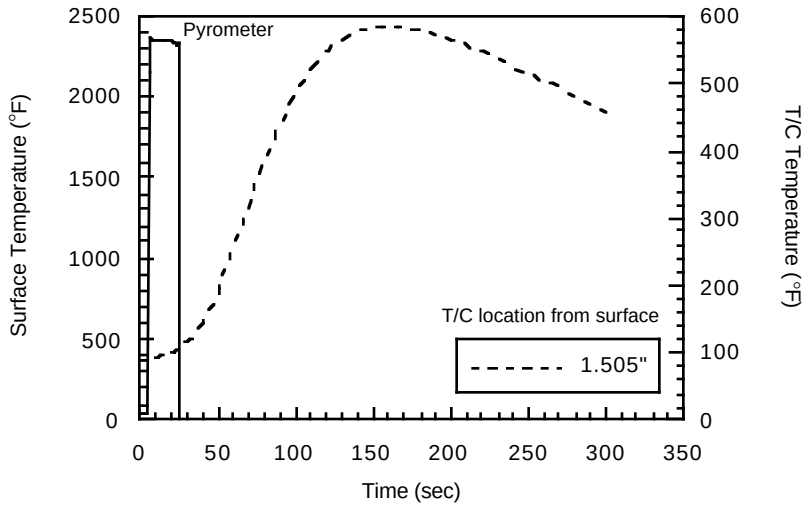

Figure 22. In-depth temperature response of carbon Fiberform.

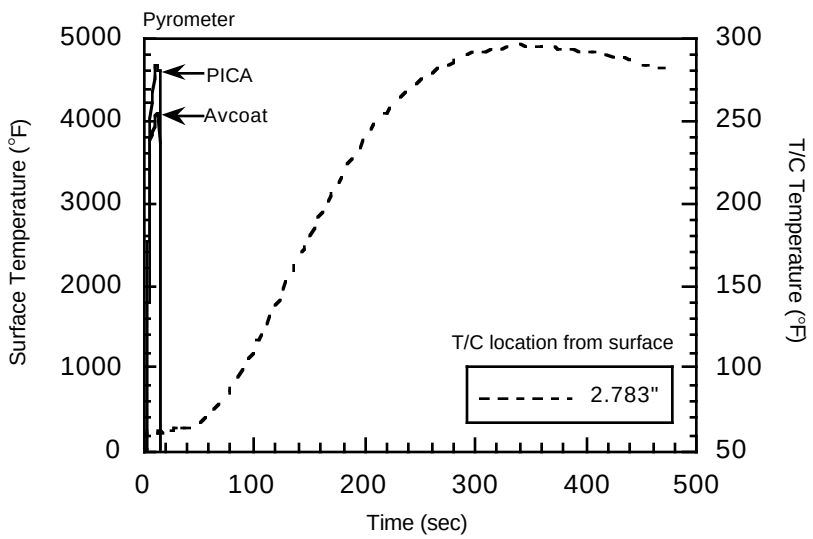

Figure 23. In-depth temperature response of Avcoat-5026.

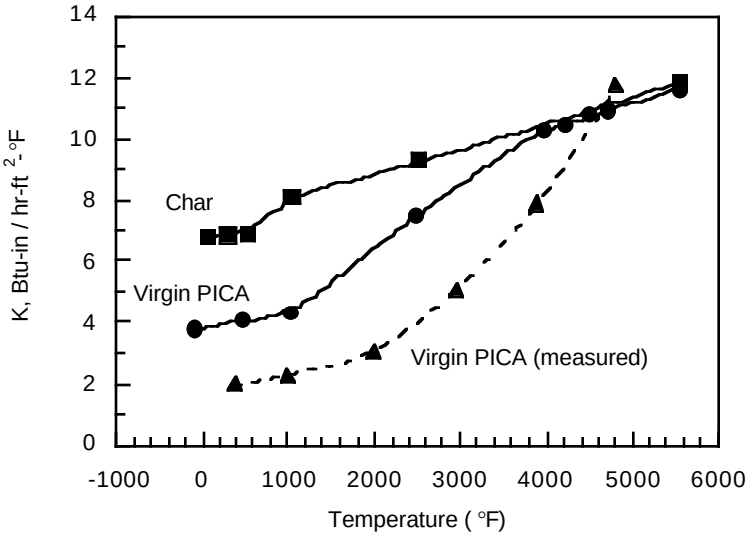

Figure 24(a). Effective thermal conductivity of standard virgin PICA and char.

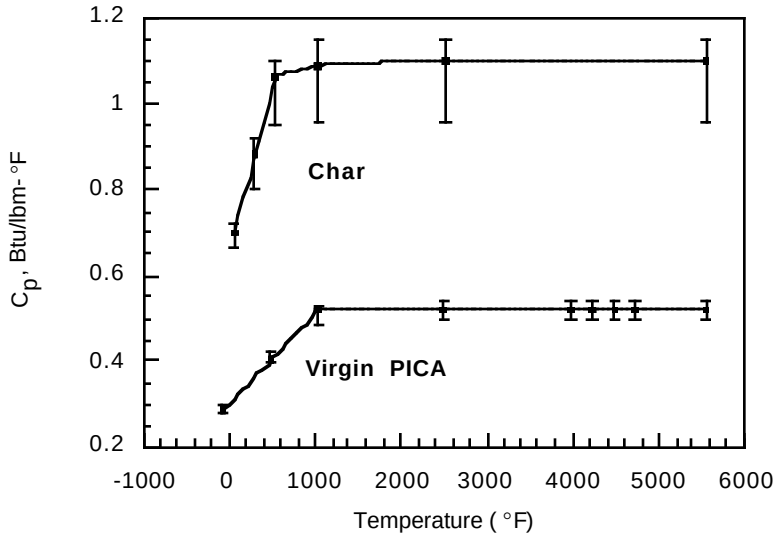

Figure 24(b). Effective specific heat of standard virgin PICA and char.

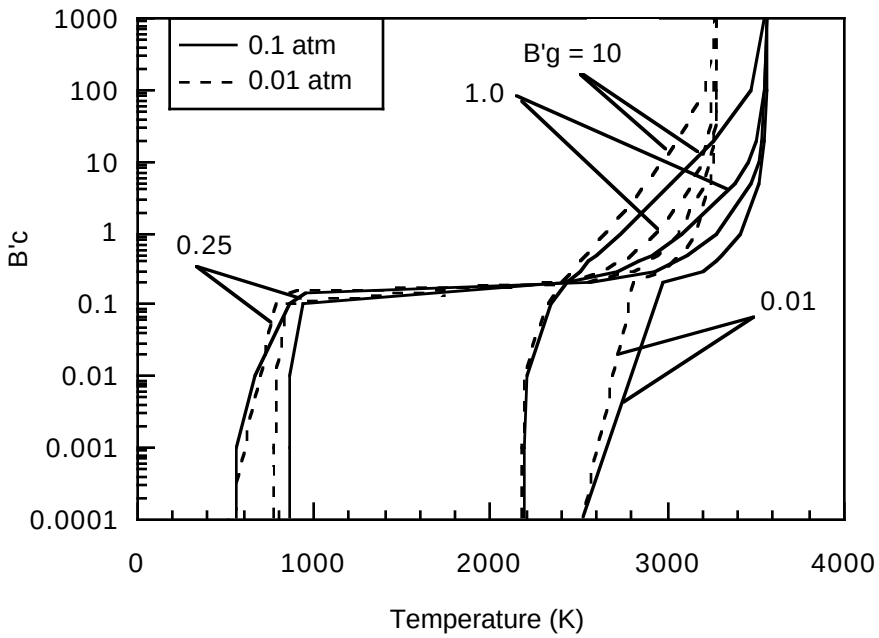

Figure 25. B' curves for standard PICA char and gas pyrolysis.

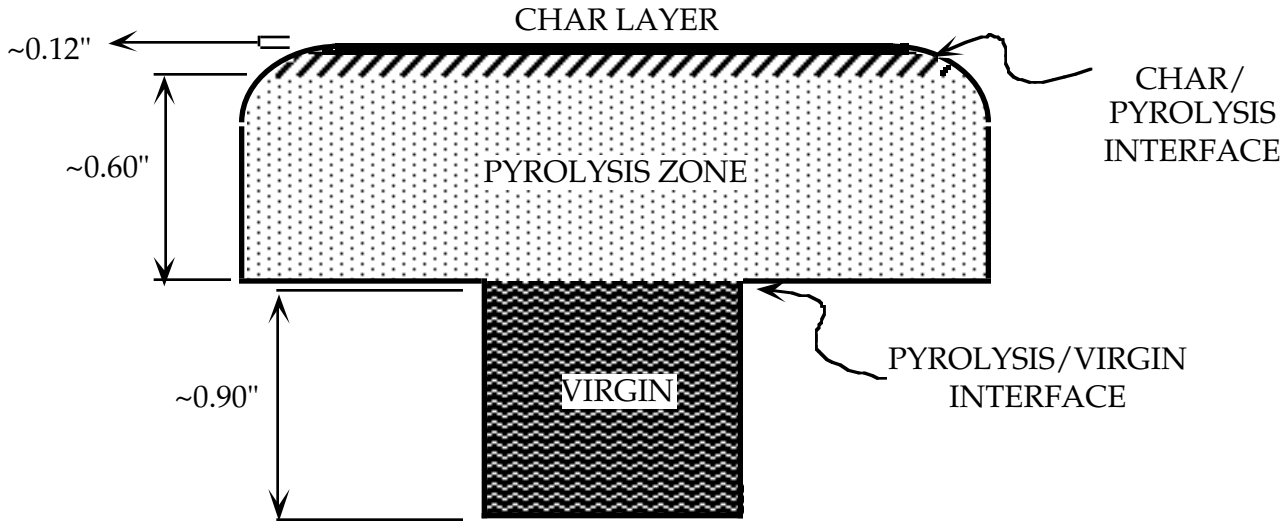

Figure 26. Regions of cross-sectioned post-test PICA-M2-7.

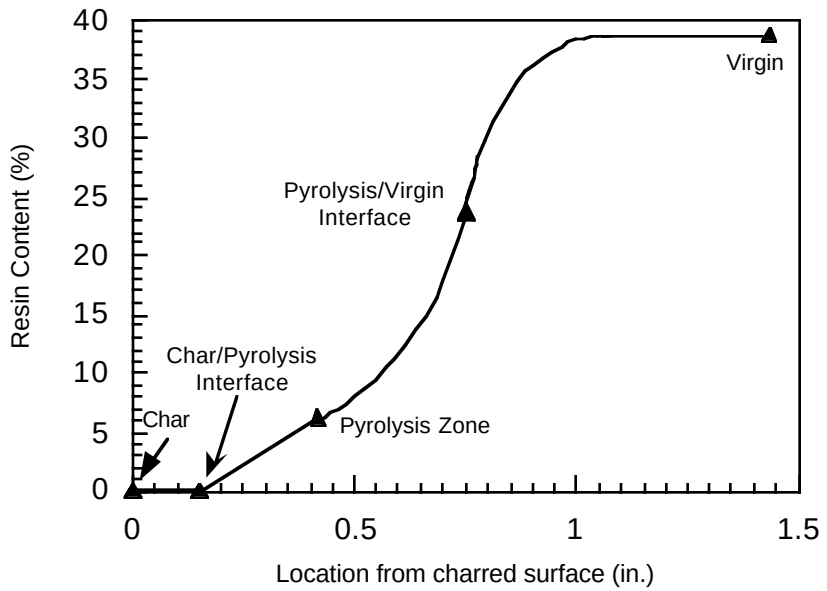

Figure 27. TGA of post-test standard PICA sample.

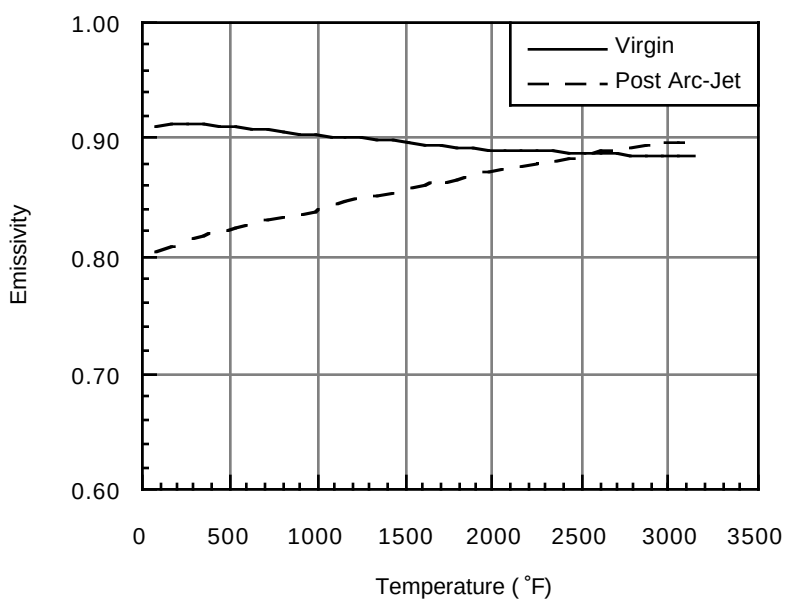

Figure 28. Emissivity of virgin and charred standard PICA.

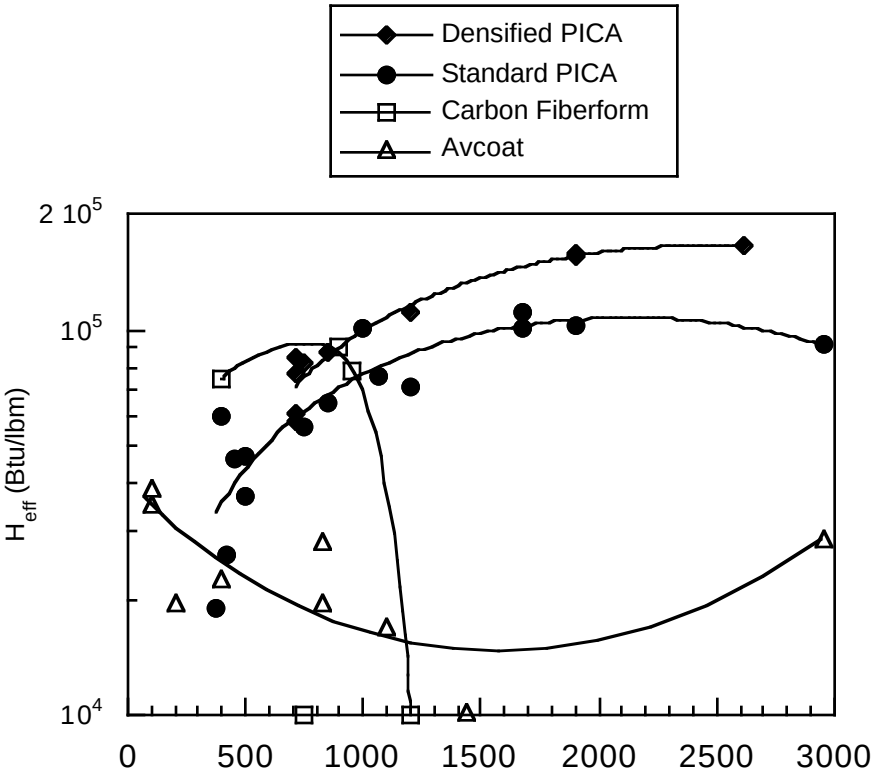

Notes: Carbon failures plotted at bottom of scale, not zero, for easier viewing

Avcoat data below 2960 Btu/ft^{2}sec heat flux are at P_{t2} = 0.014 to 0.141 atm from previous test series (ref. 1)

Figure 29. Summary of performance for tested materials.

Appendix A

In-Depth Thermal Response for Standard PICA

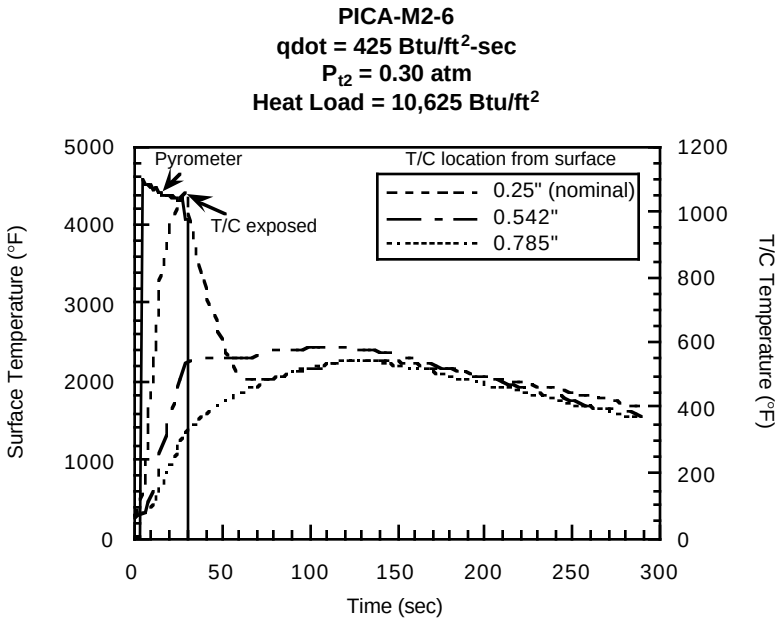

Figure A1. In-depth thermal response for standard PICA.

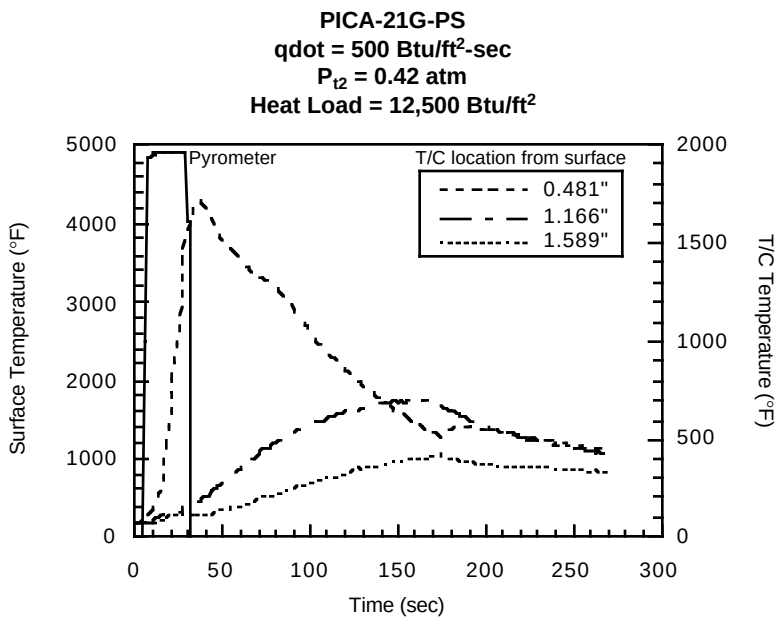

Figure A2. In-depth thermal response for standard PICA.

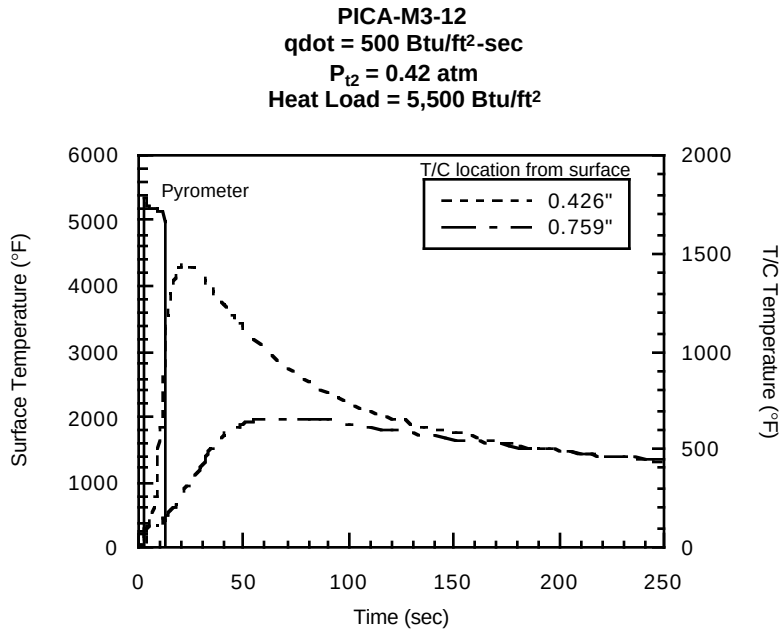

Figure A3. In-depth thermal response for standard PICA.

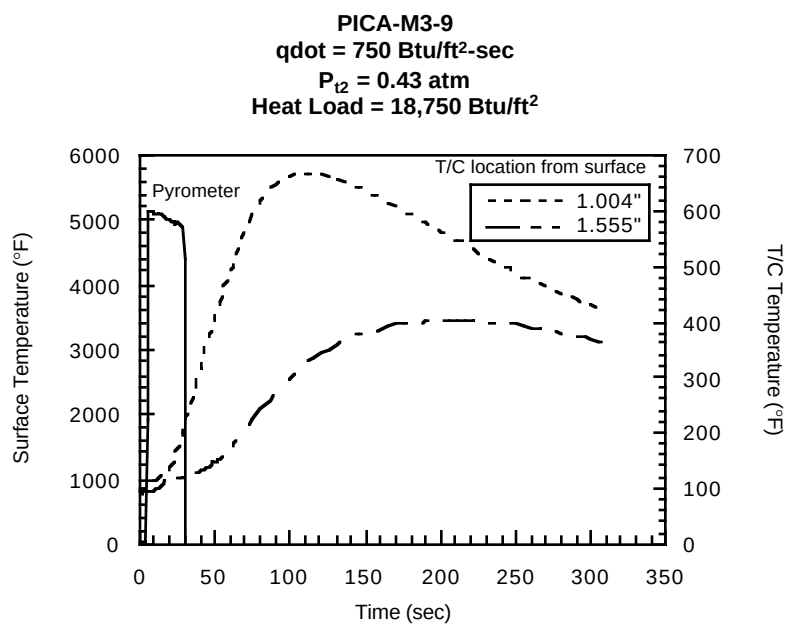

Figure A4. In-depth thermal response for standard PICA.

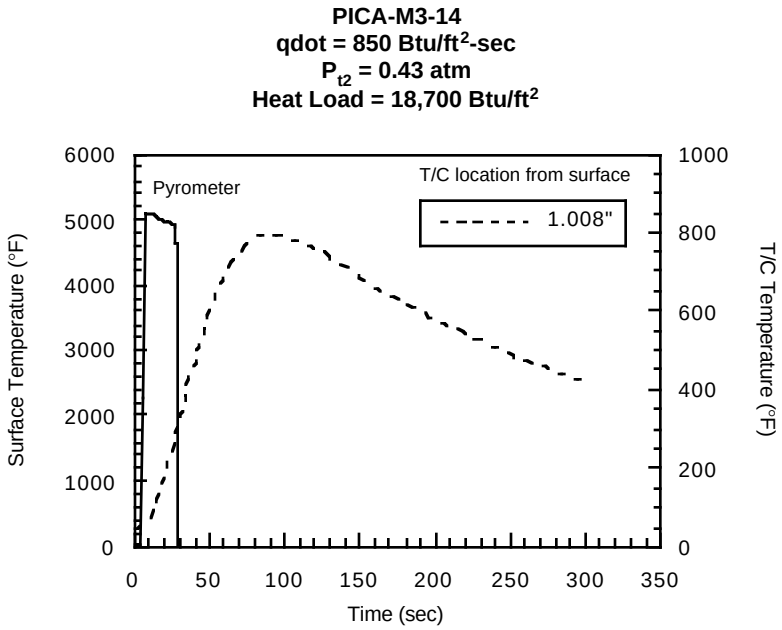

Figure A5. In-depth thermal response for standard PICA.

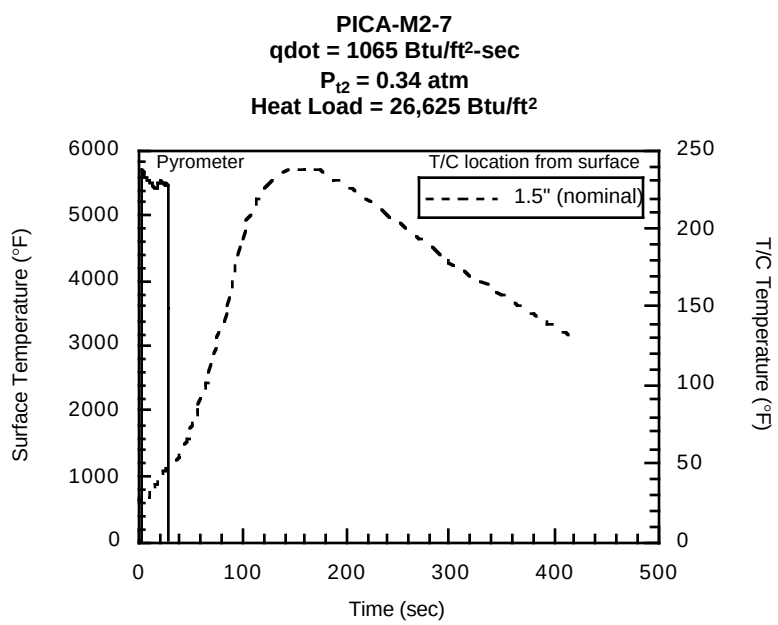

Figure A6. In-depth thermal response for standard PICA.

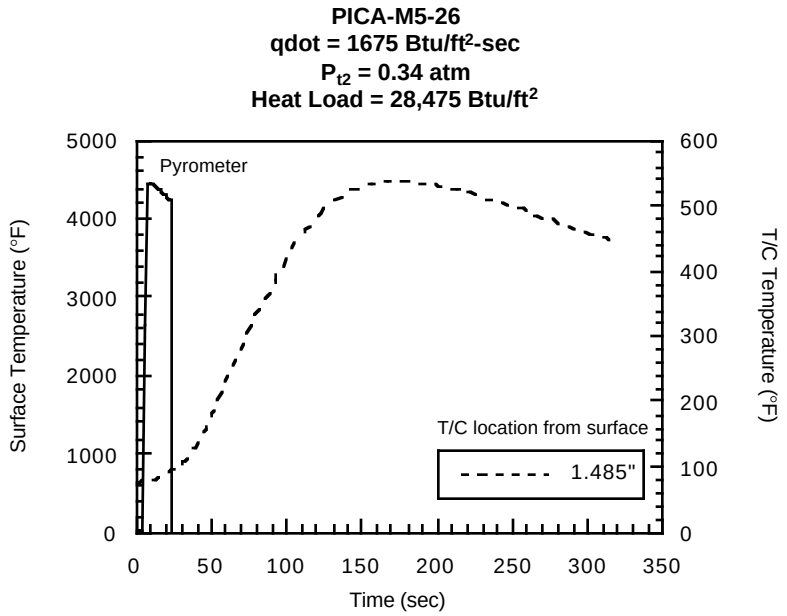

Figure A7. In-depth thermal response for standard PICA.

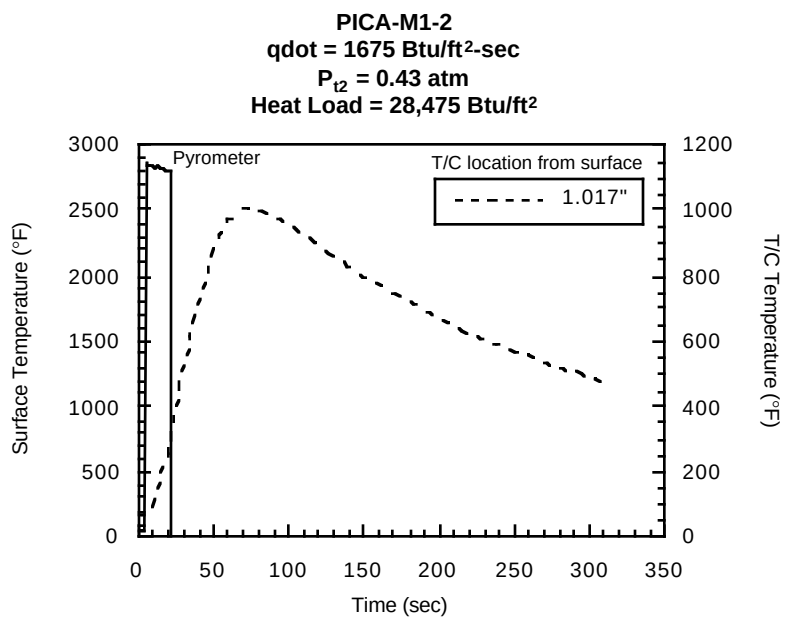

Figure A8. In-depth thermal response for standard PICA.

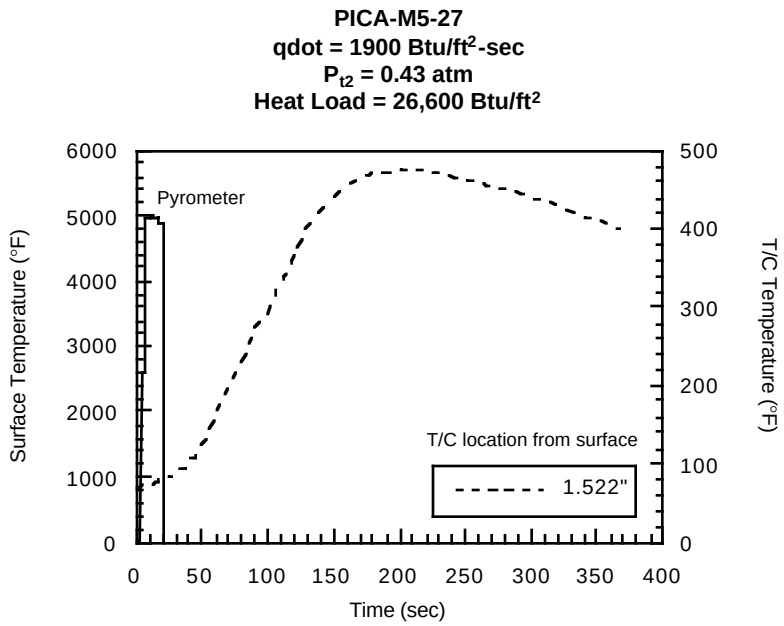

Figure A9. In-depth thermal response for standard PICA.

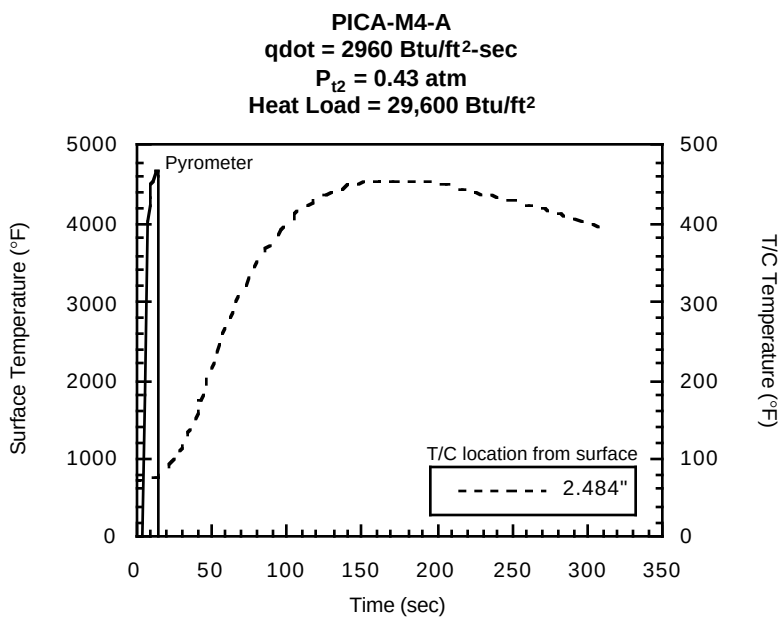

Figure A10. In-depth thermal response for standard PICA.

Appendix B

In-Depth Thermal Response for Densified PICA

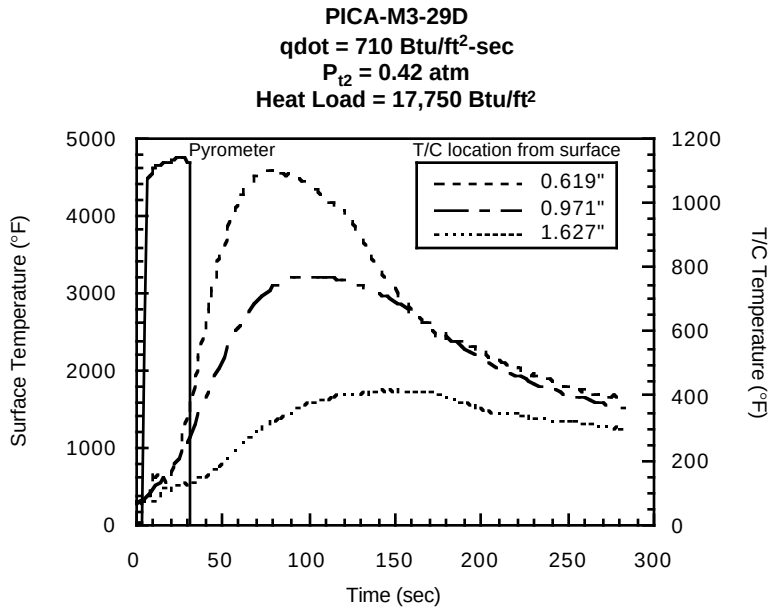

Figure B1. In-depth thermal response for densified PICA.

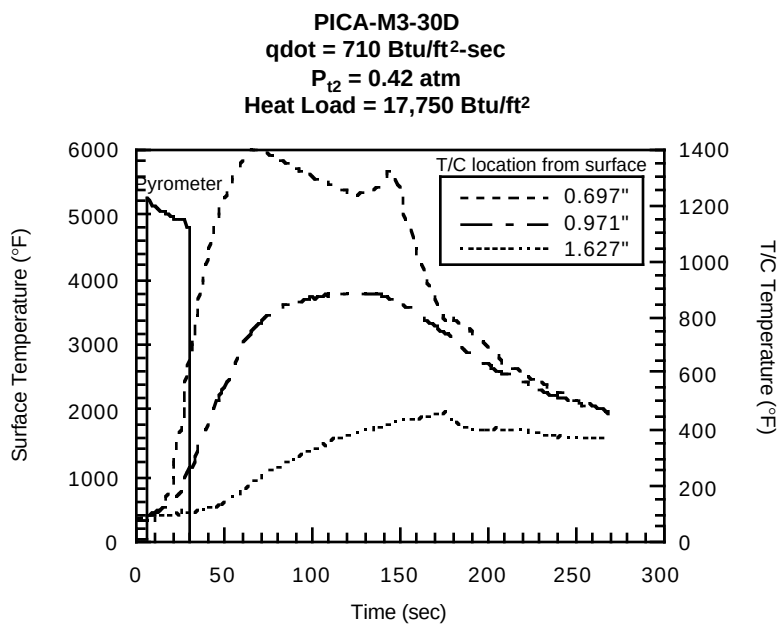

Figure B2. In-depth thermal response for densified PICA.

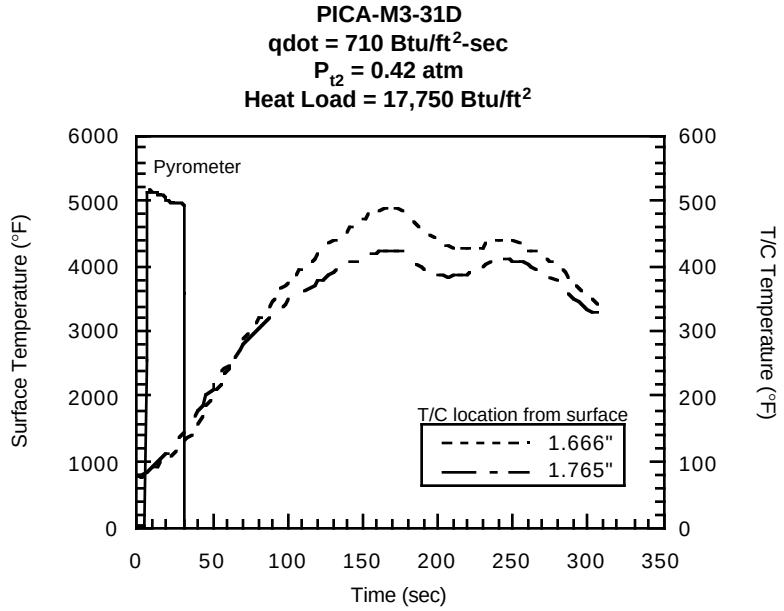

Figure B3. In-depth thermal response for densified PICA (cold air was discharged on model during cool-down period).

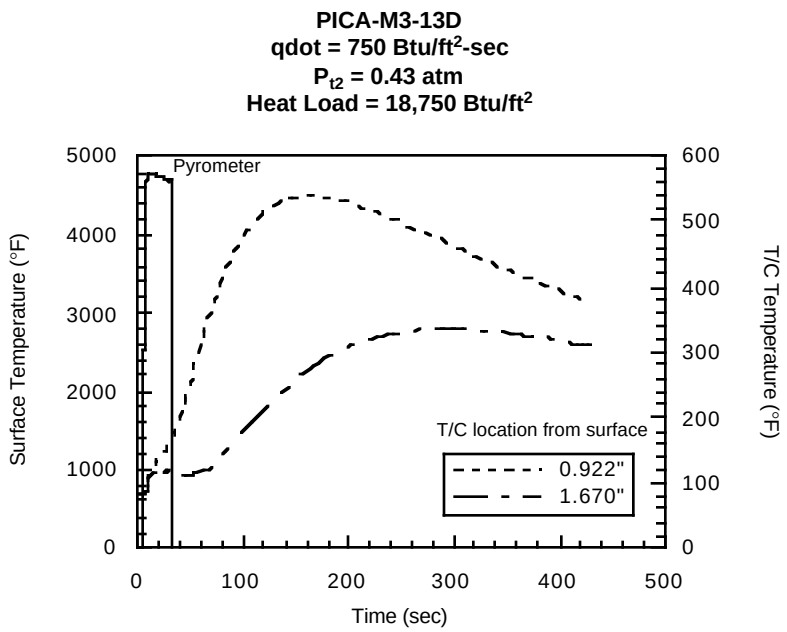

Figure B4. In-depth thermal response for densified PICA.

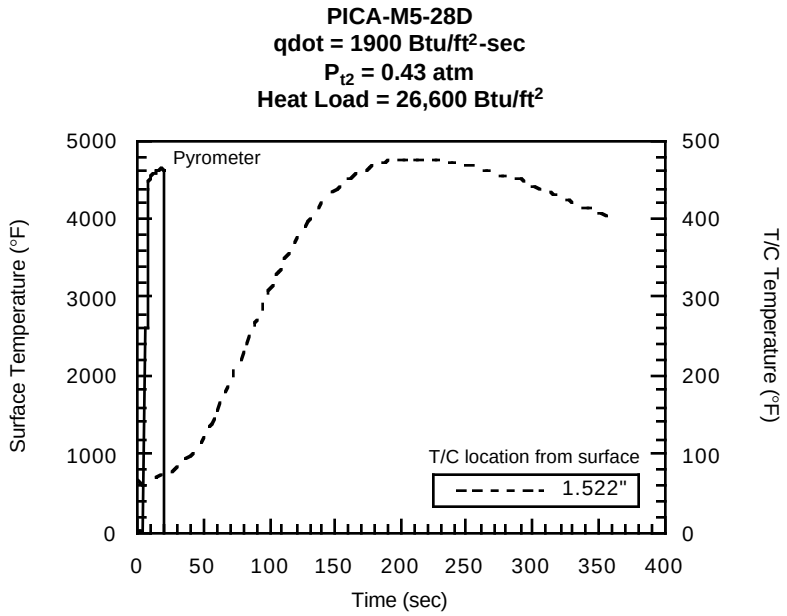

Figure B5. In-depth thermal response for densified PICA.

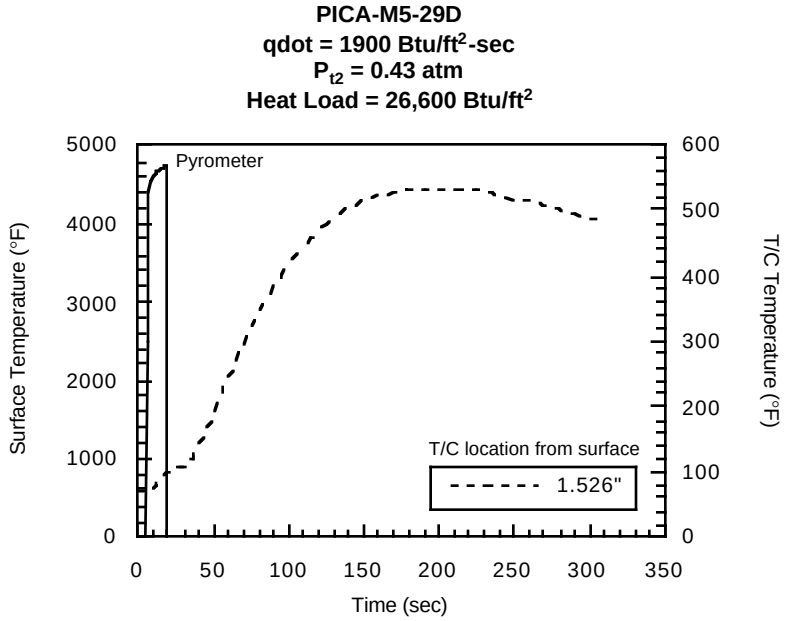

Figure B6. In-depth thermal response for densified PICA.

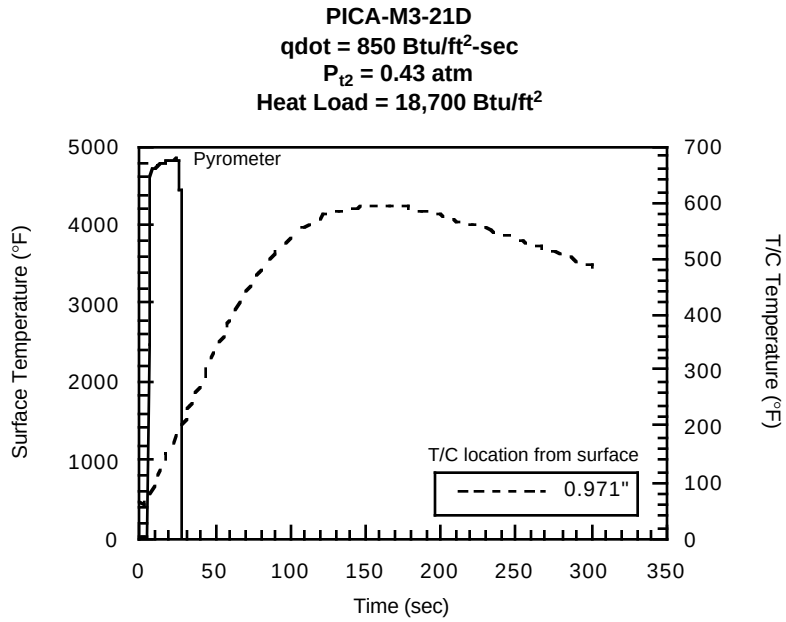

Figure B7. In-depth thermal response for densified PICA.

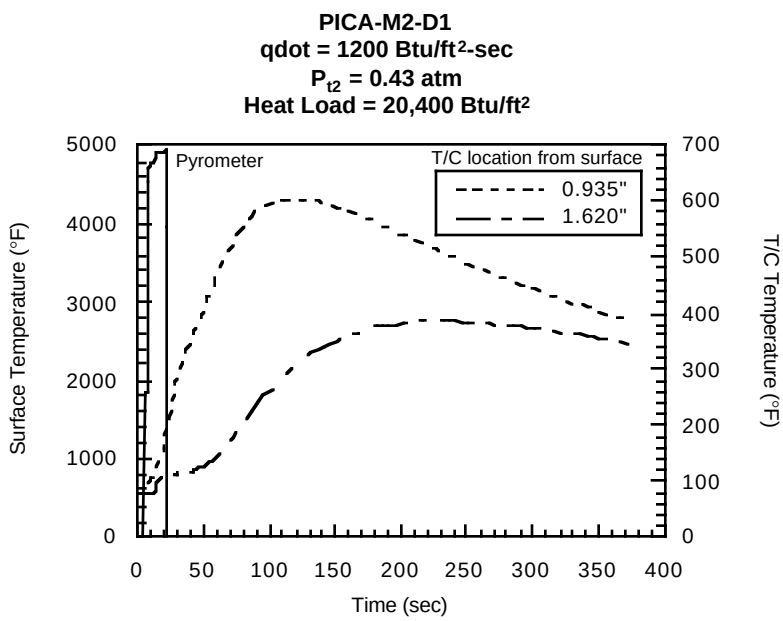

Figure B8. In-depth thermal response for densified PICA.

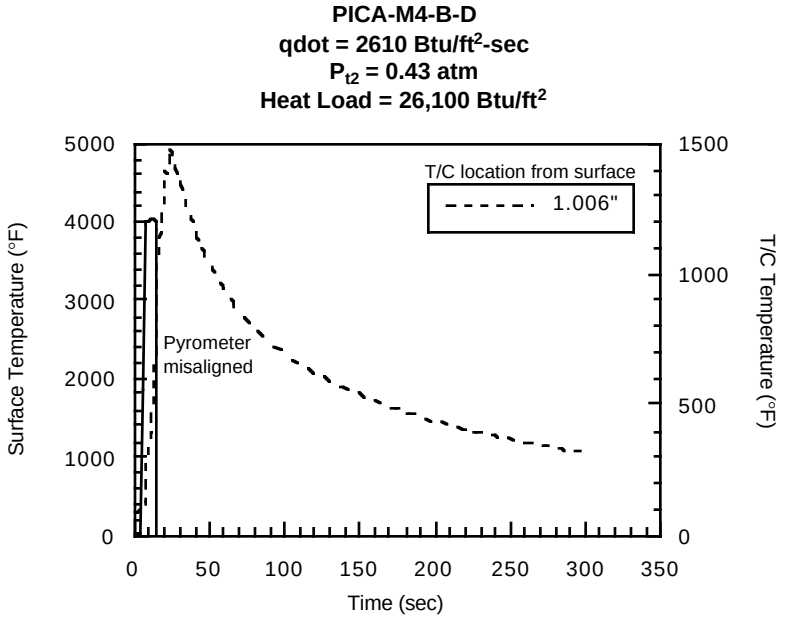

Figure B9. In-depth thermal response for densified PICA.

Appendix C

CMA Input Deck

```
CMA INPUT DECK FOR PICA (Y.K. Chen, Thermosciences Institute)

-376.5  0.0  0.0  536.0
  0.0646
DECOMPOSITION KINETIC DATA (SURFACE)
 14.2500     0.000000E+00  14000.0E-00  3.00000      15400.0      1000.00
 60.7500      49.5000     0.448000E+10  3.00000      36800.0      600.000
 10.0000      10.0000     0.000000E+00 0.000000E+00 0.000000E+00  90000.0
MATERIAL PROPERTIES
    400.0  0.34600 0.88046E-04  0.80  0.80
    950.0  0.46200 0.94046E-04  0.80  0.80
   1500.1  0.55900 1.00453E-04  0.80  0.80
   2971.1  0.58900 1.74453E-04  0.80  0.80
   4442.1  0.58900 2.47753E-04  0.80  0.80
   4694.7  0.58900 2.50900E-04  0.80  0.80
   4947.4  0.58900 2.58348E-04  0.80  0.80
   5200.0  0.58900 2.63796E-04  0.80  0.80
  -6000.0  0.58900 2.69796E-04  0.80  0.80
    530.0  0.70000 0.15700E-03  0.90  0.90
    765.0  0.90000 0.15900E-03  0.90  0.90
   1000.0  1.10000 0.16100E-03  0.90  0.90
   1500.0  1.10000 0.18800E-03  0.90  0.90
   3000.0  1.10000 0.21500E-03  0.90  0.90
  -6000.0  1.10000 0.27500E-03  0.90  0.90
PYROLYSIS GAS ENTHALPY TABLES
     720.0000  -0.38767E+04
    1440.0000  -0.26533E+04
    2160.0000  -0.97516E+02
    2880.0000   0.55346E+03
    3600.0000   0.12448E+04
    4320.0000   0.22410E+04
    5040.0000   0.41789E+04
    5760.0000   0.82321E+04
    6480.0000   0.14307E+05
    7200.0000   0.19156E+05
    7920.0000   0.21496E+05
   -8640.0000   0.22855E+05
THERMOCHEMISTRY TABLES
 0.43000      10.000      1000.0     0.00000E+00  3755.3    0.000  6770.843  6770.843 1  C*
 0.43000      10.000      100.00     0.00000E+00  3660.6    0.000  6049.868  6049.868 1  C*
 0.43000      10.000      20.000     0.00000E+00  3392.1    0.000  4917.841  4917.841 1  C*
 0.43000      10.000      10.000     0.00000E+00  3252.2    0.000  4295.873  4295.873 1  C*
 0.43000      10.000      5.0000     0.00000E+00  3112.8    0.000  3556.798  3556.798 1  C*
 0.43000      10.000      1.0000     0.00000E+00  2774.5    0.000  2011.067  2011.067 1  C*
 0.43000      10.000     0.50000     0.00000E+00  2624.3    0.000  1575.272  1575.272 1  C*
 0.43000      10.000     0.40000     0.00000E+00  2577.8    0.000  1465.819  1465.819 1  C*
 0.43000      10.000     0.30000     0.00000E+00  2520.7    0.000  1344.542  1344.542 1  C*
 0.43000      10.000     0.20000     0.00000E+00  2447.3    0.000  1207.109  1207.109 1  C*
 0.43000      10.000     0.10000     0.00000E+00  2345.8    0.000  1044.502  1044.502 1  C*
 0.43000      10.000     1.00000E-02 0.00000E+00  2202.8    0.000   855.237   855.237 1  C*
 0.43000      10.000     1.00000E-03 0.00000E+00  2183.1    0.000   831.938   831.938 1  C*
 0.43000      10.000     1.00000E-04 0.00000E+00  2181.0    0.000   829.539   829.539 1  C*
 0.43000      10.000     1.00000E-04 0.00000E+00  2000.0    0.000   648.694   648.694 0  CHAR
 0.43000      10.000     1.00000E-04 0.00000E+00  1500.0    0.000   195.090   195.090 0  CHAR
 0.43000      10.000     1.00000E-04 0.00000E+00  1000.0    0.000  -345.540  -345.540 0  CHAR
 0.43000      10.000     1.00000E-04 0.00000E+00  500.00    0.000 -1874.312 -1874.312 0  CHAR
 0.43000      2.5000      1000.0     0.00000E+00  3762.9    0.000  6843.188  6843.188 1  C*
 0.43000      2.5000      100.00     0.00000E+00  3737.0    0.000  6581.418  6581.418 1  C*
```

0.43000	2.5000	20.000	0.00000E+00	3627.8	0.000	5724.627	5724.627	1	C*
0.43000	2.5000	10.000	0.00000E+00	3517.1	0.000	5121.651	5121.651	1	C*
0.43000	2.5000	5.0000	0.00000E+00	3376.7	0.000	4456.418	4456.418	1	C*
0.43000	2.5000	1.0000	0.00000E+00	3015.4	0.000	2589.865	2589.865	1	C*
0.43000	2.5000	0.50000	0.00000E+00	2819.3	0.000	1827.591	1827.591	1	C*
0.43000	2.5000	0.40000	0.00000E+00	2742.7	0.000	1604.218	1604.218	1	C*
0.43000	2.5000	0.30000	0.00000E+00	2628.7	0.000	1332.927	1332.927	1	C*
0.43000	2.5000	0.20000	0.00000E+00	2424.6	0.000	979.144	979.144	1	C*
0.43000	2.5000	0.10000	0.00000E+00	1132.3	0.000	-128.127	-128.127	1	C*
0.43000	2.5000	1.00000E-02	0.00000E+00	994.15	0.000	-357.861	-357.861	1	C*
0.43000	2.5000	1.00000E-03	0.00000E+00	988.42	0.000	-374.831	-374.831	1	C*
0.43000	2.5000	1.00000E-04	0.00000E+00	987.87	0.000	-376.517	-376.517	1	C*
0.43000	2.5000	1.00000E-04	0.00000E+00	500.00	0.000	-1610.618	-1610.618	0	CHAR
0.43000	1.0000	1000.0	0.00000E+00	3764.5	0.000	6857.973	6857.973	1	C*
0.43000	1.0000	100.00	0.00000E+00	3752.3	0.000	6716.176	6716.176	1	C*
0.43000	1.0000	20.000	0.00000E+00	3701.2	0.000	6154.708	6154.708	1	C*
0.43000	1.0000	10.000	0.00000E+00	3641.8	0.000	5605.109	5605.109	1	C*
0.43000	1.0000	5.0000	0.00000E+00	3540.0	0.000	4859.923	4859.923	1	C*
0.43000	1.0000	1.0000	0.00000E+00	3183.1	0.000	2838.995	2838.995	1	C*
0.43000	1.0000	0.50000	0.00000E+00	2981.7	0.000	1949.287	1949.287	1	C*
0.43000	1.0000	0.40000	0.00000E+00	2898.5	0.000	1671.716	1671.716	1	C*
0.43000	1.0000	0.30000	0.00000E+00	2762.2	0.000	1315.846	1315.846	1	C*
0.43000	1.0000	0.20000	0.00000E+00	2444.2	0.000	799.224	799.224	1	C*
0.43000	1.0000	0.10000	0.00000E+00	998.97	0.000	-289.474	-289.474	1	C*
0.43000	1.0000	1.00000E-02	0.00000E+00	915.65	0.000	-541.574	-541.574	1	C*
0.43000	1.0000	1.00000E-03	0.00000E+00	908.70	0.000	-568.059	-568.059	1	C*
0.43000	1.0000	1.00000E-04	0.00000E+00	908.01	0.000	-570.739	-570.739	1	C*
0.43000	1.0000	1.00000E-04	0.00000E+00	500.00	0.000	-1320.550	-1320.550	0	CHAR
0.43000	0.25000	1000.0	0.00000E+00	3765.2	0.000	6865.405	6865.405	1	C*
0.43000	0.25000	100.00	0.00000E+00	3759.9	0.000	6787.375	6787.375	1	C*
0.43000	0.25000	20.000	0.00000E+00	3738.7	0.000	6447.661	6447.661	1	C*
0.43000	0.25000	10.000	0.00000E+00	3714.4	0.000	6060.677	6060.677	1	C*
0.43000	0.25000	5.0000	0.00000E+00	3670.3	0.000	5407.101	5407.101	1	C*
0.43000	0.25000	1.0000	0.00000E+00	3418.9	0.000	2978.184	2978.184	1	C*
0.43000	0.25000	0.50000	0.00000E+00	3222.7	0.000	1954.327	1954.327	1	C*
0.43000	0.25000	0.40000	0.00000E+00	3141.1	0.000	1649.586	1649.586	1	C*
0.43000	0.25000	0.30000	0.00000E+00	3004.2	0.000	1259.958	1259.958	1	C*
0.43000	0.25000	0.20000	0.00000E+00	2577.2	0.000	624.999	624.999	1	C*
0.43000	0.25000	0.15000	0.00000E+00	1016.1	0.000	-198.660	-198.660	1	C*
0.43000	0.25000	0.10000	0.00000E+00	916.00	0.000	-380.793	-380.793	1	C*
0.43000	0.25000	1.00000E-02	0.00000E+00	642.42	0.000	-831.958	-831.958	1	C*
0.43000	0.25000	1.00000E-03	0.00000E+00	540.77	0.000	-897.590	-897.590	1	C*
0.43000	0.25000	1.00000E-04	0.00000E+00	533.99	0.000	-901.313	-901.313	1	C*
0.43000	0.25000	1.00000E-04	0.00000E+00	500.00	0.000	-914.795	-914.795	0	CHAR
0.43000	1.00000E-02	1000.0	0.00000E+00	3765.5	0.000	6867.789	6867.789	1	C*
0.43000	1.00000E-02	100.00	0.00000E+00	3762.4	0.000	6810.703	6810.703	1	C*
0.43000	1.00000E-02	20.000	0.00000E+00	3750.6	0.000	6553.632	6553.632	1	C*
0.43000	1.00000E-02	10.000	0.00000E+00	3737.7	0.000	6248.973	6248.973	1	C*
0.43000	1.00000E-02	5.0000	0.00000E+00	3715.0	0.000	5706.447	5706.447	1	C*
0.43000	1.00000E-02	1.0000	0.00000E+00	3589.6	0.000	3261.265	3261.265	1	C*
0.43000	1.00000E-02	0.50000	0.00000E+00	3481.7	0.000	2008.390	2008.390	1	C*
0.43000	1.00000E-02	0.40000	0.00000E+00	3433.3	0.000	1643.149	1643.149	1	C*
0.43000	1.00000E-02	0.30000	0.00000E+00	3350.4	0.000	1211.992	1211.992	1	C*
0.43000	1.00000E-02	0.20000	0.00000E+00	3082.0	0.000	650.153	650.153	1	C*
0.43000	1.00000E-02	1.00000E-04	0.00000E+00	2500.0	0.000	609.960	609.960	0	CHAR
0.43000	1.00000E-02	1.00000E-04	0.00000E+00	2000.0	0.000	413.034	413.034	0	CHAR
0.43000	1.00000E-02	1.00000E-04	0.00000E+00	1500.0	0.000	255.750	255.750	0	CHAR
0.43000	1.00000E-02	1.00000E-04	0.00000E+00	1000.0	0.000	109.957	109.957	0	CHAR

0.43000	1.00000E-02	1.00000E-04	0.00000E+00	500.00	0.000	-24.390	-24.390	0	CHAR
0.43000	1.00000E-03	1000.0	0.00000E+00	3765.5	0.000	6867.878	6867.878	1	C*
0.43000	1.00000E-03	100.00	0.00000E+00	3762.5	0.000	6811.583	6811.583	1	C*
0.43000	1.00000E-03	20.000	0.00000E+00	3751.0	0.000	6557.724	6557.724	1	C*
0.43000	1.00000E-03	10.000	0.00000E+00	3738.6	0.000	6256.464	6256.464	1	C*
0.43000	1.00000E-03	5.0000	0.00000E+00	3716.6	0.000	5719.103	5719.103	1	C*
0.43000	1.00000E-03	1.0000	0.00000E+00	3596.5	0.000	3283.375	3283.375	1	C*
0.43000	1.00000E-03	0.50000	0.00000E+00	3495.2	0.000	2025.107	2025.107	1	C*
0.43000	1.00000E-03	0.40000	0.00000E+00	3450.6	0.000	1656.623	1656.623	1	C*
0.43000	1.00000E-03	0.30000	0.00000E+00	3376.3	0.000	1220.785	1220.785	1	C*
0.43000	1.00000E-03	0.20000	0.00000E+00	3162.5	0.000	662.860	662.860	1	C*
0.43000	1.00000E-03	1.00000E-04	0.00000E+00	2500.0	0.000	656.949	656.949	0	CHAR
0.43000	1.00000E-03	1.00000E-04	0.00000E+00	2000.0	0.000	472.246	472.246	0	CHAR
0.43000	1.00000E-03	1.00000E-04	0.00000E+00	1500.0	0.000	318.430	318.430	0	CHAR
0.43000	1.00000E-03	1.00000E-04	0.00000E+00	1000.0	0.000	174.919	174.919	0	CHAR
0.43000	1.00000E-03	1.00000E-04	0.00000E+00	500.00	0.000	42.402	42.402	0	CHAR
0.43000	1.00000E-05	1000.0	0.00000E+00	3765.5	0.000	6867.888	6867.888	1	C*
0.43000	1.00000E-05	100.00	0.00000E+00	3762.5	0.000	6811.680	6811.680	1	C*
0.43000	1.00000E-05	20.000	0.00000E+00	3751.1	0.000	6558.174	6558.174	1	C*
0.43000	1.00000E-05	10.000	0.00000E+00	3738.7	0.000	6257.290	6257.290	1	C*
0.43000	1.00000E-05	5.0000	0.00000E+00	3716.8	0.000	5720.501	5720.501	1	C*
0.43000	1.00000E-05	1.0000	0.00000E+00	3597.3	0.000	3285.873	3285.873	1	C*
0.43000	1.00000E-05	0.50000	0.00000E+00	3496.7	0.000	2027.085	2027.085	1	C*
0.43000	1.00000E-05	0.40000	0.00000E+00	3452.5	0.000	1658.279	1658.279	1	C*
0.43000	1.00000E-05	0.30000	0.00000E+00	3379.1	0.000	1221.980	1221.980	1	C*
0.43000	1.00000E-05	0.20000	0.00000E+00	3171.4	0.000	664.437	664.437	1	C*
0.43000	1.00000E-05	1.00000E-04	0.00000E+00	2500.0	0.000	660.119	660.119	0	CHAR
0.43000	1.00000E-05	1.00000E-04	0.00000E+00	2000.0	0.000	478.473	478.473	0	CHAR
0.43000	1.00000E-05	1.00000E-04	0.00000E+00	1500.0	0.000	325.380	325.380	0	CHAR
0.43000	1.00000E-05	1.00000E-04	0.00000E+00	1000.0	0.000	182.136	182.136	0	CHAR
0.43000	1.00000E-05	1.00000E-04	0.00000E+00	500.00	0.000	49.822	49.822	0	CHAR
0.10000	10.000	1000.0	0.00000E+00	3551.2	0.000	6767.795	6767.795	1	C*
0.10000	10.000	100.00	0.00000E+00	3474.1	0.000	6241.203	6241.203	1	C*
0.10000	10.000	20.000	0.00000E+00	3263.6	0.000	5356.912	5356.912	1	C*
0.10000	10.000	10.000	0.00000E+00	3143.0	0.000	4811.536	4811.536	1	C*
0.10000	10.000	5.0000	0.00000E+00	3020.5	0.000	4085.281	4085.281	1	C*
0.10000	10.000	1.0000	0.00000E+00	2727.8	0.000	2342.197	2342.197	1	C*
0.10000	10.000	0.50000	0.00000E+00	2597.2	0.000	1803.461	1803.461	1	C*
0.10000	10.000	0.40000	0.00000E+00	2555.9	0.000	1665.011	1665.011	1	C*
0.10000	10.000	0.30000	0.00000E+00	2504.4	0.000	1510.539	1510.539	1	C*
0.10000	10.000	0.20000	0.00000E+00	2436.8	0.000	1335.034	1335.034	1	C*
0.10000	10.000	0.10000	0.00000E+00	2340.8	0.000	1129.324	1129.324	1	C*
0.10000	10.000	1.00000E-02	0.00000E+00	2202.2	0.000	898.650	898.650	1	C*
0.10000	10.000	1.00000E-03	0.00000E+00	2183.0	0.000	871.284	871.284	1	C*
0.10000	10.000	1.00000E-04	0.00000E+00	2181.0	0.000	868.481	868.481	1	C*
0.10000	10.000	1.00000E-04	0.00000E+00	2000.0	0.000	661.769	661.769	0	CHAR
0.10000	10.000	1.00000E-04	0.00000E+00	1500.0	0.000	210.133	210.133	0	CHAR
0.10000	10.000	1.00000E-04	0.00000E+00	1000.0	0.000	-241.110	-241.110	0	CHAR
0.10000	10.000	1.00000E-04	0.00000E+00	500.00	0.000	-1863.696	-1863.696	0	CHAR
0.10000	2.5000	1000.0	0.00000E+00	3557.8	0.000	6820.425	6820.425	1	C*
0.10000	2.5000	100.00	0.00000E+00	3535.5	0.000	6615.251	6615.251	1	C*
0.10000	2.5000	20.000	0.00000E+00	3448.3	0.000	5942.487	5942.487	1	C*
0.10000	2.5000	10.000	0.00000E+00	3363.6	0.000	5441.438	5441.438	1	C*
0.10000	2.5000	5.0000	0.00000E+00	3250.1	0.000	4851.487	4851.487	1	C*
0.10000	2.5000	1.0000	0.00000E+00	2937.0	0.000	2992.201	2992.201	1	C*
0.10000	2.5000	0.50000	0.00000E+00	2768.8	0.000	2123.338	2123.338	1	C*
0.10000	2.5000	0.40000	0.00000E+00	2703.1	0.000	1855.738	1855.738	1	C*
0.10000	2.5000	0.30000	0.00000E+00	2603.9	0.000	1521.718	1521.718	1	C*

0.10000	2.5000	0.20000	0.00000E+00	2417.3	0.000	1074.526	1074.526	1	C*
0.10000	2.5000	0.10000	0.00000E+00	1070.7	0.000	-157.365	-157.365	1	C*
0.10000	2.5000	1.00000E-02	0.00000E+00	931.86	0.000	-365.488	-365.488	1	C*
0.10000	2.5000	1.00000E-03	0.00000E+00	926.75	0.000	-380.293	-380.293	1	C*
0.10000	2.5000	1.00000E-04	0.00000E+00	926.26	0.000	-381.766	-381.766	1	C*
0.10000	2.5000	1.00000E-04	0.00000E+00	500.00	0.000	-1601.830	-1601.830	0	CHAR
0.10000	1.0000	1000.0	0.00000E+00	3559.2	0.000	6831.225	6831.225	1	C*
0.10000	1.0000	100.00	0.00000E+00	3548.6	0.000	6712.168	6712.168	1	C*
0.10000	1.0000	20.000	0.00000E+00	3505.7	0.000	6239.424	6239.424	1	C*
0.10000	1.0000	10.000	0.00000E+00	3458.3	0.000	5772.719	5772.719	1	C*
0.10000	1.0000	5.0000	0.00000E+00	3379.8	0.000	5116.939	5116.939	1	C*
0.10000	1.0000	1.0000	0.00000E+00	3083.3	0.000	3178.828	3178.828	1	C*
0.10000	1.0000	0.50000	0.00000E+00	2909.2	0.000	2236.331	2236.331	1	C*
0.10000	1.0000	0.40000	0.00000E+00	2838.2	0.000	1924.980	1924.980	1	C*
0.10000	1.0000	0.30000	0.00000E+00	2721.9	0.000	1511.145	1511.145	1	C*
0.10000	1.0000	0.20000	0.00000E+00	2437.0	0.000	875.904	875.904	1	C*
0.10000	1.0000	0.10000	0.00000E+00	933.04	0.000	-307.779	-307.779	1	C*
0.10000	1.0000	1.00000E-02	0.00000E+00	861.14	0.000	-534.159	-534.159	1	C*
0.10000	1.0000	1.00000E-03	0.00000E+00	855.38	0.000	-557.493	-557.493	1	C*
0.10000	1.0000	1.00000E-04	0.00000E+00	854.81	0.000	-559.845	-559.845	1	C*
0.10000	1.0000	1.00000E-04	0.00000E+00	500.00	0.000	-1313.784	-1313.784	0	CHAR
0.10000	0.25000	1000.0	0.00000E+00	3559.9	0.000	6836.660	6836.660	1	C*
0.10000	0.25000	100.00	0.00000E+00	3555.2	0.000	6763.859	6763.859	1	C*
0.10000	0.25000	20.000	0.00000E+00	3536.9	0.000	6445.549	6445.549	1	C*
0.10000	0.25000	10.000	0.00000E+00	3516.3	0.000	6082.956	6082.956	1	C*
0.10000	0.25000	5.0000	0.00000E+00	3479.5	0.000	5470.078	5470.078	1	C*
0.10000	0.25000	1.0000	0.00000E+00	3278.9	0.000	3140.568	3140.568	1	C*
0.10000	0.25000	0.50000	0.00000E+00	3116.4	0.000	2116.613	2116.613	1	C*
0.10000	0.25000	0.40000	0.00000E+00	3046.6	0.000	1805.530	1805.530	1	C*
0.10000	0.25000	0.30000	0.00000E+00	2929.5	0.000	1397.809	1397.809	1	C*
0.10000	0.25000	0.20000	0.00000E+00	2562.4	0.000	686.429	686.429	1	C*
0.10000	0.25000	0.15000	0.00000E+00	944.81	0.000	-223.149	-223.149	1	C*
0.10000	0.25000	0.10000	0.00000E+00	857.44	0.000	-396.920	-396.920	1	C*
0.10000	0.25000	1.00000E-02	0.00000E+00	662.92	0.000	-785.190	-785.190	1	C*
0.10000	0.25000	1.00000E-03	0.00000E+00	553.38	0.000	-882.769	-882.769	1	C*
0.10000	0.25000	1.00000E-04	0.00000E+00	544.56	0.000	-888.754	-888.754	1	C*
0.10000	0.25000	1.00000E-04	0.00000E+00	500.00	0.000	-911.250	-911.250	0	CHAR
0.10000	1.00000E-02	1000.0	0.00000E+00	3560.1	0.000	6838.404	6838.404	1	C*
0.10000	1.00000E-02	100.00	0.00000E+00	3557.4	0.000	6780.872	6780.872	1	C*
0.10000	1.00000E-02	20.000	0.00000E+00	3547.2	0.000	6521.520	6521.520	1	C*
0.10000	1.00000E-02	10.000	0.00000E+00	3536.1	0.000	6214.882	6214.882	1	C*
0.10000	1.00000E-02	5.0000	0.00000E+00	3516.3	0.000	5669.958	5669.958	1	C*
0.10000	1.00000E-02	1.0000	0.00000E+00	3406.6	0.000	3223.187	3223.187	1	C*
0.10000	1.00000E-02	0.50000	0.00000E+00	3312.3	0.000	1974.076	1974.076	1	C*
0.10000	1.00000E-02	0.40000	0.00000E+00	3270.2	0.000	1610.725	1610.725	1	C*
0.10000	1.00000E-02	0.30000	0.00000E+00	3198.7	0.000	1182.708	1182.708	1	C*
0.10000	1.00000E-02	0.20000	0.00000E+00	2974.5	0.000	632.339	632.339	1	C*
0.10000	1.00000E-02	1.00000E-04	0.00000E+00	2500.0	0.000	640.799	640.799	0	CHAR
0.10000	1.00000E-02	1.00000E-04	0.00000E+00	2000.0	0.000	414.930	414.930	0	CHAR
0.10000	1.00000E-02	1.00000E-04	0.00000E+00	1500.0	0.000	255.783	255.783	0	CHAR
0.10000	1.00000E-02	1.00000E-04	0.00000E+00	1000.0	0.000	109.957	109.957	0	CHAR
0.10000	1.00000E-02	1.00000E-04	0.00000E+00	500.00	0.000	-24.390	-24.390	0	CHAR
0.10000	1.00000E-03	1000.0	0.00000E+00	3560.1	0.000	6838.470	6838.470	1	C*
0.10000	1.00000E-03	100.00	0.00000E+00	3557.4	0.000	6781.515	6781.515	1	C*
0.10000	1.00000E-03	20.000	0.00000E+00	3547.6	0.000	6524.471	6524.471	1	C*
0.10000	1.00000E-03	10.000	0.00000E+00	3536.8	0.000	6220.188	6220.188	1	C*
0.10000	1.00000E-03	5.0000	0.00000E+00	3517.7	0.000	5678.593	5678.593	1	C*
0.10000	1.00000E-03	1.0000	0.00000E+00	3412.0	0.000	3233.171	3233.171	1	C*

0.10000	1.00000E-03	0.50000	0.00000E+00	3322.2	0.000	1974.896	1974.896	1	C*
0.10000	1.00000E-03	0.40000	0.00000E+00	3282.7	0.000	1607.326	1607.326	1	C*
0.10000	1.00000E-03	0.30000	0.00000E+00	3216.8	0.000	1173.559	1173.559	1	C*
0.10000	1.00000E-03	0.20000	0.00000E+00	3028.0	0.000	622.968	622.968	1	C*
0.10000	1.00000E-03	1.00000E-04	0.00000E+00	3000.0	0.000	1086.733	1086.733	0	CHAR
0.10000	1.00000E-03	1.00000E-04	0.00000E+00	2500.0	0.000	679.903	679.903	0	CHAR
0.10000	1.00000E-03	1.00000E-04	0.00000E+00	2000.0	0.000	473.520	473.520	0	CHAR
0.10000	1.00000E-03	1.00000E-04	0.00000E+00	1500.0	0.000	318.445	318.445	0	CHAR
0.10000	1.00000E-03	1.00000E-04	0.00000E+00	1000.0	0.000	174.919	174.919	0	CHAR
0.10000	1.00000E-03	1.00000E-04	0.00000E+00	500.00	0.000	42.402	42.402	0	CHAR
0.10000	1.00000E-05	1000.0	0.00000E+00	3560.1	0.000	6838.477	6838.477	1	C*
0.10000	1.00000E-05	100.00	0.00000E+00	3557.5	0.000	6781.585	6781.585	1	C*
0.10000	1.00000E-05	20.000	0.00000E+00	3547.7	0.000	6524.796	6524.796	1	C*
0.10000	1.00000E-05	10.000	0.00000E+00	3536.9	0.000	6220.773	6220.773	1	C*
0.10000	1.00000E-05	5.0000	0.00000E+00	3517.9	0.000	5679.549	5679.549	1	C*
0.10000	1.00000E-05	1.0000	0.00000E+00	3412.6	0.000	3234.315	3234.315	1	C*
0.10000	1.00000E-05	0.50000	0.00000E+00	3323.3	0.000	1975.067	1975.067	1	C*
0.10000	1.00000E-05	0.40000	0.00000E+00	3284.0	0.000	1607.043	1607.043	1	C*
0.10000	1.00000E-05	0.30000	0.00000E+00	3218.7	0.000	1172.649	1172.649	1	C*
0.10000	1.00000E-05	0.20000	0.00000E+00	3033.9	0.000	621.833	621.833	1	C*
0.10000	1.00000E-05	1.00000E-04	0.00000E+00	3000.0	0.000	1082.304	1082.304	0	CHAR
0.10000	1.00000E-05	1.00000E-04	0.00000E+00	2500.0	0.000	681.553	681.553	0	CHAR
0.10000	1.00000E-05	1.00000E-04	0.00000E+00	2000.0	0.000	479.521	479.521	0	CHAR
0.10000	1.00000E-05	1.00000E-04	0.00000E+00	1500.0	0.000	325.387	325.387	0	CHAR
0.10000	1.00000E-05	1.00000E-04	0.00000E+00	1000.0	0.000	182.136	182.136	0	CHAR
0.10000	1.00000E-05	1.00000E-04	0.00000E+00	500.00	0.000	49.822	49.822	0	CHAR
5.00000E-02	10.000	1000.0	0.00000E+00	3461.4	0.000	6764.434	6764.434	1	C*
5.00000E-02	10.000	100.00	0.00000E+00	3391.1	0.000	6331.689	6331.689	1	C*
5.00000E-02	10.000	20.000	0.00000E+00	3203.6	0.000	5589.528	5589.528	1	C*
5.00000E-02	10.000	10.000	0.00000E+00	3092.0	0.000	5101.508	5101.508	1	C*
5.00000E-02	10.000	5.0000	0.00000E+00	2976.8	0.000	4400.519	4400.519	1	C*
5.00000E-02	10.000	1.0000	0.00000E+00	2702.6	0.000	2561.554	2561.554	1	C*
5.00000E-02	10.000	0.50000	0.00000E+00	2580.8	0.000	1961.979	1961.979	1	C*
5.00000E-02	10.000	0.40000	0.00000E+00	2542.2	0.000	1805.626	1805.626	1	C*
5.00000E-02	10.000	0.30000	0.00000E+00	2493.6	0.000	1630.080	1630.080	1	C*
5.00000E-02	10.000	0.20000	0.00000E+00	2429.3	0.000	1429.426	1429.426	1	C*
5.00000E-02	10.000	0.10000	0.00000E+00	2336.9	0.000	1193.607	1193.607	1	C*
5.00000E-02	10.000	1.00000E-02	0.00000E+00	2201.1	0.000	931.892	931.892	1	C*
5.00000E-02	10.000	1.00000E-03	0.00000E+00	2182.0	0.000	901.329	901.329	1	C*
5.00000E-02	10.000	1.00000E-04	0.00000E+00	2180.1	0.000	898.208	898.208	1	C*
5.00000E-02	10.000	1.00000E-04	0.00000E+00	2000.0	0.000	671.845	671.845	0	CHAR
5.00000E-02	10.000	1.00000E-04	0.00000E+00	1500.0	0.000	214.461	214.461	0	CHAR
5.00000E-02	10.000	1.00000E-04	0.00000E+00	1000.0	0.000	-225.884	-225.884	0	CHAR
5.00000E-02	10.000	1.00000E-04	0.00000E+00	500.00	0.000	-1855.597	-1855.597	0	CHAR
5.00000E-02	2.5000	1000.0	0.00000E+00	3467.7	0.000	6807.321	6807.321	1	C*
5.00000E-02	2.5000	100.00	0.00000E+00	3446.9	0.000	6630.033	6630.033	1	C*
5.00000E-02	2.5000	20.000	0.00000E+00	3368.0	0.000	6046.412	6046.412	1	C*
5.00000E-02	2.5000	10.000	0.00000E+00	3293.0	0.000	5601.097	5601.097	1	C*
5.00000E-02	2.5000	5.0000	0.00000E+00	3191.0	0.000	5061.160	5061.160	1	C*
5.00000E-02	2.5000	1.0000	0.00000E+00	2899.0	0.000	3240.191	3240.191	1	C*
5.00000E-02	2.5000	0.50000	0.00000E+00	2742.1	0.000	2317.213	2317.213	1	C*
5.00000E-02	2.5000	0.40000	0.00000E+00	2681.1	0.000	2024.675	2024.675	1	C*
5.00000E-02	2.5000	0.30000	0.00000E+00	2588.7	0.000	1653.665	1653.665	1	C*
5.00000E-02	2.5000	0.20000	0.00000E+00	2411.9	0.000	1146.147	1146.147	1	C*
5.00000E-02	2.5000	0.10000	0.00000E+00	1038.3	0.000	-176.390	-176.390	1	C*
5.00000E-02	2.5000	1.00000E-02	0.00000E+00	903.26	0.000	-375.488	-375.488	1	C*
5.00000E-02	2.5000	1.00000E-03	0.00000E+00	898.43	0.000	-389.613	-389.613	1	C*
5.00000E-02	2.5000	1.00000E-04	0.00000E+00	897.97	0.000	-391.016	-391.016	1	C*

5.00000E-02	2.5000	1.00000E-04	0.00000E+00	500.00	0.000	-1595.092	-1595.092	0	CHAR
5.00000E-02	1.0000	1000.0	0.00000E+00	3469.0	0.000	6816.143	6816.143	1	C*
5.00000E-02	1.0000	100.00	0.00000E+00	3459.1	0.000	6708.451	6708.451	1	C*
5.00000E-02	1.0000	20.000	0.00000E+00	3419.4	0.000	6279.041	6279.041	1	C*
5.00000E-02	1.0000	10.000	0.00000E+00	3376.6	0.000	5852.298	5852.298	1	C*
5.00000E-02	1.0000	5.0000	0.00000E+00	3306.7	0.000	5242.988	5242.988	1	C*
5.00000E-02	1.0000	1.0000	0.00000E+00	3036.5	0.000	3373.236	3373.236	1	C*
5.00000E-02	1.0000	0.50000	0.00000E+00	2873.7	0.000	2414.504	2414.504	1	C*
5.00000E-02	1.0000	0.40000	0.00000E+00	2807.6	0.000	2086.682	2086.682	1	C*
5.00000E-02	1.0000	0.30000	0.00000E+00	2699.7	0.000	1641.628	1641.628	1	C*
5.00000E-02	1.0000	0.20000	0.00000E+00	2431.7	0.000	933.526	933.526	1	C*
5.00000E-02	1.0000	0.10000	0.00000E+00	903.70	0.000	-318.850	-318.850	1	C*
5.00000E-02	1.0000	1.00000E-02	0.00000E+00	836.21	0.000	-537.230	-537.230	1	C*
5.00000E-02	1.0000	1.00000E-03	0.00000E+00	830.85	0.000	-559.626	-559.626	1	C*
5.00000E-02	1.0000	1.00000E-04	0.00000E+00	830.31	0.000	-561.881	-561.881	1	C*
5.00000E-02	1.0000	1.00000E-04	0.00000E+00	500.00	0.000	-1308.571	-1308.571	0	CHAR
5.00000E-02	0.25000	1000.0	0.00000E+00	3469.6	0.000	6820.584	6820.584	1	C*
5.00000E-02	0.25000	100.00	0.00000E+00	3465.3	0.000	6750.507	6750.507	1	C*
5.00000E-02	0.25000	20.000	0.00000E+00	3448.2	0.000	6443.201	6443.201	1	C*
5.00000E-02	0.25000	10.000	0.00000E+00	3429.0	0.000	6092.832	6092.832	1	C*
5.00000E-02	0.25000	5.0000	0.00000E+00	3395.1	0.000	5499.791	5499.791	1	C*
5.00000E-02	0.25000	1.0000	0.00000E+00	3214.1	0.000	3221.716	3221.716	1	C*
5.00000E-02	0.25000	0.50000	0.00000E+00	3066.4	0.000	2204.617	2204.617	1	C*
5.00000E-02	0.25000	0.40000	0.00000E+00	3002.0	0.000	1893.512	1893.512	1	C*
5.00000E-02	0.25000	0.30000	0.00000E+00	2893.3	0.000	1480.824	1480.824	1	C*
5.00000E-02	0.25000	0.20000	0.00000E+00	2552.7	0.000	730.446	730.446	1	C*
5.00000E-02	0.25000	0.15000	0.00000E+00	914.27	0.000	-234.022	-234.022	1	C*
5.00000E-02	0.25000	0.10000	0.00000E+00	831.99	0.000	-404.934	-404.934	1	C*
5.00000E-02	0.25000	1.00000E-02	0.00000E+00	656.01	0.000	-774.435	-774.435	1	C*
5.00000E-02	0.25000	1.00000E-03	0.00000E+00	564.31	0.000	-868.187	-868.187	1	C*
5.00000E-02	0.25000	1.00000E-04	0.00000E+00	553.84	0.000	-876.535	-876.535	1	C*
5.00000E-02	0.25000	1.00000E-04	0.00000E+00	500.00	0.000	-908.510	-908.510	0	CHAR
5.00000E-02	1.00000E-02	1000.0	0.00000E+00	3469.8	0.000	6822.010	6822.010	1	C*
5.00000E-02	1.00000E-02	100.00	0.00000E+00	3467.3	0.000	6764.386	6764.386	1	C*
5.00000E-02	1.00000E-02	20.000	0.00000E+00	3457.8	0.000	6504.410	6504.410	1	C*
5.00000E-02	1.00000E-02	10.000	0.00000E+00	3447.4	0.000	6197.288	6197.288	1	C*
5.00000E-02	1.00000E-02	5.0000	0.00000E+00	3428.8	0.000	5651.890	5651.890	1	C*
5.00000E-02	1.00000E-02	1.0000	0.00000E+00	3325.5	0.000	3205.913	3205.913	1	C*
5.00000E-02	1.00000E-02	0.50000	0.00000E+00	3236.8	0.000	1958.594	1958.594	1	C*
5.00000E-02	1.00000E-02	0.40000	0.00000E+00	3197.3	0.000	1596.010	1596.010	1	C*
5.00000E-02	1.00000E-02	0.30000	0.00000E+00	3130.5	0.000	1169.260	1169.260	1	C*
5.00000E-02	1.00000E-02	0.20000	0.00000E+00	2923.7	0.000	623.646	623.646	1	C*
5.00000E-02	1.00000E-02	1.00000E-04	0.00000E+00	2500.0	0.000	664.435	664.435	0	CHAR
5.00000E-02	1.00000E-02	1.00000E-04	0.00000E+00	2000.0	0.000	416.331	416.331	0	CHAR
5.00000E-02	1.00000E-02	1.00000E-04	0.00000E+00	1500.0	0.000	255.806	255.806	0	CHAR
5.00000E-02	1.00000E-02	1.00000E-04	0.00000E+00	1000.0	0.000	109.957	109.957	0	CHAR
5.00000E-02	1.00000E-02	1.00000E-04	0.00000E+00	500.00	0.000	-24.390	-24.390	0	CHAR
5.00000E-02	1.00000E-03	1000.0	0.00000E+00	3469.8	0.000	6822.064	6822.064	1	C*
5.00000E-02	1.00000E-03	100.00	0.00000E+00	3467.4	0.000	6764.910	6764.910	1	C*
5.00000E-02	1.00000E-03	20.000	0.00000E+00	3458.2	0.000	6506.795	6506.795	1	C*
5.00000E-02	1.00000E-03	10.000	0.00000E+00	3448.1	0.000	6201.519	6201.519	1	C*
5.00000E-02	1.00000E-03	5.0000	0.00000E+00	3430.1	0.000	5658.566	5658.566	1	C*
5.00000E-02	1.00000E-03	1.0000	0.00000E+00	3330.4	0.000	3210.271	3210.271	1	C*
5.00000E-02	1.00000E-03	0.50000	0.00000E+00	3245.4	0.000	1952.274	1952.274	1	C*
5.00000E-02	1.00000E-03	0.40000	0.00000E+00	3208.0	0.000	1585.132	1585.132	1	C*
5.00000E-02	1.00000E-03	0.30000	0.00000E+00	3145.6	0.000	1152.265	1152.265	1	C*
5.00000E-02	1.00000E-03	0.20000	0.00000E+00	2967.1	0.000	604.756	604.756	1	C*
5.00000E-02	1.00000E-03	1.00000E-04	0.00000E+00	2500.0	0.000	697.663	697.663	0	CHAR

5.00000E-02	1.00000E-03	1.00000E-04	0.00000E+00	2000.0	0.000	474.502	474.502	0	CHAR
5.00000E-02	1.00000E-03	1.00000E-04	0.00000E+00	1500.0	0.000	318.455	318.455	0	CHAR
5.00000E-02	1.00000E-03	1.00000E-04	0.00000E+00	1000.0	0.000	174.919	174.919	0	CHAR
5.00000E-02	1.00000E-03	1.00000E-04	0.00000E+00	500.00	0.000	42.402	42.402	0	CHAR
5.00000E-02	1.00000E-05	1000.0	0.00000E+00	3469.8	0.000	6822.070	6822.070	1	C*
5.00000E-02	1.00000E-05	100.00	0.00000E+00	3467.4	0.000	6764.968	6764.968	1	C*
5.00000E-02	1.00000E-05	20.000	0.00000E+00	3458.2	0.000	6507.058	6507.058	1	C*
5.00000E-02	1.00000E-05	10.000	0.00000E+00	3448.2	0.000	6201.986	6201.986	1	C*
5.00000E-02	1.00000E-05	5.0000	0.00000E+00	3430.3	0.000	5659.305	5659.305	1	C*
5.00000E-02	1.00000E-05	1.0000	0.00000E+00	3330.9	0.000	3210.786	3210.786	1	C*
5.00000E-02	1.00000E-05	0.50000	0.00000E+00	3246.3	0.000	1951.633	1951.633	1	C*
5.00000E-02	1.00000E-05	0.40000	0.00000E+00	3209.2	0.000	1583.993	1583.993	1	C*
5.00000E-02	1.00000E-05	0.30000	0.00000E+00	3147.2	0.000	1150.444	1150.444	1	C*
5.00000E-02	1.00000E-05	0.20000	0.00000E+00	2971.9	0.000	602.500	602.500	1	C*
5.00000E-02	1.00000E-05	1.00000E-04	0.00000E+00	2500.0	0.000	698.366	698.366	0	CHAR
5.00000E-02	1.00000E-05	1.00000E-04	0.00000E+00	2000.0	0.000	480.356	480.356	0	CHAR
5.00000E-02	1.00000E-05	1.00000E-04	0.00000E+00	1500.0	0.000	325.392	325.392	0	CHAR
5.00000E-02	1.00000E-05	1.00000E-04	0.00000E+00	1000.0	0.000	182.136	182.136	0	CHAR
5.00000E-02	1.00000E-05	1.00000E-04	0.00000E+00	500.00	0.000	49.822	49.822	0	CHAR
1.00000E-02	10.000	1000.0	0.00000E+00	3269.3	0.000	6754.827	6754.827	1	C*
1.00000E-02	10.000	100.00	0.00000E+00	3211.4	0.000	6524.163	6524.163	1	C*
1.00000E-02	10.000	20.000	0.00000E+00	3066.4	0.000	6139.077	6139.077	1	C*
1.00000E-02	10.000	10.000	0.00000E+00	2975.3	0.000	5836.831	5836.831	1	C*
1.00000E-02	10.000	5.0000	0.00000E+00	2876.6	0.000	5272.982	5272.982	1	C*
1.00000E-02	10.000	1.0000	0.00000E+00	2638.9	0.000	3270.811	3270.811	1	C*
1.00000E-02	10.000	0.50000	0.00000E+00	2535.3	0.000	2503.233	2503.233	1	C*
1.00000E-02	10.000	0.40000	0.00000E+00	2502.4	0.000	2294.675	2294.675	1	C*
1.00000E-02	10.000	0.30000	0.00000E+00	2460.8	0.000	2055.971	2055.971	1	C*
1.00000E-02	10.000	0.20000	0.00000E+00	2405.0	0.000	1776.909	1776.909	1	C*
1.00000E-02	10.000	0.10000	0.00000E+00	2322.5	0.000	1441.066	1441.066	1	C*
1.00000E-02	10.000	1.00000E-02	0.00000E+00	2195.9	0.000	1066.003	1066.003	1	C*
1.00000E-02	10.000	1.00000E-03	0.00000E+00	2177.7	0.000	1023.029	1023.029	1	C*
1.00000E-02	10.000	1.00000E-04	0.00000E+00	2175.8	0.000	1018.656	1018.656	1	C*
1.00000E-02	10.000	1.00000E-04	0.00000E+00	2000.0	0.000	714.018	714.018	0	CHAR
1.00000E-02	10.000	1.00000E-04	0.00000E+00	1500.0	0.000	218.921	218.921	0	CHAR
1.00000E-02	10.000	1.00000E-04	0.00000E+00	1000.0	0.000	-218.454	-218.454	0	CHAR
1.00000E-02	10.000	1.00000E-04	0.00000E+00	500.00	0.000	-1824.460	-1824.460	0	CHAR
1.00000E-02	2.5000	1000.0	0.00000E+00	3274.8	0.000	6776.542	6776.542	1	C*
1.00000E-02	2.5000	100.00	0.00000E+00	3256.8	0.000	6659.670	6659.670	1	C*
1.00000E-02	2.5000	20.000	0.00000E+00	3192.9	0.000	6269.177	6269.177	1	C*
1.00000E-02	2.5000	10.000	0.00000E+00	3135.1	0.000	5957.102	5957.102	1	C*
1.00000E-02	2.5000	5.0000	0.00000E+00	3055.9	0.000	5557.133	5557.133	1	C*
1.00000E-02	2.5000	1.0000	0.00000E+00	2810.4	0.000	3960.333	3960.333	1	C*
1.00000E-02	2.5000	0.50000	0.00000E+00	2675.7	0.000	2933.053	2933.053	1	C*
1.00000E-02	2.5000	0.40000	0.00000E+00	2624.0	0.000	2577.678	2577.678	1	C*
1.00000E-02	2.5000	0.30000	0.00000E+00	2545.9	0.000	2106.018	2106.018	1	C*
1.00000E-02	2.5000	0.20000	0.00000E+00	2393.3	0.000	1416.113	1416.113	1	C*
1.00000E-02	2.5000	0.10000	0.00000E+00	963.21	0.000	-223.062	-223.062	1	C*
1.00000E-02	2.5000	1.00000E-02	0.00000E+00	841.46	0.000	-404.576	-404.576	1	C*
1.00000E-02	2.5000	1.00000E-03	0.00000E+00	837.24	0.000	-417.664	-417.664	1	C*
1.00000E-02	2.5000	1.00000E-04	0.00000E+00	836.83	0.000	-418.966	-418.966	1	C*
1.00000E-02	2.5000	1.00000E-04	0.00000E+00	500.00	0.000	-1569.011	-1569.011	0	CHAR
1.00000E-02	1.0000	1000.0	0.00000E+00	3275.9	0.000	6781.050	6781.050	1	C*
1.00000E-02	1.0000	100.00	0.00000E+00	3267.3	0.000	6698.149	6698.149	1	C*
1.00000E-02	1.0000	20.000	0.00000E+00	3233.9	0.000	6362.161	6362.161	1	C*
1.00000E-02	1.0000	10.000	0.00000E+00	3199.2	0.000	6021.755	6021.755	1	C*
1.00000E-02	1.0000	5.0000	0.00000E+00	3144.5	0.000	5519.453	5519.453	1	C*
1.00000E-02	1.0000	1.0000	0.00000E+00	2928.8	0.000	3875.429	3875.429	1	C*

1.00000E-02	1.0000	0.50000	0.00000E+00	2790.2	0.000	2934.419	2934.419	1	C*
1.00000E-02	1.0000	0.40000	0.00000E+00	2733.7	0.000	2578.899	2578.899	1	C*
1.00000E-02	1.0000	0.30000	0.00000E+00	2642.5	0.000	2063.709	2063.709	1	C*
1.00000E-02	1.0000	0.20000	0.00000E+00	2413.8	0.000	1150.452	1150.452	1	C*
1.00000E-02	1.0000	0.10000	0.00000E+00	841.31	0.000	-346.086	-346.086	1	C*
1.00000E-02	1.0000	1.00000E-02	0.00000E+00	782.27	0.000	-552.574	-552.574	1	C*
1.00000E-02	1.0000	1.00000E-03	0.00000E+00	777.56	0.000	-573.625	-573.625	1	C*
1.00000E-02	1.0000	1.00000E-04	0.00000E+00	777.10	0.000	-575.737	-575.737	1	C*
1.00000E-02	1.0000	1.00000E-04	0.00000E+00	500.00	0.000	-1288.237	-1288.237	0	CHAR
1.00000E-02	0.25000	1000.0	0.00000E+00	3276.5	0.000	6783.326	6783.326	1	C*
1.00000E-02	0.25000	100.00	0.00000E+00	3272.7	0.000	6719.266	6719.266	1	C*
1.00000E-02	0.25000	20.000	0.00000E+00	3258.0	0.000	6436.154	6436.154	1	C*
1.00000E-02	0.25000	10.000	0.00000E+00	3241.6	0.000	6112.327	6112.327	1	C*
1.00000E-02	0.25000	5.0000	0.00000E+00	3213.2	0.000	5561.777	5561.777	1	C*
1.00000E-02	0.25000	1.0000	0.00000E+00	3068.1	0.000	3400.996	3400.996	1	C*
1.00000E-02	0.25000	0.50000	0.00000E+00	2950.7	0.000	2414.765	2414.765	1	C*
1.00000E-02	0.25000	0.40000	0.00000E+00	2898.2	0.000	2113.433	2113.433	1	C*
1.00000E-02	0.25000	0.30000	0.00000E+00	2808.1	0.000	1707.555	1707.555	1	C*
1.00000E-02	0.25000	0.20000	0.00000E+00	2523.7	0.000	883.866	883.866	1	C*
1.00000E-02	0.25000	0.17500	0.00000E+00	2109.9	0.000	350.170	350.170	1	C*
1.00000E-02	0.25000	0.16250	0.00000E+00	902.49	0.000	-204.442	-204.442	1	C*
1.00000E-02	0.25000	0.15000	0.00000E+00	850.64	0.000	-257.178	-257.178	1	C*
1.00000E-02	0.25000	0.10000	0.00000E+00	778.36	0.000	-423.379	-423.379	1	C*
1.00000E-02	0.25000	1.00000E-04	0.00000E+00	500.00	0.000	-897.806	-897.806	0	CHAR
1.00000E-02	1.00000E-02	1000.0	0.00000E+00	3276.6	0.000	6784.057	6784.057	1	C*
1.00000E-02	1.00000E-02	100.00	0.00000E+00	3274.5	0.000	6726.307	6726.307	1	C*
1.00000E-02	1.00000E-02	20.000	0.00000E+00	3266.3	0.000	6465.336	6465.336	1	C*
1.00000E-02	1.00000E-02	10.000	0.00000E+00	3257.3	0.000	6157.535	6157.535	1	C*
1.00000E-02	1.00000E-02	5.0000	0.00000E+00	3241.1	0.000	5611.618	5611.618	1	C*
1.00000E-02	1.00000E-02	1.0000	0.00000E+00	3150.8	0.000	3168.000	3168.000	1	C*
1.00000E-02	1.00000E-02	0.50000	0.00000E+00	3073.3	0.000	1923.941	1923.941	1	C*
1.00000E-02	1.00000E-02	0.40000	0.00000E+00	3038.9	0.000	1562.726	1562.726	1	C*
1.00000E-02	1.00000E-02	0.30000	0.00000E+00	2981.0	0.000	1138.239	1138.239	1	C*
1.00000E-02	1.00000E-02	0.20000	0.00000E+00	2807.2	0.000	601.812	601.812	1	C*
1.00000E-02	1.00000E-02	1.00000E-04	0.00000E+00	2500.0	0.000	757.219	757.219	0	CHAR
1.00000E-02	1.00000E-02	1.00000E-04	0.00000E+00	2000.0	0.000	421.841	421.841	0	CHAR
1.00000E-02	1.00000E-02	1.00000E-04	0.00000E+00	1500.0	0.000	255.882	255.882	0	CHAR
1.00000E-02	1.00000E-02	1.00000E-04	0.00000E+00	1000.0	0.000	109.957	109.957	0	CHAR
1.00000E-02	1.00000E-02	1.00000E-04	0.00000E+00	500.00	0.000	-24.390	-24.390	0	CHAR
1.00000E-02	1.00000E-03	1000.0	0.00000E+00	3276.6	0.000	6784.084	6784.084	1	C*
1.00000E-02	1.00000E-03	100.00	0.00000E+00	3274.5	0.000	6726.574	6726.574	1	C*
1.00000E-02	1.00000E-03	20.000	0.00000E+00	3266.6	0.000	6466.490	6466.490	1	C*
1.00000E-02	1.00000E-03	10.000	0.00000E+00	3257.9	0.000	6159.432	6159.432	1	C*
1.00000E-02	1.00000E-03	5.0000	0.00000E+00	3242.2	0.000	5614.070	5614.070	1	C*
1.00000E-02	1.00000E-03	1.0000	0.00000E+00	3154.6	0.000	3160.701	3160.701	1	C*
1.00000E-02	1.00000E-03	0.50000	0.00000E+00	3079.4	0.000	1903.227	1903.227	1	C*
1.00000E-02	1.00000E-03	0.40000	0.00000E+00	3046.2	0.000	1536.893	1536.893	1	C*
1.00000E-02	1.00000E-03	0.30000	0.00000E+00	2990.9	0.000	1105.757	1105.757	1	C*
1.00000E-02	1.00000E-03	0.20000	0.00000E+00	2833.1	0.000	564.410	564.410	1	C*
1.00000E-02	1.00000E-03	1.00000E-04	0.00000E+00	2500.0	0.000	768.080	768.080	0	CHAR
1.00000E-02	1.00000E-03	1.00000E-04	0.00000E+00	2000.0	0.000	478.504	478.504	0	CHAR
1.00000E-02	1.00000E-03	1.00000E-04	0.00000E+00	1500.0	0.000	318.494	318.494	0	CHAR
1.00000E-02	1.00000E-03	1.00000E-04	0.00000E+00	1000.0	0.000	174.919	174.919	0	CHAR
1.00000E-02	1.00000E-03	1.00000E-04	0.00000E+00	500.00	0.000	42.402	42.402	0	CHAR
1.00000E-02	1.00000E-05	1000.0	0.00000E+00	3276.6	0.000	6784.087	6784.087	1	C*
1.00000E-02	1.00000E-05	100.00	0.00000E+00	3274.5	0.000	6726.603	6726.603	1	C*
1.00000E-02	1.00000E-05	20.000	0.00000E+00	3266.7	0.000	6466.618	6466.618	1	C*
1.00000E-02	1.00000E-05	10.000	0.00000E+00	3257.9	0.000	6159.641	6159.641	1	C*

1.00000E-02	1.00000E-05	5.0000	0.00000E+00	3242.4	0.000	5614.343	5614.343	1	C*
1.00000E-02	1.00000E-05	1.0000	0.00000E+00	3155.0	0.000	3159.913	3159.913	1	C*
1.00000E-02	1.00000E-05	0.50000	0.00000E+00	3080.1	0.000	1900.958	1900.958	1	C*
1.00000E-02	1.00000E-05	0.40000	0.00000E+00	3047.1	0.000	1534.052	1534.052	1	C*
1.00000E-02	1.00000E-05	0.30000	0.00000E+00	2992.0	0.000	1102.160	1102.160	1	C*
1.00000E-02	1.00000E-05	0.20000	0.00000E+00	2836.0	0.000	560.066	560.066	1	C*
1.00000E-02	1.00000E-05	1.00000E-04	0.00000E+00	2500.0	0.000	766.076	766.076	0	CHAR
1.00000E-02	1.00000E-05	1.00000E-04	0.00000E+00	2000.0	0.000	483.868	483.868	0	CHAR
1.00000E-02	1.00000E-05	1.00000E-04	0.00000E+00	1500.0	0.000	325.415	325.415	0	CHAR
1.00000E-02	1.00000E-05	1.00000E-04	0.00000E+00	1000.0	0.000	182.136	182.136	0	CHAR
1.00000E-02	1.00000E-05	1.00000E-04	0.00000E+00	500.00	0.000	49.822	49.822	0	CHAR
1.00000E-03	10.000	1000.0	0.00000E+00	3028.6	0.000	6740.558	6740.558	1	C*
1.00000E-03	10.000	100.00	0.00000E+00	2982.8	0.000	6725.463	6725.463	1	C*
1.00000E-03	10.000	20.000	0.00000E+00	2877.0	0.000	6792.191	6792.191	1	C*
1.00000E-03	10.000	10.000	0.00000E+00	2810.7	0.000	6792.845	6792.845	1	C*
1.00000E-03	10.000	5.0000	0.00000E+00	2735.3	0.000	6592.032	6592.032	1	C*
1.00000E-03	10.000	1.0000	0.00000E+00	2541.9	0.000	4840.952	4840.952	1	C*
1.00000E-03	10.000	0.50000	0.00000E+00	2457.7	0.000	3843.843	3843.843	1	C*
1.00000E-03	10.000	0.40000	0.00000E+00	2431.3	0.000	3546.051	3546.051	1	C*
1.00000E-03	10.000	0.30000	0.00000E+00	2398.1	0.000	3191.062	3191.062	1	C*
1.00000E-03	10.000	0.20000	0.00000E+00	2353.5	0.000	2755.680	2755.680	1	C*
1.00000E-03	10.000	0.10000	0.00000E+00	2286.8	0.000	2198.419	2198.419	1	C*
1.00000E-03	10.000	1.00000E-02	0.00000E+00	2179.5	0.000	1526.786	1526.786	1	C*
1.00000E-03	10.000	1.00000E-03	0.00000E+00	2163.4	0.000	1446.975	1446.975	1	C*
1.00000E-03	10.000	1.00000E-04	0.00000E+00	2161.7	0.000	1438.833	1438.833	1	C*
1.00000E-03	10.000	1.00000E-04	0.00000E+00	2000.0	0.000	877.997	877.997	0	CHAR
1.00000E-03	10.000	1.00000E-04	0.00000E+00	1500.0	0.000	221.687	221.687	0	CHAR
1.00000E-03	10.000	1.00000E-04	0.00000E+00	1000.0	0.000	-217.235	-217.235	0	CHAR
1.00000E-03	10.000	1.00000E-04	0.00000E+00	500.00	0.000	-1731.553	-1731.553	0	CHAR
1.00000E-03	2.5000	1000.0	0.00000E+00	3033.2	0.000	6739.676	6739.676	1	C*
1.00000E-03	2.5000	100.00	0.00000E+00	3018.4	0.000	6687.004	6687.004	1	C*
1.00000E-03	2.5000	20.000	0.00000E+00	2968.6	0.000	6504.425	6504.425	1	C*
1.00000E-03	2.5000	10.000	0.00000E+00	2925.9	0.000	6351.887	6351.887	1	C*
1.00000E-03	2.5000	5.0000	0.00000E+00	2868.8	0.000	6146.591	6146.591	1	C*
1.00000E-03	2.5000	1.0000	0.00000E+00	2684.0	0.000	5164.460	5164.460	1	C*
1.00000E-03	2.5000	0.50000	0.00000E+00	2575.8	0.000	4219.221	4219.221	1	C*
1.00000E-03	2.5000	0.40000	0.00000E+00	2534.2	0.000	3816.166	3816.166	1	C*
1.00000E-03	2.5000	0.30000	0.00000E+00	2471.9	0.000	3218.424	3218.424	1	C*
1.00000E-03	2.5000	0.20000	0.00000E+00	2351.0	0.000	2203.711	2203.711	1	C*
1.00000E-03	2.5000	0.15000	0.00000E+00	2201.5	0.000	1335.404	1335.404	1	C*
1.00000E-03	2.5000	0.12500	0.00000E+00	2018.0	0.000	746.061	746.061	1	C*
1.00000E-03	2.5000	0.11250	0.00000E+00	1795.4	0.000	402.068	402.068	1	C*
1.00000E-03	2.5000	0.10938	0.00000E+00	1671.7	0.000	284.767	284.767	1	C*
1.00000E-03	2.5000	0.10781	0.00000E+00	1559.6	0.000	195.818	195.818	1	C*
1.00000E-03	2.5000	0.10703	0.00000E+00	1456.0	0.000	120.368	120.368	1	C*
1.00000E-03	2.5000	0.10625	0.00000E+00	1055.1	0.000	-153.738	-153.738	1	C*
1.00000E-03	2.5000	0.10000	0.00000E+00	866.61	0.000	-284.871	-284.871	1	C*
1.00000E-03	2.5000	1.00000E-02	0.00000E+00	765.42	0.000	-448.589	-448.589	1	C*
1.00000E-03	2.5000	1.00000E-03	0.00000E+00	761.90	0.000	-460.951	-460.951	1	C*
1.00000E-03	2.5000	1.00000E-04	0.00000E+00	761.56	0.000	-462.183	-462.183	1	C*
1.00000E-03	2.5000	1.00000E-04	0.00000E+00	500.00	0.000	-1490.521	-1490.521	0	CHAR
1.00000E-03	1.0000	1000.0	0.00000E+00	3034.2	0.000	6739.568	6739.568	1	C*
1.00000E-03	1.0000	100.00	0.00000E+00	3027.0	0.000	6683.038	6683.038	1	C*
1.00000E-03	1.0000	20.000	0.00000E+00	3000.0	0.000	6445.881	6445.881	1	C*
1.00000E-03	1.0000	10.000	0.00000E+00	2973.0	0.000	6198.069	6198.069	1	C*
1.00000E-03	1.0000	5.0000	0.00000E+00	2932.0	0.000	5819.026	5819.026	1	C*
1.00000E-03	1.0000	1.0000	0.00000E+00	2774.8	0.000	4541.218	4541.218	1	C*
1.00000E-03	1.0000	0.50000	0.00000E+00	2669.2	0.000	3804.747	3804.747	1	C*

1.00000E-03	1.0000	0.40000	0.00000E+00	2624.9	0.000	3489.904	3489.904	1	C*
1.00000E-03	1.0000	0.30000	0.00000E+00	2552.9	0.000	2966.848	2966.848	1	C*
1.00000E-03	1.0000	0.20000	0.00000E+00	2373.1	0.000	1774.951	1774.951	1	C*
1.00000E-03	1.0000	0.17500	0.00000E+00	2237.9	0.000	1143.774	1143.774	1	C*
1.00000E-03	1.0000	0.16250	0.00000E+00	2097.6	0.000	728.527	728.527	1	C*
1.00000E-03	1.0000	0.15000	0.00000E+00	1725.1	0.000	249.472	249.472	1	C*
1.00000E-03	1.0000	0.14844	0.00000E+00	1566.8	0.000	144.260	144.260	1	C*
1.00000E-03	1.0000	0.14766	0.00000E+00	1347.2	0.000	16.807	16.807	1	C*
1.00000E-03	1.0000	0.14688	0.00000E+00	934.76	0.000	-209.857	-209.857	1	C*
1.00000E-03	1.0000	0.14375	0.00000E+00	859.53	0.000	-255.396	-255.396	1	C*
1.00000E-03	1.0000	0.13750	0.00000E+00	822.74	0.000	-285.851	-285.851	1	C*
1.00000E-03	1.0000	0.12500	0.00000E+00	793.36	0.000	-323.534	-323.534	1	C*
1.00000E-03	1.0000	0.10000	0.00000E+00	765.47	0.000	-383.456	-383.456	1	C*
1.00000E-03	1.0000	1.00000E-02	0.00000E+00	715.37	0.000	-582.257	-582.257	1	C*
1.00000E-03	1.0000	1.00000E-03	0.00000E+00	711.28	0.000	-602.507	-602.507	1	C*
1.00000E-03	1.0000	1.00000E-04	0.00000E+00	710.87	0.000	-604.539	-604.539	1	C*
1.00000E-03	1.0000	1.00000E-04	0.00000E+00	500.00	0.000	-1226.405	-1226.405	0	CHAR
1.00000E-03	0.25000	1000.0	0.00000E+00	3034.6	0.000	6739.522	6739.522	1	C*
1.00000E-03	0.25000	100.00	0.00000E+00	3031.5	0.000	6681.783	6681.783	1	C*
1.00000E-03	0.25000	20.000	0.00000E+00	3019.4	0.000	6424.141	6424.141	1	C*
1.00000E-03	0.25000	10.000	0.00000E+00	3006.0	0.000	6128.084	6128.084	1	C*
1.00000E-03	0.25000	5.0000	0.00000E+00	2983.2	0.000	5621.632	5621.632	1	C*
1.00000E-03	0.25000	1.0000	0.00000E+00	2871.9	0.000	3592.172	3592.172	1	C*
1.00000E-03	0.25000	0.50000	0.00000E+00	2785.6	0.000	2659.345	2659.345	1	C*
1.00000E-03	0.25000	0.40000	0.00000E+00	2747.4	0.000	2384.252	2384.252	1	C*
1.00000E-03	0.25000	0.30000	0.00000E+00	2681.5	0.000	2028.266	2028.266	1	C*
1.00000E-03	0.25000	0.20000	0.00000E+00	2468.1	0.000	1247.910	1247.910	1	C*
1.00000E-03	0.25000	0.17500	0.00000E+00	2110.6	0.000	447.404	447.404	1	C*
1.00000E-03	0.25000	0.16875	0.00000E+00	1629.7	0.000	98.552	98.552	1	C*
1.00000E-03	0.25000	0.16836	0.00000E+00	1505.0	0.000	45.460	45.460	1	C*
1.00000E-03	0.25000	0.16816	0.00000E+00	1375.2	0.000	-6.999	-6.999	1	C*
1.00000E-03	0.25000	0.16797	0.00000E+00	990.95	0.000	-156.463	-156.463	1	C*
1.00000E-03	0.25000	0.16719	0.00000E+00	886.65	0.000	-197.898	-197.898	1	C*
1.00000E-03	0.25000	0.16563	0.00000E+00	846.83	0.000	-216.890	-216.890	1	C*
1.00000E-03	0.25000	0.16250	0.00000E+00	816.78	0.000	-236.313	-236.313	1	C*
1.00000E-03	0.25000	0.15000	0.00000E+00	774.35	0.000	-285.434	-285.434	1	C*
1.00000E-03	0.25000	0.10000	0.00000E+00	713.10	0.000	-447.758	-447.758	1	C*
1.00000E-03	0.25000	1.00000E-02	0.00000E+00	574.39	0.000	-770.578	-770.578	1	C*
1.00000E-03	0.25000	1.00000E-03	0.00000E+00	543.61	0.000	-814.761	-814.761	1	C*
1.00000E-03	0.25000	1.00000E-04	0.00000E+00	540.09	0.000	-819.699	-819.699	1	C*
1.00000E-03	0.25000	1.00000E-04	0.00000E+00	500.00	0.000	-865.928	-865.928	0	CHAR
1.00000E-03	1.00000E-02	1000.0	0.00000E+00	3034.8	0.000	6739.509	6739.509	1	C*
1.00000E-03	1.00000E-02	100.00	0.00000E+00	3033.0	0.000	6681.497	6681.497	1	C*
1.00000E-03	1.00000E-02	20.000	0.00000E+00	3026.3	0.000	6419.127	6419.127	1	C*
1.00000E-03	1.00000E-02	10.000	0.00000E+00	3018.8	0.000	6110.326	6110.326	1	C*
1.00000E-03	1.00000E-02	5.0000	0.00000E+00	3005.4	0.000	5563.381	5563.381	1	C*
1.00000E-03	1.00000E-02	1.0000	0.00000E+00	2929.7	0.000	3119.321	3119.321	1	C*
1.00000E-03	1.00000E-02	0.50000	0.00000E+00	2864.5	0.000	1876.694	1876.694	1	C*
1.00000E-03	1.00000E-02	0.40000	0.00000E+00	2835.7	0.000	1516.320	1516.320	1	C*
1.00000E-03	1.00000E-02	0.30000	0.00000E+00	2787.4	0.000	1093.567	1093.567	1	C*
1.00000E-03	1.00000E-02	0.20000	0.00000E+00	2646.4	0.000	565.927	565.927	1	C*
1.00000E-03	1.00000E-02	1.00000E-04	0.00000E+00	2500.0	0.000	1029.801	1029.801	0	CHAR
1.00000E-03	1.00000E-02	1.00000E-04	0.00000E+00	2000.0	0.000	441.927	441.927	0	CHAR
1.00000E-03	1.00000E-02	1.00000E-04	0.00000E+00	1500.0	0.000	256.098	256.098	0	CHAR
1.00000E-03	1.00000E-02	1.00000E-04	0.00000E+00	1000.0	0.000	109.957	109.957	0	CHAR
1.00000E-03	1.00000E-02	1.00000E-04	0.00000E+00	500.00	0.000	-24.390	-24.390	0	CHAR
1.00000E-03	1.00000E-03	1000.0	0.00000E+00	3034.8	0.000	6739.508	6739.508	1	C*
1.00000E-03	1.00000E-03	100.00	0.00000E+00	3033.0	0.000	6681.488	6681.488	1	C*

1.00000E-03	1.00000E-03	20.000	0.00000E+00	3026.6	0.000	6418.962	6418.962	1	C*
1.00000E-03	1.00000E-03	10.000	0.00000E+00	3019.3	0.000	6109.731	6109.731	1	C*
1.00000E-03	1.00000E-03	5.0000	0.00000E+00	3006.3	0.000	5561.360	5561.360	1	C*
1.00000E-03	1.00000E-03	1.0000	0.00000E+00	2932.4	0.000	3100.252	3100.252	1	C*
1.00000E-03	1.00000E-03	0.50000	0.00000E+00	2868.6	0.000	1841.921	1841.921	1	C*
1.00000E-03	1.00000E-03	0.40000	0.00000E+00	2840.3	0.000	1476.050	1476.050	1	C*
1.00000E-03	1.00000E-03	0.30000	0.00000E+00	2793.1	0.000	1046.361	1046.361	1	C*
1.00000E-03	1.00000E-03	0.20000	0.00000E+00	2658.6	0.000	511.419	511.419	1	C*
1.00000E-03	1.00000E-03	1.00000E-04	0.00000E+00	2500.0	0.000	988.747	988.747	0	CHAR
1.00000E-03	1.00000E-03	1.00000E-04	0.00000E+00	2000.0	0.000	493.529	493.529	0	CHAR
1.00000E-03	1.00000E-03	1.00000E-04	0.00000E+00	1500.0	0.000	318.619	318.619	0	CHAR
1.00000E-03	1.00000E-03	1.00000E-04	0.00000E+00	1000.0	0.000	174.919	174.919	0	CHAR
1.00000E-03	1.00000E-03	1.00000E-04	0.00000E+00	500.00	0.000	42.402	42.402	0	CHAR
1.00000E-03	1.00000E-05	1000.0	0.00000E+00	3034.8	0.000	6739.508	6739.508	1	C*
1.00000E-03	1.00000E-05	100.00	0.00000E+00	3033.1	0.000	6681.487	6681.487	1	C*
1.00000E-03	1.00000E-05	20.000	0.00000E+00	3026.6	0.000	6418.944	6418.944	1	C*
1.00000E-03	1.00000E-05	10.000	0.00000E+00	3019.4	0.000	6109.666	6109.666	1	C*
1.00000E-03	1.00000E-05	5.0000	0.00000E+00	3006.4	0.000	5561.138	5561.138	1	C*
1.00000E-03	1.00000E-05	1.0000	0.00000E+00	2932.7	0.000	3098.151	3098.151	1	C*
1.00000E-03	1.00000E-05	0.50000	0.00000E+00	2869.0	0.000	1838.075	1838.075	1	C*
1.00000E-03	1.00000E-05	0.40000	0.00000E+00	2840.8	0.000	1471.588	1471.588	1	C*
1.00000E-03	1.00000E-05	0.30000	0.00000E+00	2793.7	0.000	1041.113	1041.113	1	C*
1.00000E-03	1.00000E-05	0.20000	0.00000E+00	2659.9	0.000	505.248	505.248	1	C*
1.00000E-03	1.00000E-05	1.00000E-04	0.00000E+00	2500.0	0.000	982.887	982.887	0	CHAR
1.00000E-03	1.00000E-05	1.00000E-04	0.00000E+00	2000.0	0.000	497.475	497.475	0	CHAR
1.00000E-03	1.00000E-05	1.00000E-04	0.00000E+00	1500.0	0.000	325.502	325.502	0	CHAR
1.00000E-03	1.00000E-05	1.00000E-04	0.00000E+00	1000.0	0.000	182.136	182.136	0	CHAR
1.00000E-03	1.00000E-05	1.00000E-04	0.00000E+00	500.00	0.000	49.822	49.822	0	CHAR

Appendix D

IR Reflectant Spectra for Selected Post-Test Samples

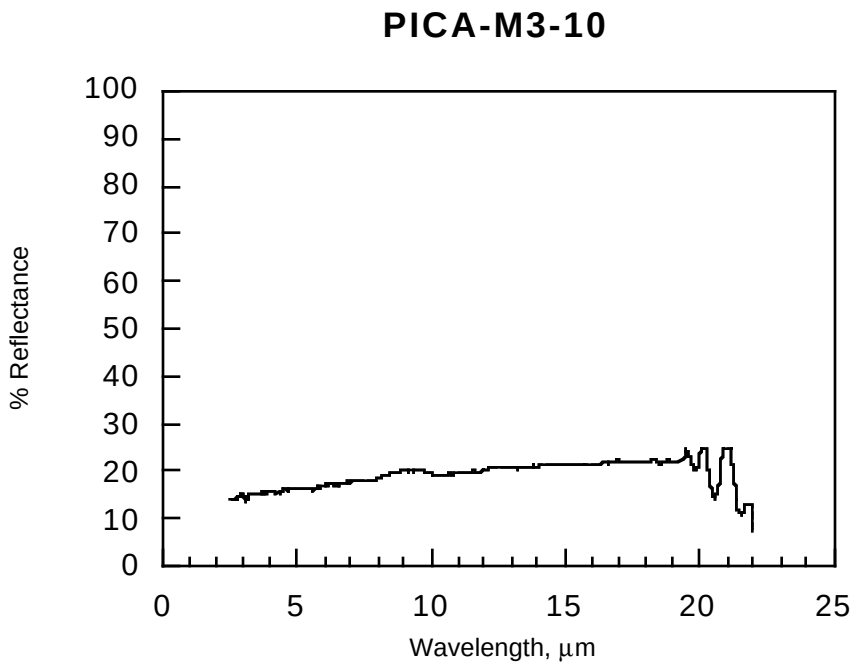

Figure D1. IR reflectant spectra for post-test standard PICA.

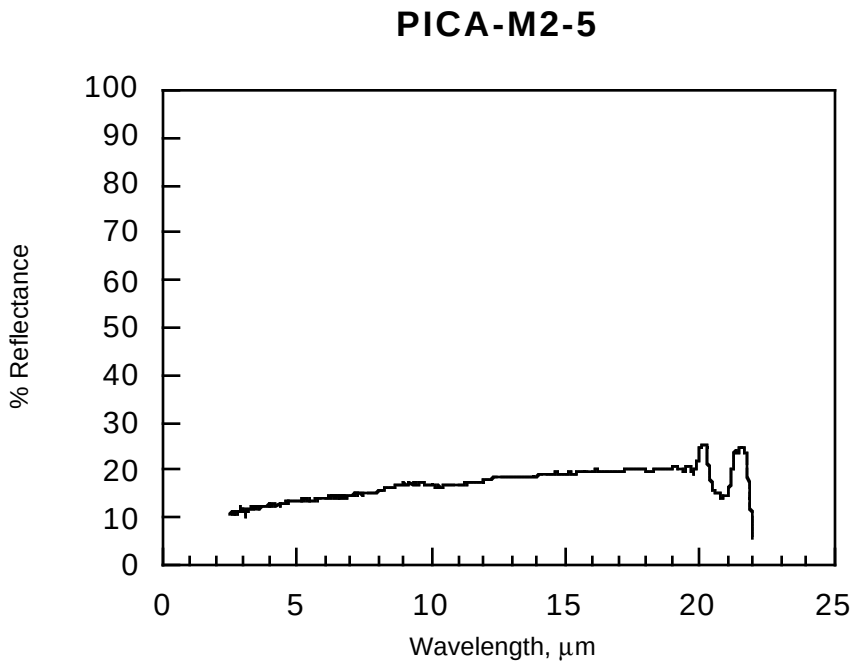

Figure D2. IR reflectant spectra for post-test standard PICA.

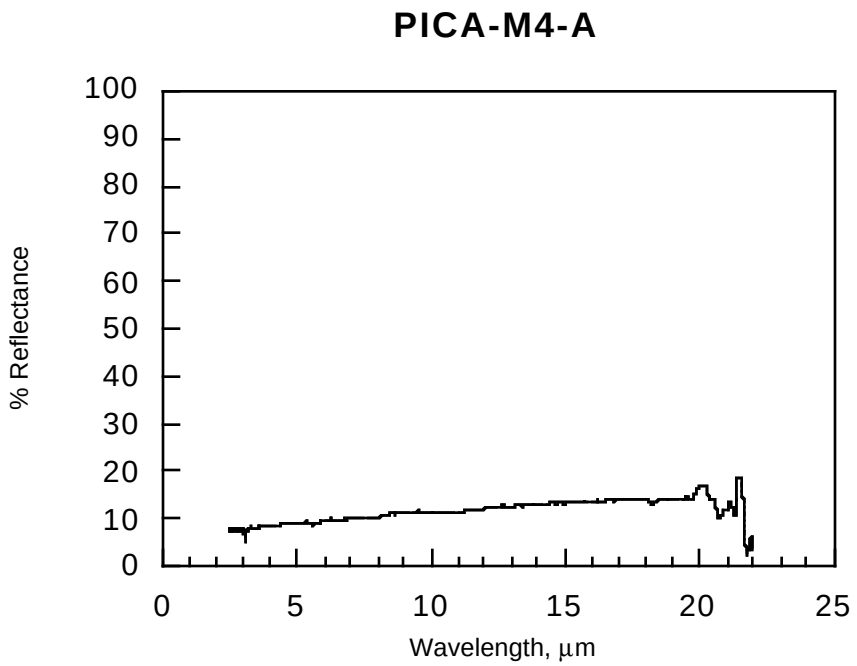

Figure D3. IR reflectant spectra for post-test standard PICA.

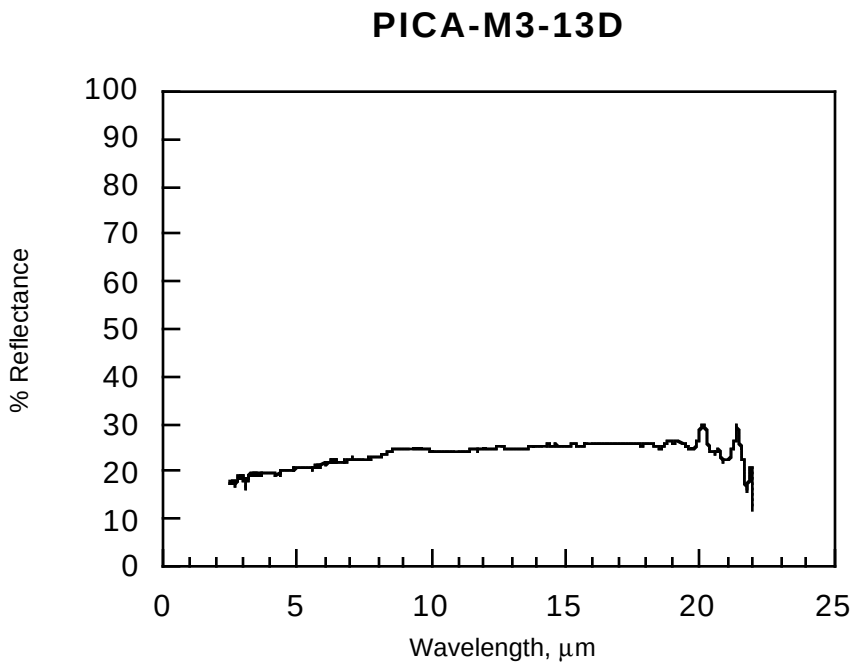

Figure D4. IR reflectant spectra for post-test densified PICA.

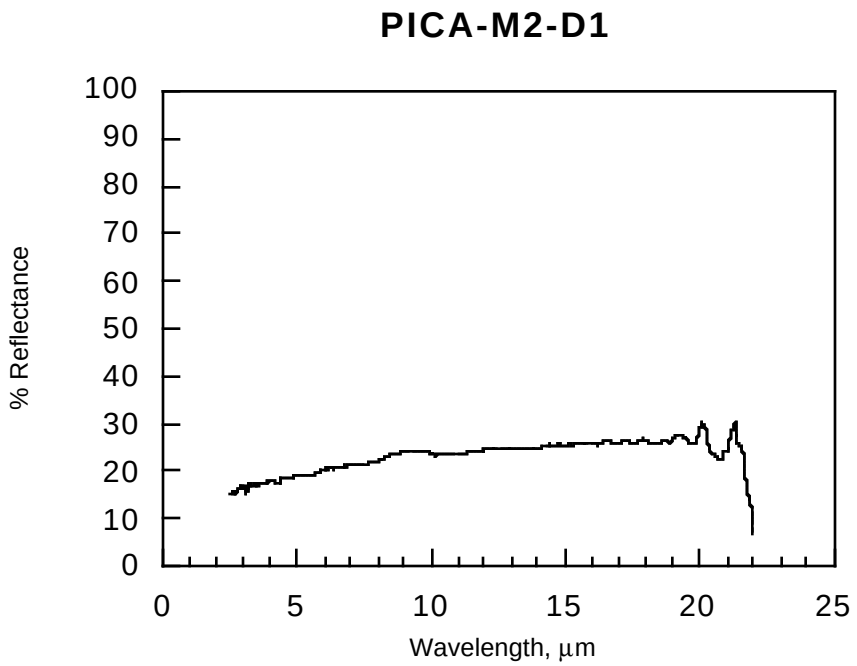

Figure D5. IR reflectant spectra for post-test densified PICA.

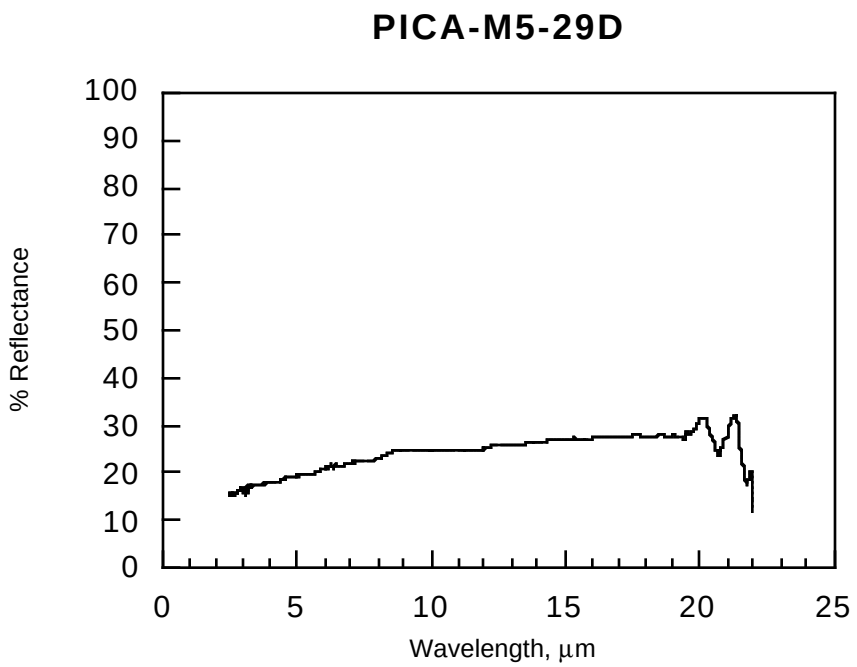

Figure D6. IR reflectant spectra for post-test densified PICA.

Appendix E

Photographs

Figure E1. Pre-test photograph of PICA-M3-8.

Figure E2. Post-test photograph of PICA-M3-8 tested at 400 Btu/ft^2-s, 0.11 atm stagnation pressure for 25 seconds.

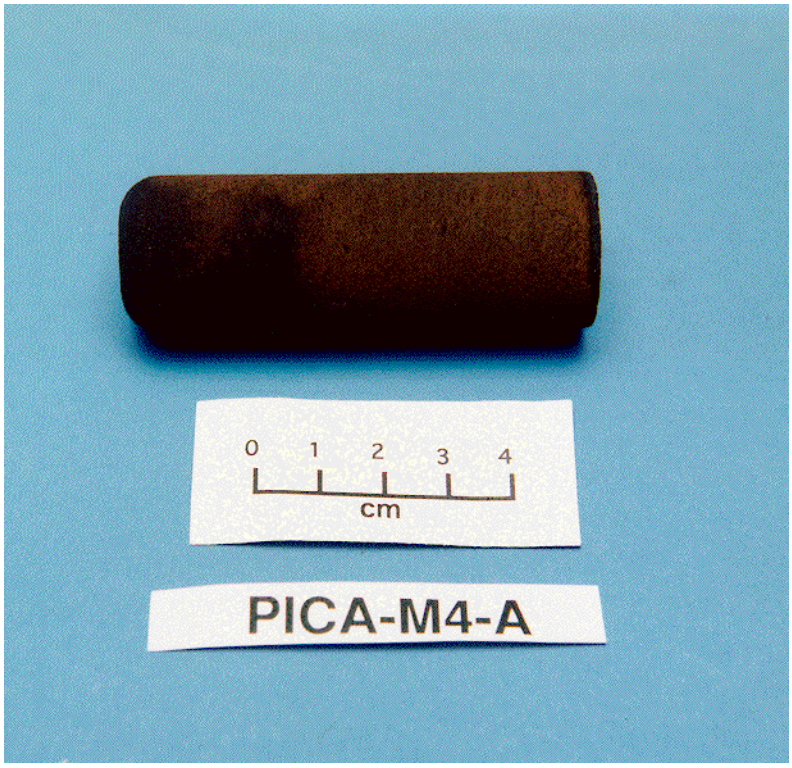

Figure E3. Pre-test photograph of PICA-M4-A (side view).

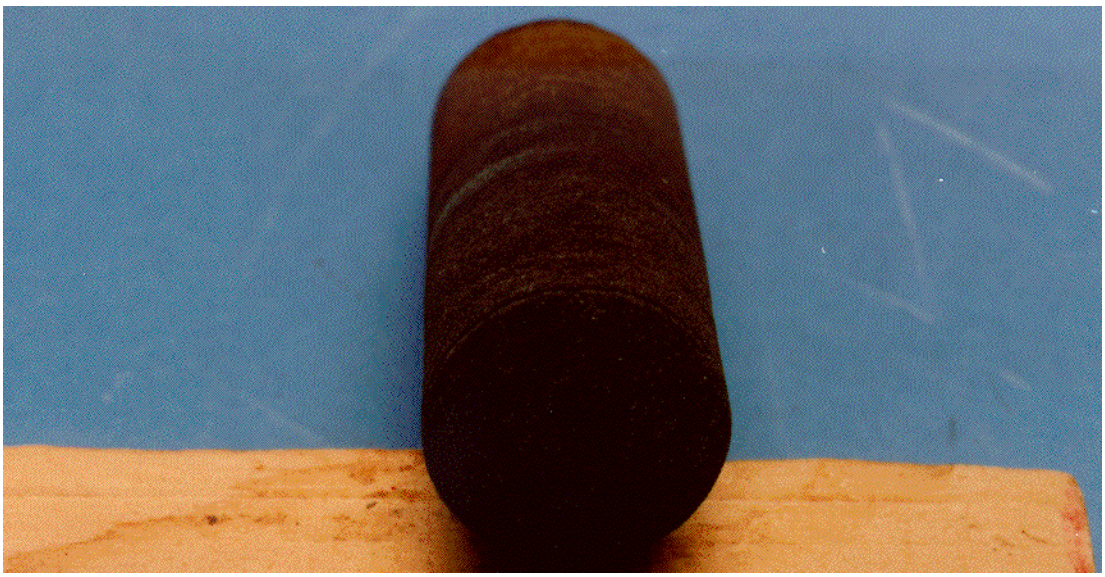

Figure E4. Post-test photograph of PICA-M4-A (front view) tested at 2960 Btu/ft^2-s, 0.43 atm stagnation pressure, for 10 seconds.

REPORT DOCUMENTATION PAGE

Form Approved
OMB No. 0704-0188

Public reporting burden for this collection of information is estimated to average 1 hour per response, including the time for reviewing instructions, searching existing data sources, gathering and maintaining the data needed, and completing and reviewing the collection of information. Send comments regarding this burden estimate or any other aspect of this collection of information, including suggestions for reducing this burden, to Washington Headquarters Services, Directorate for information Operations and Reports, 1215 Jefferson Davis Highway, Suite 1204, Arlington, VA 22202-4302, and to the Office of Management and Budget, Paperwork Reduction Project (0704-0188), Washington, DC 20503.

1. AGENCY USE ONLY *(Leave blank)*

2. REPORT DATE
April 1997

3. REPORT TYPE AND DATES COVERED
Technical Memorandum

4. TITLE AND SUBTITLE
Phenolic Impregnated Carbon Ablators (PICA) as Thermal Protection Systems for Discovery Missions

5. FUNDING NUMBERS
242-80-01

6. AUTHOR(S)
Huy Tran, Christine Johnson, Daniel Rasky, Frank Hui, Ming-Ta Hsu, Timothy Chen, Y. K. Chen, Daniel Paragas, and Loreen Kobayashi

7. PERFORMING ORGANIZATION NAME(S) AND ADDRESS(ES)
Ames Research Center
Moffett Field, CA 94035-1000

8. PERFORMING ORGANIZATION REPORT NUMBER
A-976112

9. SPONSORING/MONITORING AGENCY NAME(S) AND ADDRESS(ES)
National Aeronautics and Space Administration
Washington, DC 20546-0001

10. SPONSORING/MONITORING AGENCY REPORT NUMBER
NASA TM-110440

11. SUPPLEMENTARY NOTES
Point of Contact: Christine Johnson, Ames Research Center, MS 234-1, Moffett Field, CA 94035-1000
(415) 604-6163

12a. DISTRIBUTION/AVAILABILITY STATEMENT
Unclassified — Unlimited
Subject Category 24

12b. DISTRIBUTION CODE

13. ABSTRACT *(Maximum 200 words)*
This paper presents the development of the light weight Phenolic Impregnated Carbon Ablators (PICA) and its thermal performance in a simulated heating environment for planetary entry vehicles. The PICA material was developed as a member of the Light Weight Ceramic Ablators (LCAs), and the manufacturing process of this material has since been significantly improved. The density of PICA material ranges from 14 to 20 lbm/ft^3, having uniform resin distribution with and without a densified top surface. The thermal performance of PICA was evaluated in the Ames arc-jet facility at cold wall heat fluxes from 375 to 2,960 Btu/ft^2-s and surface pressures of 0.1 to 0.43 atm. Heat loads used in these tests varied from 5,500 to 29,600 Btu/ft^2 and are representative of the entry conditions of the proposed Discovery Class Missions. Surface and in-depth temperatures were measured using optical pyrometers and thermocouples. Surface recession was also measured by using a template and a height gage. The ablation characteristics and efficiency of PICA are quantified by using the effective heat of ablation, and the thermal penetration response is evaluated from the thermal soak data. In addition, a comparison of thermal performance of standard and surface densified PICA is also discussed.

14. SUBJECT TERMS
PICA, Ablator, Thermal protection system

15. NUMBER OF PAGES
61

16. PRICE CODE
A04

17. SECURITY CLASSIFICATION OF REPORT
Unclassified

18. SECURITY CLASSIFICATION OF THIS PAGE
Unclassified

19. SECURITY CLASSIFICATION OF ABSTRACT

20. LIMITATION OF ABSTRACT